

SUPERSYMMETRIC LEPTOPHILIC MODELS OF  
ELECTROWEAK SYMMETRY BREAKING

Gardner Rush Marshall

Charlottesville, Virginia

Master of Science, College of William and Mary, 2009  
Bachelor of Science, University of Mary Washington, 2007

A Dissertation presented to the Graduate Faculty  
of the College of William and Mary in Candidacy for the Degree of  
Doctor of Philosophy

Department of Physics

The College of William and Mary  
August 2012

©2012  
Gardner Rush Marshall  
All rights reserved.

# APPROVAL PAGE

This Dissertation is submitted in partial fulfillment of  
the requirements for the degree of

Doctor of Philosophy

*Gardner R. Marshall*

---

Gardner Rush Marshall

Approved by the Committee, May, 2012

*Marc Sher*

---

Committee Chair  
Professor Marc Sher, Physics  
The College of William and Mary

*Christopher Carone*

---

Professor Christopher Carone, Physics  
The College of William and Mary

*Joshua Erlich*

---

Associate Professor Joshua Erlich, Physics  
The College of William and Mary

*Patricia L. Vahle*

---

Assistant Professor Patricia Vahle, Physics  
The College of William and Mary

*José Goity*

---

Professor José Goity, Physics  
Hampton University

## ABSTRACT PAGE

Over the years, the Standard Model has proved itself to be an extremely durable theory. In spite of its success, very few empirical clues have emerged about the nature of the electroweak symmetry breaking that lies at its heart. With results from the LHC around the corner, this will hopefully change soon. In this dissertation we examine several possibilities for electroweak symmetry breaking and discuss various extensions to the Standard Model to resolve known problems. We begin by providing a brief overview of electroweak symmetry breaking, two Higgs doublet models, and supersymmetry. We then present a supersymmetric model that allows for small, Dirac neutrino masses. We find that it yields dramatic multi-lepton signatures, which have extremely small backgrounds. Next we discuss the leptophilic two Higgs doublet model and construct its supersymmetric analogue. Bounds on this model as well as its phenomenology are presented. We then show that an extension of this model includes a dark matter candidate that is capable of explaining a possibly observed excess of gamma-rays coming from the Galactic Center.

## TABLE OF CONTENTS

	Page
<b>Dedication</b> . . . . .	<b>iv</b>
<b>Acknowledgments</b> . . . . .	<b>v</b>
<b>List of Tables</b> . . . . .	<b>vi</b>
<b>List of Figures</b> . . . . .	<b>vii</b>
 <b>Chapter</b>	
<b>1 Introduction</b> . . . . .	<b>1</b>
1.1 Electroweak Symmetry Breaking . . . . .	2
1.2 Two Higgs Doublet Models . . . . .	4
1.3 Supersymmetry . . . . .	8
1.4 The Higgs Sector in The MSSM . . . . .	11
1.5 Thesis Layout . . . . .	16
<b>2 A Supersymmetric Model with Dirac Neutrino Masses</b> . . . . .	<b>18</b>
2.1 Introduction . . . . .	18
2.2 The Model . . . . .	20
2.3 Phenomenology of The Nu-Higgs Scalars . . . . .	23

2.4	Phenomenology of The Nu-Higgsinos . . . . .	26
2.4.1	Production . . . . .	26
2.4.2	Decays . . . . .	29
2.4.3	Signatures . . . . .	31
2.5	Conclusion . . . . .	36
<b>3</b>	<b>The Supersymmetric Leptophilic Higgs Model . . . . .</b>	<b>38</b>
3.1	Introduction . . . . .	38
3.2	The Leptophilic Two Higgs Doublet Model . . . . .	41
3.3	The Supersymmetric Leptophilic Higgs Model . . . . .	42
3.4	Constraints on The Supersymmetric Leptophilic Higgs Model . . . . .	47
3.4.1	Yukawa Coupling Perturbativity . . . . .	47
3.4.2	Tree Level Unitarity . . . . .	48
3.4.3	The Anomalous Muon Magnetic Moment . . . . .	49
3.4.4	LEP Higgs Search Data . . . . .	51
3.5	Phenomenology . . . . .	55
3.6	Conclusion . . . . .	60
<b>4</b>	<b>A Supersymmetric Leptophilic Higgs to Explain an Observed Gamma Ray Excess from The Galactic Center . . . . .</b>	<b>62</b>
4.1	Introduction . . . . .	62
4.2	The Model . . . . .	65
4.3	Annihilation to Fermions . . . . .	72
4.4	Direct Detection . . . . .	76
4.5	Bounds on The Model . . . . .	78
4.6	Conclusion . . . . .	81

## Appendices

**A The PMNS Mixing Matrix Parameters . . . . . 84**

**B Gauge Boson Masses in The SLHM . . . . . 86**

**C Derivation of  $\xi^2$  in The SLHM . . . . . 89**

**D Breaking Terms . . . . . 93**

**E List of Benchmark Points . . . . . 97**

**References . . . . . 99**

**Vita . . . . . 107**

## DEDICATION

This thesis is dedicated to the spirit of curiosity that makes physics so interesting.

## ACKNOWLEDGMENTS

While I have been at William & Mary, many people have contributed greatly to both my physics education and the work that lead to this thesis. I am very lucky to have had fellow graduate students in my year concentrate in high energy physics with me. Conversations with Dylan Albrecht and Reinard Primulando have been critical to my development as a student of physics. I appreciate the many key insights offered to me by Dylan, and I am particularly indebted to Reinard for being a constant source of physics knowledge and continually offering his extremely skillful assistance. I have learned a tremendous amount from him.

I am very grateful to my advisor, Marc Sher, for his guidance and mentorship. He has demonstrated an obvious concern for the success and development of his students. I can see that he planned projects designed to ease me into the process of performing physics research, and he has always had my interests in mind when guiding me through my years at William & Mary.

I am grateful to Chris Carone for inviting me to work with him on a dark Matter project with his undergraduate student, and also for teaching me general relativity. I don't think it's possible to explain the material more clearly than he did. I am also grateful to Josh Erlich, for the many questions he has answered and all the time he has spent explaining things to me.

I must also acknowledge all of the help and general support I received from my fellow graduate students: Doug, Dylan, Jeremy, Matt, Megan, and Reinard. Great times include all nighters doing homework in (the old) Small Hall, shoveling cream filled cups of sugerwater down our throats at Sno-To-Go, and endless nights playing Age of Empires together.

I want to thank my parents for doing a first rate job in parenting and encouraging me to pursue what I enjoy. And lastly, I must express profound thanks to my wife, Jennifer, for being by my side, and thereby making the world perfect.

## LIST OF TABLES

1	Possibilities for 2HDM couplings . . . . .	7
2	Various Higgs couplings to fermions in 2HDMs . . . . .	8
3	Chiral superfields of the MSSM . . . . .	13
4	Collider cuts used to extract the two lepton, two neutrino signal . . .	27
5	Normal hierarchy decay branching fractions for the nu-Higgsinos . . .	30
6	Inverted hierarchy decay branching fractions for the nu-Higgsinos . .	31
7	Cross sections for hexalepton signatures . . . . .	32
8	Cross sections, for tetralepton signatures . . . . .	34
9	Cross sections, for pentalepton signatures . . . . .	36
10	Benchmark point A: possible point in parameter space . . . . .	71
11	Benchmark point B: possible point in parameter space . . . . .	72
12	Mass spectrum and bounds for benchmark points A and B . . . . .	79
13	Transformation rule for the $\mathbb{Z}_{3q} \times \mathbb{Z}_{3\ell}$ symmetry . . . . .	93
14	List of generated superpotential and $V_{\text{soft}}$ terms . . . . .	95
15	Additional benchmark points for the model of Chapter 4 . . . . .	97
15	Continuation of previous table . . . . .	98

## LIST OF FIGURES

1	Production cross sections of charged and neutral nu-Higgsinos . . . . .	28
2	Exclusion plot showing viable regions of parameter space . . . . .	53
3	Exclusion plot showing additional regions of viable parameter space .	54
4	Various values of the quantity $\text{BR}(h \rightarrow b\bar{b})\xi^2$ . . . . .	55
5	Various values of the quantity $\text{BR}(h \rightarrow \tau^+\tau^-)\xi^2$ . . . . .	56
6	Various values of $\kappa$ . . . . .	57
7	Production of the lightest neutral scalar by gluon fusion . . . . .	58
8	Dominant diagram for dark matter annihilation into fermions . . . . .	73

SUPERSYMMETRIC LEPTOPHILIC MODELS OF  
ELECTROWEAK SYMMETRY BREAKING

# CHAPTER 1

## 1 Introduction

Over the last few decades, the Standard Model has been repeatedly validated by an increasingly impressive list of experiments. Measurements of most of its parameters have been refined, and only a few hints of its incompleteness have been uncovered. One key aspect of the Standard Model is electroweak symmetry breaking (EWSB). Despite all that has been learned, very little is known about the nature of how this is accomplished. The favored mechanism is known as the Higgs mechanism and entails the addition of one or more scalar fields to the theory. These fields receive nonzero vacuum expectation values (vevs) and spontaneously break the gauge symmetries under which they transform nontrivially. This is the scenario assumed in the Standard Model, which implements this in the simplest possible way by including a single, complex scalar doublet.

Until recently, there has not been any direct evidence for the physical particles arising from the additional scalar fields. With the Large Hadron Collider (LHC) now running, this is changing, and there is growing support for a Higgs boson at around 125 GeV. This is consistent with the predictions of the Standard Model. The possibility for more complicated scalar sectors, however, is very much open. Once the LHC is up and running full force, it may find additional scalars or other exotic particles not contained in the Standard Model. A great deal of work has been done

in anticipation of what the LHC might see.

In this thesis we will discuss possible extensions to the Standard Model's scalar sector to accomplish EWSB using multiple scalar doublets and supersymmetry. We will address a variety of issues that such extensions can explain, beginning with how the neutrinos might obtain small masses, and ending with explanations for dark matter that is capable of describing possibly anomalous observations at cosmic ray observatories.

## 1.1 Electroweak Symmetry Breaking

Before reviewing the Standard Model extensions addressed in this thesis, we will begin with a brief review of electroweak symmetry and its breaking. The electroweak symmetry is the  $SU(2)_L \times U(1)$  gauge symmetry of the Standard Model. Gauge symmetries, unlike global symmetries, entail the invariance of the action under transformations that depend on the spacetime coordinates of the fields. In order to connect the fields at infinitesimally separated points, one must introduce new degrees of freedom designed to transform in precisely the right way to compensate for the discrepancy between how the matter fields transform.

The simplest gauge symmetry is a  $U(1)$  symmetry. In this case, a spin 1/2 field,  $\psi$ , transforms as  $\psi \rightarrow e^{i\alpha}\psi$ . Since this is a local transformation, the value of  $\alpha$  is a function of the coordinates. As a consequence, derivatives of the field do not transform in the same way as the field itself  $\partial_\mu\psi \rightarrow e^{i\alpha}\partial_\mu\psi + ie^{i\alpha}\psi\partial_\mu\alpha$ . The extra term spoiling the equivalence arises because of the discrepancy in how the field transforms at infinitesimal separations. The introduction of a  $U(1)$  gauge field,  $A_\mu$ , eliminates this discrepancy by transforming in a way that exactly compensates:  $A_\mu \rightarrow A_\mu - \frac{1}{g}\partial_\mu\alpha$ . When coupled to the matter field,  $\psi$ , the net result is that the

combination  $\partial_\mu\psi + igA_\mu\psi$  does transform in the same way as the field,  $\psi$ , itself

$$\begin{aligned}
\partial_\mu\psi + igA_\mu\psi &\rightarrow e^{i\alpha}\partial_\mu\psi + ie^{i\alpha}\psi\partial_\mu\alpha + ig\left(A_\mu - \frac{1}{g}\partial_\mu\alpha\right)e^{i\alpha}\psi \\
&= e^{i\alpha}\partial_\mu\psi + ie^{i\alpha}\psi\partial_\mu\alpha + ig e^{i\alpha}A_\mu\psi - ie^{i\alpha}\psi\partial_\mu\alpha \\
&= e^{i\alpha}(\partial_\mu\psi + igA_\mu\psi).
\end{aligned} \tag{1}$$

The result is that ordinary derivatives must be exchanged for new operators called covariant derivatives defined by  $\partial_\mu \rightarrow \mathcal{D}_\mu = \partial_\mu + igA_\mu$ . When this is done, the disruption caused by a coordinate dependent transformation is smoothed out by the presence of the new gauge field.

To interpret the new field as dynamical it must have a kinetic term. This term must not violate the gauge symmetry. To construct such a kinetic term we use the combination  $F_{\mu\nu} = \partial_\mu A_\nu - \partial_\nu A_\mu$ , since it is invariant under a gauge transformation

$$\begin{aligned}
F_{\mu\nu} &\rightarrow \partial_\mu A_\nu - \frac{1}{g}\partial_\mu\partial_\nu\alpha - \partial_\nu A_\mu + \frac{1}{g}\partial_\nu\partial_\mu\alpha \\
&= \partial_\mu A_\nu - \partial_\nu A_\mu.
\end{aligned} \tag{2}$$

The kinetic term is therefore proportional to  $F_{\mu\nu}F^{\mu\nu}$ . An important fact is that a mass term  $M_A A_\mu A^\mu$  would violate the gauge symmetry and is therefore prohibited. Following the requirements of a postulated gauge symmetry gives rise to a lagrangian describing a massless vector field interacting with a spinor field.

In the Standard Model, the  $W$  and  $Z$  bosons acquire mass via the simplest possible Higgs mechanism, consisting of a single, scalar  $SU(2)$  doublet. Subsequent chapters of this thesis will concentrate on possible models for the Higgs mechanism that include supersymmetry. There will also be a focus on ‘‘leptophilic’’ models, in which at least one Higgs field has an enhanced coupling to leptons.

## 1.2 Two Higgs Doublet Models

One of the simplest and most studied extensions of the Standard Model is the Two Higgs Doublet Model (2HDM), in which two scalar doublets are jointly responsible for electroweak symmetry breaking and fermion mass acquisition [1, 2, 3]. This model has a very rich phenomenology, including charged scalars and pseudoscalars. Among the earliest motivations for the 2HDM is the possibility of additional CP violation relative to the Standard Model [4, 5, 6, 7, 8, 9, 10], which can provide an additional source of baryogenesis and contribute to the relative abundance of matter to antimatter in the universe [11, 12]. It was also motivated by the fact that supersymmetric models and models with a Peccei-Quinn symmetry [13] will always require a minimum of two Higgs doublets.

Two Higgs doublet models generally have eight real degrees of freedom since each of the two doublets contains two complex degrees of freedom. Assuming the pattern of gauge symmetry breaking is  $SU(2) \times U(1) \rightarrow U(1)$ , the potential is minimized when the fields receive the following vevs

$$\langle H_1 \rangle = \frac{1}{\sqrt{2}} \begin{pmatrix} 0 \\ v_1 \end{pmatrix}, \quad \text{and} \quad \langle H_2 \rangle = \frac{1}{\sqrt{2}} \begin{pmatrix} 0 \\ v_2 \end{pmatrix}. \quad (3)$$

In general, the vev of the second doublet can have a CP violating phase  $v_2 \rightarrow v_2 e^{i\theta}$ . In supersymmetric models, however, this phase can be eliminated by a redefinition of one of the fields. In the gauge eigenstate basis, the Higgs fields can be expressed as

$$H_1 = \begin{pmatrix} \Phi_1^+ \\ \frac{1}{\sqrt{2}}(v_1 + \phi_1 + i\eta_1) \end{pmatrix}, \quad H_2 = \begin{pmatrix} \Phi_2^+ \\ \frac{1}{\sqrt{2}}(v_2 + \phi_2 + i\eta_2) \end{pmatrix} \quad (4)$$

where the  $\Phi_i^+$  are complex and the  $\phi_i, \eta_i$  are real. The eight real degrees of freedom

give rise to two neutral scalars, a pseudoscalar, one charged pair, a charged goldstone boson, and a neutral goldstone boson. By defining the parameter  $\tan \beta = v_2/v_1$  we can express the goldstone bosons as

$$\begin{aligned} G^\pm &= \Phi_1^\pm \cos \beta + \Phi_2^\pm \sin \beta, \\ G^0 &= \eta_1 \cos \beta + \eta_2 \sin \beta. \end{aligned} \tag{5}$$

The physical charged scalar and pseudoscalar are orthogonal to the goldstone bosons, we therefore have

$$\begin{aligned} H^\pm &= -\Phi_1^\pm \sin \beta + \Phi_2^\pm \cos \beta, \\ A^0 &= -\eta_1 \sin \beta + \eta_2 \cos \beta. \end{aligned} \tag{6}$$

The goldstone bosons are eaten by the  $W$  and  $Z$ , giving them mass and acting as their longitudinal degrees of freedom. The remaining two degrees of freedom from the Higgs doublets give rise to the two neutral scalars, which can be expressed in terms of the mixing angle  $\alpha$  as

$$\begin{aligned} h^0 &= \phi_1 \sin \alpha - \phi_2 \cos \alpha \\ H^0 &= -\phi_1 \cos \alpha - \phi_2 \sin \alpha. \end{aligned} \tag{7}$$

The mixing angle is given by  $\tan 2\alpha = 2C/(A - B)$ , where  $A, B$ , and  $C$  are the 1-1, 2-2, and off-diagonal entries of the neutral scalar mass matrix. While the parameter  $\tan \beta$  depends on the relative sizes of  $v_1$  and  $v_2$ , the magnitude of their square sum is related to the  $Z$  mass by  $M_Z^2 = \frac{v^2}{4}(g_1^2 + g_2^2)$ , where  $v^2 = v_1^2 + v_2^2$ . Here  $g_1$  and  $g_2$  are the  $SU(2)_L$  and  $U(1)$  gauge couplings respectively.

When adding a second Higgs doublet, one encounters the potential phenomenological danger of generating unobserved flavor-changing neutral currents (FCNCs).

The Standard Model contains only a single Higgs doublet, which is responsible for giving mass to the fermions. Consequently, diagonalizing the fermion mass matrices to obtain the physical states also diagonalizes the Yukawa interactions. With a second Higgs doublet, this is no longer the case. In order to avoid this difficulty, the Glashow-Weinberg theorem [14] is often used to construct models with no tree-level FCNCs. The Glashow-Weinberg theorem states that FCNCs will be absent at tree-level if fermions of a given charge only couple to a single Higgs doublet. The most familiar models with this approach are Model I, in which one doublet couples to all fermions and the other couples to no fermions, and Model II, in which one doublet couples to the  $Q = 2/3$  quarks and the other couples to the  $Q = -1/3$  quarks and leptons. As will be discussed in Section 1.4, the latter is a feature of supersymmetric models [15]. These couplings are generally restricted by imposing a discrete  $\mathbb{Z}_2$  symmetry.

Another possible approach, Model III, has no such discrete symmetry but has tree-level FCNCs [16]. With the ansatz that the flavor-changing couplings scale as the geometric mean of the fermion masses, bounds from the FCNCs can be eluded without requiring extremely massive intermediate neutral scalars. It has been shown that this is indeed the case if the fermion mass hierarchy is due to approximate flavor symmetries [17]. There are also other versions of the 2HDM in the literature, which differ in the couplings of the Higgs doublets to fermions.

We will henceforth restrict our attention to 2HDMs that avoid tree-level FCNCs by requiring that fermions with the same quantum numbers couple to the same Higgs doublet. In this case, there are only two choices for the quarks. The first possibility is that one Higgs doublet, which we shall denote by  $H_1$ , does not couple to any quarks, while the other Higgs doublet, denoted  $H_2$ , couples to both the up-type quarks and the down-type quarks. The second possibility is that the down-type

	Model I	Model II	Leptophilic	Flipped
$u$	$H_2$	$H_2$	$H_2$	$H_2$
$d$	$H_2$	$H_1$	$H_2$	$H_1$
$\ell$	$H_2$	$H_1$	$H_1$	$H_2$

Table 1: Possibilities for 2HDM couplings with symmetries eliminating tree-level FCNCs. The first column lists the fermions with which the Higgs doublets may couple (up-type quarks, down-type quarks, and leptons respectively).

quarks couple to one doublet,  $H_1$ , while the up-type quarks couple to the second doublet  $H_2$ . For each of these scenarios there are two choices for the leptons.

Typically one assumes that the leptons always couple to the same doublet as the down-type quarks. In this case, the former of the above scenarios has one doublet coupling to all fermions and the other coupling to none, while the latter has one doublet coupling to the  $Q = 2/3$  quarks and the other coupling to the  $Q = -1/3$  quarks and leptons. As mentioned previously, these are called Model I and Model II respectively. The Yukawa structure of Model I can be enforced by a simple  $\mathbb{Z}_2$  symmetry under which the first Higgs doublet transforms as  $H_1 \rightarrow -H_1$ . To enforce the structure of Model II, simply choose  $H_1 \rightarrow -H_1$ ,  $d_R^i \rightarrow -d_R^i$ , and  $e_R^i \rightarrow -e_R^i$ .

It is not necessary that the leptons couple to the same doublet as the down-type quarks. If they do not, then the resulting possibilities are the ‘‘Leptophilic’’ Model and the ‘‘Flipped’’ Model. In the Leptophilic Model, the leptons couple to one doublet,  $H_1$ , while the up-type and down-type quarks couple to the second doublet  $H_2$ . In the Flipped Model, the down-type quarks couple to one doublet,  $H_1$ , while the leptons and up-type quarks couple to the second doublet  $H_2$ . Note that the convention is such that the  $H_2$  doublet always couples to the up-type quarks. All four possible models are summarized in Table 1.

The structure of the different 2HDMs differ by their couplings to fermions. The

Model	$\lambda_u^h$	$\lambda_d^h$	$\lambda_\ell^h$	$\lambda_u^H$	$\lambda_d^H$	$\lambda_\ell^H$	$\lambda_u^A$	$\lambda_d^A$	$\lambda_\ell^A$
I	$c_\alpha/s_\beta$	$c_\alpha/s_\beta$	$c_\alpha/s_\beta$	$s_\alpha/s_\beta$	$s_\alpha/s_\beta$	$s_\alpha/s_\beta$	$\cot \beta$	$-\cot \beta$	$-\cot \beta$
II	$c_\alpha/s_\beta$	$-s_\alpha/c_\beta$	$-s_\alpha/c_\beta$	$s_\alpha/s_\beta$	$c_\alpha/c_\beta$	$c_\alpha/c_\beta$	$\cot \beta$	$\tan \beta$	$\tan \beta$
L	$c_\alpha/s_\beta$	$c_\alpha/s_\beta$	$-s_\alpha/c_\beta$	$s_\alpha/s_\beta$	$s_\alpha/s_\beta$	$c_\alpha/c_\beta$	$\cot \beta$	$-\cot \beta$	$\tan \beta$
F	$c_\alpha/s_\beta$	$-s_\alpha/c_\beta$	$c_\alpha/s_\beta$	$s_\alpha/s_\beta$	$c_\alpha/c_\beta$	$s_\alpha/s_\beta$	$\cot \beta$	$\tan \beta$	$\cot \beta$

Table 2: Various Higgs couplings to fermions in 2HDMs. Rows correspond to Model I, Model II, the Leptophilic Model, and the Flipped Model respectively. This table has been reproduced from Reference [37].

Yukawa lagrangian can generally be expressed in terms of the physical states as

$$\begin{aligned} \mathcal{L}_Y = & - \sum_{i=u,d,\ell} \frac{m_i}{v} \left( \lambda_i^h \bar{\psi}_i \psi_i h^0 + \lambda_i^H \bar{\psi}_i \psi_i H^0 - i \lambda_i^A \bar{\psi}_i \gamma_5 \psi_i A^0 \right) \\ & - \frac{\sqrt{2}}{v} \left[ \bar{u} (A - B \gamma_5) V_{ud} d H^+ + \lambda_\ell^A m_\ell \bar{\nu}_L \ell_R H^+ + \text{h.c.} \right], \end{aligned} \quad (8)$$

where  $A = \frac{1}{2}(m_u \lambda_u^A + m_d \lambda_d^A)$  and  $B = \frac{1}{2}(m_u \lambda_u^A - m_d \lambda_d^A)$ . The sum is over up-type quarks, down-type quarks, and leptons, but an additional sum over generations is understood. The factor  $V_{ud}$  is the  $u$ - $d$  component of the CKM matrix, and the couplings  $\lambda_i^j$  for  $i = u, d, \ell$  and  $j = h, H, A$  are given in Table 2.

### 1.3 Supersymmetry

Supersymmetry entails the idea of incorporating symmetries under transformations that change the spin of the states upon which they act. Before the development of supersymmetry, the only kinds of transformations considered were bosonic, meaning that they mapped bosons to bosons and fermions to fermions. On the other hand, in supersymmetric theories, one considers fermionic transformations, which change a state's spin by  $1/2$ . Such transformations send bosons to fermions and fermions to bosons. Fermionic transformations must therefore have spinor indices so that when acting on a boson, the spinor index remains, leaving the state as a fermion. When acting on a fermion however, the transformation's spinor index contracts with the

state's spinor index, leaving the state as a boson.

A strong motivation for considering such transformations is that they provide the only means of extending the symmetries of the Poincaré group in a nontrivial way. The Poincaré group is the symmetry group consisting of Lorentz transformations and spacetime translations. The only kinds of additional bosonic symmetries one can impose are internal symmetries such as gauge symmetries [18]. This means that the overall symmetry group is just a direct product of some internal symmetries with the Poincaré group.

When one considers fermionic transformations, it is possible to introduce new symmetries whose generators mix with those of the Poincaré group. This indicates that supersymmetry is the only possible way to extend the known symmetries of nature in a nontrivial way. Whether nature makes use of this is a matter to be determined empirically, but that it is the only option is compelling motivation for studying supersymmetry.

Another strong motivation for supersymmetry is that it solves the hierarchy problem in the Standard Model. The hierarchy problem entails the apparent need for an enormous fine tuning of the Higgs bare mass. Upon calculating radiative corrections to the Higgs mass, one will encounter quadratic divergences necessitating a cutoff at an energy scale  $\Lambda$  where new physics is expected (meaning we can no longer trust the low energy results). This results in an expression for the Higgs mass  $M_h$  of the form

$$M_h^2 = M_0^2 + \mathcal{O}(\Lambda^2), \quad (9)$$

where  $M_0$  is the tree-level mass. Since  $\Lambda$  represents the scale of new physics, it is necessarily very large, possibly even on the order of the Planck scale  $10^{19}$  GeV. The Higgs mass however, is on the order of 100 GeV. The only way this can be the case is if the tree-level mass and the correction term cancel almost exactly, leaving only

an  $\mathcal{O}(100)$  GeV discrepancy between them. That is, the tree-level mass would need to be finely tuned to cancel the correction term over more than a dozen orders of magnitude.

Supersymmetry solves the hierarchy problem by introducing new particles to the theory. In order to have new, fermionic transformations, there must be particle states of the appropriate spin for the known particles to transform into. To do this for the Standard Model, the number of particles in the theory must be doubled. Every particle receives a corresponding superpartner whose spin differs by  $1/2$ . The masses of the new superpartner particles must be the same as their corresponding Standard Model counterparts in order to preserve supersymmetry. Since we do not see these extra superpartners, supersymmetry must be broken at some energy scale above that which we can currently probe.

The solution to the hierarchy problem arises from additional diagrams coming from the new superpartner particles. When calculating the Higgs mass in a supersymmetric theory, the contributions to the Higgs mass coming from diagrams with particle loops are canceled by the corresponding diagrams with superpartner loops. This eliminates the large correction term in Equation 9 and frees the theory from fine tuning. Since supersymmetry must be broken if it exists, a correction term corresponding to the scale at which supersymmetry breaks will still be present. So long as this scale is around 1 TeV or so, the issue of fine tuning will still be resolved. If supersymmetry is broken at much higher scales, it remains a viable theory, but no longer provides a solution to the hierarchy problem.

The third and final motivation for supersymmetry discussed here is that it automatically provides a dark matter candidate. In order to prevent unwanted terms in the lagrangian that lead to proton decay, most formulations of supersymmetry include a  $\mathbb{Z}_2$  symmetry called R-parity. R-parity is a multiplicative quantum number

under which Standard Model particles have charge  $R = 1$ , and new superpartner particles have charge  $R = -1$ . A result of R-parity is that the new superpartners only directly interact with Standard Model particles in pairs. As a consequence of R-parity, the lightest superpartner particle is stable. This is because the decay channel of any superpartner must contain a final state with at least one other superpartner. Obviously the lightest superpartner cannot decay into a state with particles heavier than it is, and so it has no possible decay channels.

The lightest superpartner is typically referred to as the lightest stable particle (LSP), and serves as a natural dark matter candidate. In the Minimal Supersymmetric Standard Model (MSSM), the LSP is usually a neutralino, which is an electrically neutral linear combination of the gauginos, the superpartners of the gauge bosons, and the Higgsinos, the superpartners of the Higgs bosons.

## 1.4 The Higgs Sector in The MSSM

To construct the scalar sector of supersymmetric theories, one first builds the so-called superpotential,  $W$ , which is the most general possible analytic, cubic function of the scalar fields of the theory. The allowed terms in the superpotential are restricted by gauge invariance as well as any other imposed symmetries of the theory, e.g., R-parity. Since the superpotential is required to be analytic in the fields, it cannot contain complex conjugates of the fields. In general, the superpotential takes the form

$$W = a_i \phi_i + \frac{1}{2} m_{ij} \phi_i \phi_j + \frac{1}{3!} y_{ijk} \phi_i \phi_j \phi_k . \quad (10)$$

For supersymmetric models, the scalar potential is determined by the superpo-

tential. In particular, the potential is given by

$$V(\phi_i) = \sum_i \left| \frac{\partial W}{\partial \phi_i} \right|^2 + \frac{1}{2} \sum_a \left| \sum_i g^a \phi_i^\dagger T^a \phi_i + \xi^a \right|^2. \quad (11)$$

The first term in the above expression is called the  $F$ -term while the second term involving the sum over gauge group generators,  $T^a$ , is called the  $D$ -term. The so called Fayet-Iliopoulos term,  $\xi^a$ , is only nonzero for  $U(1)$  gauge fields. It is clear that the assumption of supersymmetry limits the possible scalar couplings to the extent that they are determined by the gauge couplings and the parameters of the superpotential. Interactions between the scalar and fermion fields are governed by the Yukawa lagrangian, which is given by

$$\mathcal{L}_Y = \frac{1}{2} \frac{\partial^2 W}{\partial \phi_i \partial \phi_j} \bar{\psi}_i \psi_j + \text{h.c.} \quad (12)$$

As its name suggests, the MSSM is the minimal possible extension of the Standard Model that enables supersymmetry. Every known particle receives a superpartner, with which it is paired as part of a supermultiplet. To incorporate supersymmetry, the Higgs sector must also receive a second Higgs doublet. The reason for this is twofold. First, a second doublet with opposite hypercharge assignment is needed for anomaly cancelation. Second, two doublets are required in order to give mass to both the up-type and down-type quarks due to the analyticity of the superpotential. The two scalar doublets of the MSSM are labeled according to the quark types to which they couple:  $H_u$  and  $H_d$ .

To calculate the scalar potential one merely needs to determine the superpotential. In the case of the MSSM, there are several scalar fields from which a superpotential could be built:  $Q$ , the left-handed squark doublet,  $U$  and  $D$ , the right-handed squark singlets,  $L$ , the left-handed lepton doublet,  $E$ , the right-handed

LH $\chi$ SF	Spin-0	Spin-1/2	$(SU(3), SU(2), U_Y(1))$
$U$	$\tilde{u}_R^\dagger$	$u_R^\dagger$	$(\bar{3}, 1, -\frac{2}{3})$
$D$	$\tilde{d}_R^\dagger$	$d_R^\dagger$	$(\bar{3}, 1, +\frac{1}{3})$
$E$	$\tilde{e}_R^\dagger$	$e_R^\dagger$	$(1, 1, +1)$
$Q$	$\begin{pmatrix} \tilde{u}_L \\ \tilde{d}_L \end{pmatrix}$	$\begin{pmatrix} u_L \\ d_L \end{pmatrix}$	$(3, 2, +\frac{1}{6})$
$L$	$\begin{pmatrix} \tilde{\nu}_L \\ \tilde{e}_L \end{pmatrix}$	$\begin{pmatrix} \nu_L \\ e_L \end{pmatrix}$	$(1, 2, -\frac{1}{2})$
$H_u$	$\begin{pmatrix} H_u^+ \\ H_u^0 \end{pmatrix}$	$\begin{pmatrix} \tilde{H}_u^+ \\ \tilde{H}_u^0 \end{pmatrix}$	$(1, 2, +\frac{1}{2})$
$H_d$	$\begin{pmatrix} H_d^0 \\ H_d^- \end{pmatrix}$	$\begin{pmatrix} \tilde{H}_d^0 \\ \tilde{H}_d^- \end{pmatrix}$	$(1, 2, -\frac{1}{2})$

Table 3: Chiral superfields of the MSSM. Not shown are the vector superfields that contain the gauge bosons and their corresponding gauginos. This table is an adaptation of a table that can be found in Reference [19].

lepton singlet, and the Higgs doublets  $H_u$  and  $H_d$ . These fields, along with their gauge quantum numbers, are listed in Table 3. Aside from the gauge bosons and gauginos, the table represents the full particle content of the MSSM (note that flavor indices have been suppressed, so there are really three of every field listed). It may seem that with all of these fields, the most general allowed superpotential would be enormous. However, because the superpotential must respect gauge invariance, the number of possibilities is actually quite limited. With hypercharge assignments shown in Table 3, the most general possible superpotential is given by \*

$$\begin{aligned}
W = & y_u U Q H_u - y_d D Q H_d - y_e E L H_d + m H_u H_d \\
& + y_1 E L L + y_2 D L Q + y_3 U D D + m' L H_u .
\end{aligned} \tag{13}$$

---

\*Here we have suppressed color and  $SU(2)$  indices. For  $SU(2)$  doublets, such as  $H_u$  and  $H_d$ , the notation  $H_u H_d$  is read  $\epsilon_{ij} H_u^i H_d^j$  when  $SU(2)$  indices are explicit.

The last four terms are not desired however, since they collectively violate both lepton and baryon number conservation. This is where R-parity comes in. As mentioned previously, R-parity is an additional  $\mathbb{Z}_2$  symmetry imposed on the theory. Once enforced, it prohibits all four of the unwanted terms, leaving the MSSM superpotential as

$$W_{MSSM} = y_u U Q H_u - y_d D Q H_d - y_e E L H_d + m H_u H_d . \quad (14)$$

For the purposes of this section, we will focus only on the last term,  $m H_u H_d$ , which is responsible for the Higgs sector of the MSSM. So far we have neglected the fact that in the MSSM, supersymmetry must be broken. This is accomplished by adding terms to the lagrangian that softly break supersymmetry. Such terms are simply a general parameterization of how supersymmetry may be broken (if it is true in the first place). To fully parameterize the breaking, one must add the most general possible set of soft terms. The meaning “soft” is that the new terms do not result in couplings that reintroduce the quadratic divergences that supersymmetric theories are intended to eliminate. In the case of the Higgs sector, the soft terms added to the potential are given by

$$V_{\text{soft}} = \mu_u^2 |H_u|^2 + \mu_d^2 |H_d|^2 - m_0^2 (H_u H_d + \text{h.c.}) . \quad (15)$$

Combining the soft terms with the results from Equations 11 and 14, we obtain the following Higgs potential for the MSSM

$$\begin{aligned} V = & \frac{g_1^2}{8} \sum_a \left| H_u^\dagger \sigma^a H_u - H_d^\dagger \sigma^a H_d \right|^2 + \frac{g_2^2}{8} \left( |H_u|^2 - |H_d|^2 \right)^2 \\ & + m_u^2 |H_u|^2 + m_d^2 |H_d|^2 - m_0^2 (H_u H_d + \text{h.c.}) , \end{aligned} \quad (16)$$

where  $m_u^2 = |m|^2 + \mu_u^2$ ,  $m_d^2 = |m|^2 + \mu_d^2$ , and  $\sigma^a$  ( $a = 1, 2, 3$ ) are the Pauli matrices.

By minimizing this potential with the requirement that the parameters be such that the minimum not occur at zero values for the fields, spontaneous symmetry breaking will be achieved. Upon doing this, the Higgs fields acquire the following vevs

$$\langle H_u \rangle = \frac{1}{\sqrt{2}} \begin{pmatrix} 0 \\ v_u \end{pmatrix}, \quad \text{and} \quad \langle H_d \rangle = \frac{1}{\sqrt{2}} \begin{pmatrix} v_d \\ 0 \end{pmatrix}. \quad (17)$$

To find the physical states we simply diagonalize the matrix of second partial derivatives of the potential and evaluate it at the field vevs. The result breaks up into blocks corresponding to the neutral scalars, pseudoscalars, and charged scalars. By defining the quantity  $\tan \beta = v_u/v_d$  and using the relation  $M_Z^2 = \frac{1}{4}(g_1^2 + g_2^2)(v_u^2 + v_d^2)$  we may express the resulting mass matrices in terms of the  $Z$  mass. The neutral scalar mass matrix is

$$M_N^2 = \begin{pmatrix} M_Z^2 \sin^2 \beta + m_0^2 \cot \beta & -\frac{M_Z^2}{2} \sin 2\beta - m_0^2 \\ -\frac{M_Z^2}{2} \sin 2\beta - m_0^2 & M_Z^2 \cos^2 \beta + m_0^2 \tan \beta \end{pmatrix}, \quad (18)$$

The pseudoscalar mass matrix is

$$M_A^2 = m_0^2 \begin{pmatrix} \cot \beta & 1 \\ 1 & \tan \beta \end{pmatrix}, \quad (19)$$

and the charged scalar mass matrix is

$$M_C^2 = \begin{pmatrix} M_W^2 \cos^2 \beta + m_0^2 \cot \beta & \frac{M_W^2}{2} \sin 2\beta + m_0^2 \\ \frac{M_W^2}{2} \sin 2\beta + m_0^2 & M_W^2 \sin^2 \beta + m_0^2 \tan \beta \end{pmatrix}. \quad (20)$$

Note that the charged mass matrix depends on the  $W$  mass rather than the  $Z$  mass.

This is because it has no dependency on the  $U(1)$  coupling.

Since we began with two complex Higgs doublets,  $H_u$  and  $H_d$ , we have a total of eight real degrees of freedom. These degrees of freedom give rise to five physical states: two neutral scalars, one pseudoscalar, and one charged pair. The remaining three degrees of freedom are the goldstone bosons whose existence can be seen from the fact that the determinants of the pseudoscalar and charged scalar mass matrices are zero. These are eaten by the  $W$  and  $Z$  bosons, giving them mass and acting as their longitudinal degrees of freedom.

If one subtracts  $M_Z^2$  times the identity matrix from the neutral scalar matrix and then takes the determinant, the result is  $-2M_Z^2 m_0^2 \sin(2\beta)$ . This being negative indicates that the lightest neutral scalar is necessarily lighter than the  $Z$ . Since these matrices are only valid at tree-level, the actual neutral scalar mass may exceed this upper bound. Regardless, the result is that if the MSSM is realized in nature, one expects a neutral scalar to be found with a mass not too much greater than the  $Z$  boson.

## 1.5 Thesis Layout

In the following chapters of this thesis, we will present a variety of extensions to the Standard Model's scalar sector, which will be responsible for accomplishing electroweak symmetry breaking. In Chapter 2 we will discuss a supersymmetric model in which two additional Higgs doublets are present. These doublets, called the “nu-Higgs” couple to left-handed lepton doublets and right-handed neutrinos and receive small vevs via the breaking of a global  $U(1)$  symmetry. This give rise to small Dirac neutrino masses. We find that, if kinematically allowed, the decay of the heavy MSSM scalar into the charged nu-Higgs scalars produces dramatic multi-lepton signatures with very low background.

In Chapter 3 we discuss leptophilic two Higgs doublet models and present the minimal supersymmetric model thereof. We consider constraints from perturbativity, unitarity, and LEP bounds and find that the model contains a Higgs with Standard Model couplings and a mass around 110 GeV throughout most of parameter space. The two heaviest Higgs are gauge-phobic with one decaying mostly into  $b\bar{b}$  pairs and the other almost entirely into  $\tau^+\tau^-$  pairs. The former can be produced via gluon fusion while latter is very difficult to produce.

In Chapter 4 we modify the supersymmetric leptophilic Higgs model presented in the previous chapter to obtain a model of dark matter that annihilates mostly into  $\tau^+\tau^-$  pairs. The motivation for such a model comes from a claimed excess of gamma-rays coming from the Galactic Center. A paper by Hooper and Goodenough [21] has suggested that the possible excess can be explained by 7-10 GeV annihilating dark matter with a power law profile if the dark matter annihilates predominantly into tau pairs. We use a  $\mathbb{Z}_2$  symmetry to enforce the correct Yukawa structure to achieve the desired phenomenology for explaining the gamma-ray excess. Our model yields the correct dark matter thermal relic density and avoids collider bounds from measurements of the  $Z$  width as well as direct production at LEP.

# CHAPTER 2

## 2 A Supersymmetric Model with Dirac Neutrino Masses \*

### 2.1 Introduction

As discussed in Section 1.2, the 2HDM is one of the simplest and most studied extensions of the Standard Model. The most heavily studied versions are Model I, in which one doublet couples to all fermions and the other couples to no fermions, and Model II, in which one doublet couples to the  $Q = 2/3$  quarks and the other couples to the  $Q = -1/3$  quarks and leptons. Another version of the 2HDM has one doublet coupling to all of the quarks and the second doublet coupling to the leptons. Although the basic structure of this model was proposed long ago [22], it has received a resurgence of interest [23] due to the existence of non-zero neutrino masses. A modified version, in which one doublet couples to all of the quarks and charged leptons, and the second doublet couples only to the left-handed lepton doublet and the right-handed neutrino was proposed by Gabriel and Nandi [24]. The model will allow for Dirac neutrino masses, which are small due to a very small (less than an eV) vacuum expectation value for the second doublet (as opposed to the one-doublet case in which they are small due to very small Yukawa couplings).

---

\*This chapter was previously published in Reference [20].

The model has a  $\mathbb{Z}_2$  symmetry in which the second doublet and the right-handed neutrinos are odd and all other fields are even.

The model of Gabriel and Nandi [24] has the feature that it contains a very light scalar which causes problems with standard cosmology. This feature remains even if the  $\mathbb{Z}_2$  symmetry is promoted to a  $U(1)$  (which can eliminate Majorana mass terms for the right-handed neutrinos). Very recently, Davidson and Logan (DL) proposed [25] enforcing the coupling structure with a global  $U(1)$ , but breaking the  $U(1)$  explicitly, through a dimension-2 soft term in the Higgs potential. This avoids any Goldstone bosons and other light scalars, and only requires that the soft term have a magnitude of approximately an  $(\text{MeV})^2$ . Since this term is the only  $U(1)$  breaking term, the smallness of its size is technically natural. The charged Higgs boson in the model has very distinctive signatures, decaying into a left-handed charged lepton and a neutrino, with branching ratios determined by the Pontecorvo, Maki, Nakagawa, Sakata (PMNS) neutrino mixing matrix.

In this chapter, we consider the supersymmetric version of the Davidson-Logan model. We extend the MSSM by adding two additional Higgs doublets of opposite hypercharge, which have opposite quantum numbers under the global  $U(1)$ . The right-handed neutrinos are also charged under the  $U(1)$  and all other fields are neutral. We first show that, through D-terms, the heavy neutral scalar of the MSSM will decay (if kinematically allowed) into the lightest of the  $U(1)$ -charged Higgs, leading to distinctive signatures. We then look at the supersymmetric partners of the  $U(1)$ -charged Higgs, and find some remarkable signatures at the LHC and the Tevatron, including dramatic multilepton events which have little to no background and yet accessible cross sections.

## 2.2 The Model

To ensure anomaly cancellation, we must add an even number of doublets to the MSSM. Referring to the MSSM doublets as  $H_1$  and  $H_2$ , we add two new doublets,  $H_3$  and  $H_4$  and three right-handed neutrino superfields,  $N_i$ . A global  $U(1)$  symmetry is imposed in which  $H_3$ ,  $H_4$  and  $N_i$  have charges  $-1$ ,  $+1$  and  $-1$  respectively, while all other fields are uncharged. As usual, R-parity will be conserved in the model.

The superpotential is given by

$$W = W_0 + y'NLH_4 + \mu_{34}H_3H_4, \quad (21)$$

where  $W_0$  is the MSSM superpotential and  $L$  is the left-handed lepton doublet (generation indices are understood). Since the new Higgs fields only couple to right-handed neutrinos and leptons, we refer to them as “nu-Higgs.” Due to the global  $U(1)$  symmetry, there is no mixing with the MSSM Higgs bosons at this stage. We also assume that the mass-squared parameters of the nu-Higgs fields are sufficiently large and positive that the fields do not acquire vacuum expectation values (vevs). DL show that there is a cosmological lower bound of  $1/30$  on  $y'$ ; our results will not be sensitive to  $y'$  as long as it is not extremely small (so that decays occur at the vertex).

Following Davidson and Logan, the global  $U(1)$  is broken explicitly by soft dimension-2 terms in the potential  $\mu_{14}^2 H_1 H_4 + \mu_{23}^2 H_2 H_3$ . These terms will result in vevs for the nu-Higgs fields which have the seesaw form  $v_3 = \mu_{23}^2 v_2 / M_A$  and  $v_4 = \mu_{14}^2 v_1 / M_A$ , where  $M_A$  is generally the weak scale. Since the vevs of  $H_3$  and  $H_4$  cannot be too dissimilar (due to the  $U(1)$ -conserving  $\mu_{34}$  coupling), we must have  $v_3 \sim v_4 \sim \text{eV}$  in order to give the correct neutrino masses without very small Yukawa couplings. This implies that  $\mu_{14}$  and  $\mu_{23}$  are both of the order of an MeV.

Since these soft terms are the only source of  $U(1)$  breaking, their small size is technically natural. This model does seem rather ad hoc, and one can ask about a possible ultraviolet completion, possibly in the context of a grand unified theory. Of course, this question can be asked about any leptophilic model, whether supersymmetric or not. As noted earlier, there are many discussions of leptophilic models [22, 23] in which the charged leptons (and the left-handed neutrino) have a different sign under the  $\mathbb{Z}_2$  symmetry than the quarks. It is difficult to see how to reconcile these models with grand unification, since the charged leptons and quarks are generally in the same representation. In this model, however, the charged leptons and quarks have the same sign under the  $\mathbb{Z}_2$ , and thus it is easy to incorporate into a GUT. For example, in  $SU(5)$ , one could simply promote the  $H$  fields to 5-plets, and the  $N$  fields to singlets, and impose the same discrete symmetry. Whether one can find a model which can also give terms discussed in the previous paragraph is unclear - it would possibly be more contrived than the model we have presented. Without such a detailed model, discussion of sparticle mass spectra would be premature. Nonetheless, this model would appear to be easier to embed in a GUT than other leptophilic models.

The nu-Higgs spectrum consists of two scalars, two pseudoscalars, two pairs of charged scalars, two neutral nu-Higgsinos and a pair of charged nu-Higgsinos. What are their masses? In the scalar sector, DL had several unknown quartic couplings, and thus the relative masses of the scalars was arbitrary; they had to consider cases in which the charged scalar was either heavier than or lighter than the neutral scalars, which affected the phenomenology. In this case, however, the quartic terms are completely determined by gauge couplings. Ignoring the very small corrections due to  $U(1)$  breaking, the masses were calculated in Ref. [26]. They found that the neutral scalar mass matrix depended on unknown parameters, but the pseudoscalar

mass matrix was identical to the scalar, and the charged scalar mass matrix only differed slightly. It was shown that the lightest charged scalar was a few GeV heavier than the degenerate scalar and pseudoscalar. Since the masses are similar, decays of the nu-Higgs particles into each other will be phase-space forbidden or suppressed, and the decays into leptons will predominate. As a result, we will focus on the lighter of the states, and take the scalar, pseudoscalar and charged scalar to be degenerate in mass (for phenomenological purposes, keeping in mind that the charged scalar is slightly heavier). They will be referred to as  $\chi^0, \chi_A$  and  $\chi^\pm$  respectively. The nu-Higgsino masses depend only on  $\mu_{34}$  and are completely degenerate at tree level. Note that the neutral nu-Higgsino mass matrix is completely off-diagonal, giving a mixing angle of 45 degrees when rotating to mass eigenstates. Thus, both of the neutral nu-Higgsinos as well as the charged nu-Higgsinos are degenerate in mass. For notational simplicity, we refer to them as  $\tilde{\chi}^0$  and  $\tilde{\chi}^\pm$ . Although there are two neutral states, the branching ratios will be the same for each, and we will account for the factors of two in the production cross section.

Focusing on the lighter of the nu-Higgs and on the nu-Higgsinos, we can look at their decays. The decays of the neutral nu-Higgs,  $\chi^0, \chi_A$  are into neutrinos, and are thus unobservable. The charged nu-Higgs,  $\chi^\pm$ , will decay into all nine combinations  $\ell_i \nu_j$ . Davidson and Logan show that the decay rate into  $\ell^\pm \nu$  is proportional to  $\sum_i m_{\nu_i}^2 |U_{\ell i}|^2$ , where  $U$  is the PMNS mixing matrix. For a normal neutrino mass hierarchy, with the lightest neutrino having a mass below  $10^{-3}$  eV, the decays will be into  $\mu\nu$  and  $\tau\nu$  with branching ratios between 40 and 60 percent. For an inverted hierarchy, the rate into  $e\nu$  is about 50 percent, with the balance shared equally between  $\mu\nu$  and  $\tau\nu$ . A discussion of the PMNS mixing matrix parameters used is in Appendix A. The actual width is narrow, but the decay still occurs at the vertex.

The nu-Higgsinos decay as

$$\begin{aligned}\tilde{\chi}^0 &\rightarrow \nu_L + \tilde{\nu}_R, \nu_R + \tilde{\nu}_L \\ \tilde{\chi}^\pm &\rightarrow \ell + \tilde{\nu}_R, \nu_R + \tilde{\ell}\end{aligned}$$

with equal branching ratios in the limit that the slepton and sneutrino have equal mass. Note that because the nu-Higgsino mass eigenstates are made up of equal parts of  $\tilde{H}_3$  and  $\tilde{H}_4$ , and the former does not have any two body decays, both mass eigenstates will decay similarly.

Finally, the right-handed sneutrino,  $\tilde{\nu}_R$  can only decay through a virtual nu-Higgs (plus a left-handed sneutrino or slepton) or a virtual nu-Higgsino (plus a left-handed neutrino or lepton), and has no two body decays. As a result, it can have visible decays, and thus the  $\tilde{\chi}^0$  decays above could be observable through both decay chains.

We now turn to the detailed phenomenology of these nu-Higgs particles at the LHC and the Tevatron.

### 2.3 Phenomenology of The Nu-Higgs Scalars

In the non-supersymmetric version of the model, the phenomenology of the nu-Higgs scalars was discussed by Davidson and Logan [25]. As noted above, since supersymmetry did not restrict the masses in their model, they needed to consider a range of possibilities. In the supersymmetric version, the lightest neutral nu-Higgs is only slightly lighter than the lightest charged nu-Higgs. As a result, it will only decay into neutrinos and would thus be unobservable <sup>†</sup>. The charged nu-Higgs will decay into a charged lepton and a neutrino; summing over the unobserved neutrino

---

<sup>†</sup>We are assuming here that its supersymmetric partners are not much lighter. If so, other two-body decay channels which are observable could open up.

leads to the charged lepton being approximately 50%  $\mu$ , 50%  $\tau$  (50%  $e$ , 25%  $\mu$ , 25%  $\tau$ ) for the normal (inverted) hierarchy.

This was discussed by Davidson and Logan, and the primary production mechanism was through a Drell-Yan photon or  $Z$ . In the supersymmetric version, a new production mechanism opens up, and can be substantially larger. Because of the  $SU(2)$  and  $U(1)$  D-terms, there is an interaction  $(H_1^\dagger H_1 - H_2^\dagger H_2)(H_3^\dagger H_3 - H_4^\dagger H_4)$ , and when  $H_1$  and  $H_2$  acquire vev's, this will lead to a three point interaction between an MSSM Higgs and two nu-Higgs scalars. The lightest MSSM Higgs is too light to decay into two charged nu-Higgs, but the heavier one,  $H$ , is not. One can thus produce the  $H$  of the MSSM via gluon fusion [27], and it will then decay into a pair of charged nu-Higgs scalars. Each of those will decay into a charged lepton and a neutrino.

For the production of the heavy MSSM Higgs through gluon fusion we use  $\tan\beta = 3$ . In order to calculate the pair production of the charged nu-Higgs bosons we first calculate the branching fraction of the heavy MSSM Higgs to a pair of charged nu-Higgs bosons. From the D-terms in the potential we can derive the coupling of the heavy MSSM Higgs to the charged nu-Higgs:

$$g_{H^0\chi^+\chi^-} = \left( \frac{gM_Z}{2\cos\theta_W} \right) \cos(2\theta_W) \cos(2\gamma) \cos(\alpha + \beta) \quad (22)$$

where  $\alpha$  and  $\beta$  are the standard MSSM parameters and  $\gamma$  is the mixing angle that diagonalizes the neutral nu-Higgs mass-squared matrix. The decay width of the MSSM Higgs to charged nu-Higgs bosons then can be written as

$$\Gamma(H^0 \rightarrow \chi^+\chi^-) = \frac{g_{H^0\chi^+\chi^-}^2}{16\pi M_{H^0}} \sqrt{1 - \frac{4M_{\chi^+}^2}{M_{H^0}^2}}. \quad (23)$$

For example using an MSSM Higgs of 400 GeV and an charged nu-Higgs mass

of 100 GeV we calculate the production cross section of a pair of charged nu-Higgs bosons to be 14 fb assuming  $\cos(2\gamma) = 1$ . Since both of the charged nu-Higgs bosons will each decay into a charged lepton and neutrino, the collider signature will be two leptons (which generally can be different) and missing energy.

There are two backgrounds that we consider. The primary background is  $W$ -pair production with both  $W$  bosons decaying leptonically. We also consider  $t\bar{t}$  pair production as another possible background. Due to its large production cross section ( $\sim \mathcal{O}(100 \text{ pb})$ ) it is possible for  $t\bar{t}$  events to have both tops decay semi-leptonically and both  $b$ -quarks be missed by the detector because of too large rapidity or too small transverse momentum (i.e.  $\eta_b > 2.0$  and  $p_{T,b} < 20 \text{ GeV}$ , respectively).

We generated events for the signal and both of the backgrounds using the MadGraph/MadEvent program package [28] using the CTEQ6L parton distribution functions [29]. To simulate these events in a collider we apply the following acceptance and isolation cuts on the two final state leptons:

$$p_{T,\min} = 20 \text{ GeV}, \quad (24)$$

$$|\eta_e| < 2.4, \quad |\eta_\mu| < 2.1, \quad (25)$$

$$\Delta R = \sqrt{\Delta\eta^2 + \Delta\phi^2} > 0.4, \quad (26)$$

where  $\eta$  and  $\phi$  are the pseudorapidity and azimuthal angle of a final state lepton respectively. We also apply a 90% tagging efficiency for the leptons (electrons and muons). For the final state leptons we do not include taus because of the small 40% tau tagging efficiency and a relatively large light jet mis-tagging rate  $\sim \mathcal{O}(1\%)$  [30].

To extract the signal from our background we first require that there are two final state leptons that pass the acceptance and isolation cuts. This naturally reduces the number of  $t\bar{t}$  events. Because our final state particles decay from a heavy Higgs

boson, we expect that there should be a large amount of missing transverse energy from the two energetic neutrinos as well as a large total transverse mass from the high  $p_T$  leptons. We exploit this by requiring the missing transverse energy be greater than 90 GeV and the total transverse mass be greater than 250 GeV. Applying these collider cuts using the MadAnalysis program package [28] we obtain the results given in Table 4. With  $100 \text{ fb}^{-1}$  of integrated luminosity we obtain a statistical significance near  $3\sigma$  for both values of the charged nu-Higgs mass and a heavy MSSM Higgs mass of 400 GeV. For an MSSM Higgs of 300 GeV and charged nu-Higgs mass of 100 GeV we obtained a statistical significance over  $5\sigma$  due to the larger production cross section of the MSSM Higgs and larger branching fraction to a charged nu-Higgs pair. Note we did not assume any particular hierarchical structure of the neutrino masses. If we knew more specifically what the flavor distribution of the leptons in the charged nu-Higgs decay, it may be easier to extract the signal from backgrounds.

## 2.4 Phenomenology of The Nu-Higgsinos

### 2.4.1 Production

The nu-Higgsinos cannot be produced from decays of an MSSM Higgs, thus the primary production mechanism is through a Drell-Yan process. The charged nu-Higgsino pair is produced through a Drell-Yan process involving a  $\gamma$  or  $Z$  boson while the neutral nu-Higgsino pair can only be produced through a  $Z$ . Note that the  $Z$  will only couple to two different nu-Higgsinos, but since the two neutral nu-Higgsinos are degenerate this will effectively be a pair production mechanism. Associated production of a charged and neutral nu-Higgsino can occur through a Drell-Yan process involving the  $W$  bosons.

The LHC and Tevatron production cross sections of the above channels are calculated using the MadGraph/MadEvent software package [28] with the CTEQ6L

Cut	tagging: $2\ell, 0$ jets	$E_{T,\text{miss}} > 90$ GeV	$M_{TR} > 250$ GeV
$W^+W^-$	113000	1700	1300
$t\bar{t}$	610	160	160
$M_H = 400$ GeV $M_\chi = 100$ GeV	420	120	110
$\frac{S}{\sqrt{S+B}}$	$1.2 \pm 0.06$	$2.7 \pm 0.2$	$2.8 \pm 0.3$
$M_H = 300$ GeV $M_\chi = 100$ GeV	300	150	130
$\frac{S}{\sqrt{S+B}}$	$0.9 \pm 0.05$	$3.3 \pm 0.3$	$3.3 \pm 0.3$
$M_H = 400$ GeV $M_\chi = 150$ GeV	2200	400	210
$\frac{S}{\sqrt{S+B}}$	$6.5 \pm 0.1$	$8.4 \pm 0.4$	$5.1 \pm 0.3$

Table 4: Collider cuts used to extract the two lepton, two neutrino signal from  $\chi^+\chi^-$  production from the backgrounds considered. With  $100 \text{ fb}^{-1}$  of integrated luminosity we obtain a statistical significance over  $5\sigma$  for the  $M_H = 300$  GeV case and near  $3\sigma$  for  $M_H = 400$  GeV and both values of  $M_\chi$ . It is interesting to note that for the charged nu-Higgs of 150 GeV that even though the production cross section is smaller, the larger nu-Higgs yields events with larger missing energies and total transverse mass which allows more events to pass our collider cuts.

parton distribution functions [29]. Using center of mass energies of 14 and 7 TeV for the LHC and 2 TeV for the Tevatron we calculated the Higgsino pair production cross sections for Higgsino masses within the range of 100–500 GeV. The results are given in Fig 1. For the LHC, the  $\tilde{\chi}^+\tilde{\chi}^0$  pair has the largest production cross section. Note that the  $\tilde{\chi}^+\tilde{\chi}^0$  cross section is larger than the  $\tilde{\chi}^-/\tilde{\chi}^0$  production due to the valence up-quarks used in the former process as opposed to the valence down-quark in the latter. We also note the larger charged nu-Higgsino pair production cross section compared to the neutral nu-Higgsino production from the Drell-Yan process involving a photon.

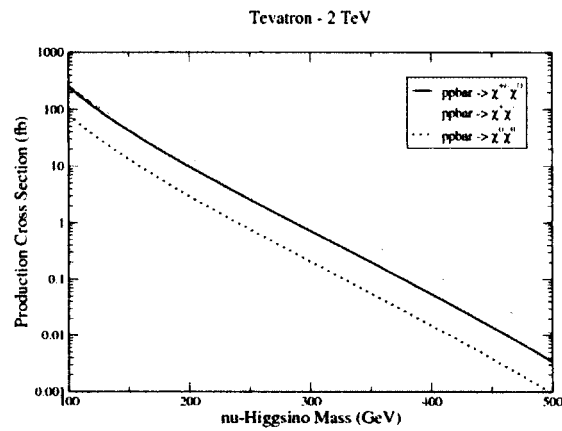
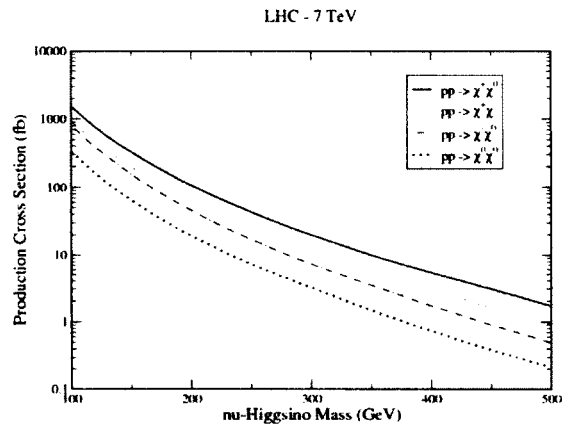
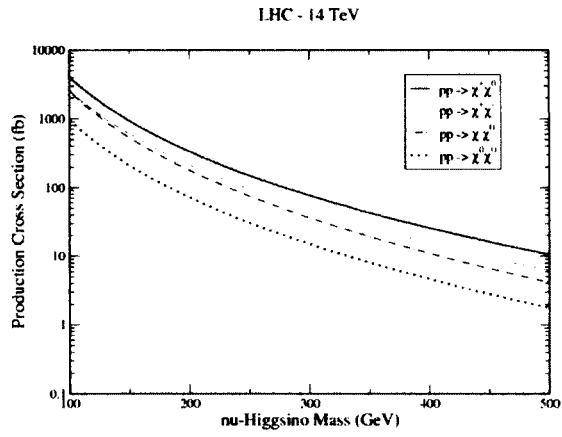


Figure 1: Production cross sections of various pairs of charged and neutral nu-Higgsinos (in fb) at the LHC with center of mass energies of (a) 14 TeV and (b) 7 TeV as well as the Tevatron with a center of mass energy of (c) 2 TeV.

### 2.4.2 Decays

We first discuss the detailed decays of the neutral and then the charged nu-Higgsinos. For simplicity, we will assume that the left and right handed sneutrinos have similar mass. The  $\tilde{\chi}^0$  decays into Branch A:  $\nu_R + \tilde{\nu}_L$  or Branch B:  $\nu_L + \tilde{\nu}_R$ . Since the mass of the neutrinos arises from the same Yukawa coupling term as this decay, the coupling is flavor diagonal and proportional to the mass.

Let us first consider Branch A. The left-handed sneutrino decays are well-studied in the MSSM. Here, we must choose a point in the mSUGRA parameter space. We will choose Snowmass point SPS-1a, which is one of the most studied to date. Using the results of Freitas et al. [31], we find that, for the normal hierarchy, the left-handed sneutrino decays into  $\tilde{B}\nu_L$  88% of the time, either  $\nu_L\tau^+\tau^-$  or  $\tilde{B}\nu_L\tau^+\tau^-$  7% of the time,  $\nu_L\tau^\pm\mu^\mp$  5% of the time, and has a negligible  $\mathcal{O}(0.2\%)$  decay into muon or electron pairs. For the inverted hierarchy, the left-handed sneutrino decays into  $\tilde{B}\nu_L$  88% of the time, either  $\nu_L\tau^+\tau^-$  or  $\tilde{B}\nu_L\tau^+\tau^-$  5% of the time,  $\nu_L\tau^\pm e^\mp$  5% of the time,  $\nu_L\tau^\pm\mu^\mp$  2% of the time, and also has a negligible  $\mathcal{O}(0.2\%)$  decay into muon or electron pairs. Since only 12% of the decays are visible in either hierarchy, the branch into the left-handed sneutrino is not as promising as for the other branch.

Let us now consider Branch B: The right-handed sneutrino decays have not been previously studied. Since there are no gauge interactions, and negligible mixing with MSSM fields, the only decays of the right-handed sneutrino are three-body decays via a virtual nu-Higgsino. One can have Branch B1:  $\nu_L\tilde{\chi}^{0*}$  or Branch B2:  $\ell\tilde{\chi}^{+*}$ , where the \* superscript indicates a virtual state. Branch B1 will give exactly the same flavor structure as Branch A, and thus we use those results. For Branch B2, however, the final state will **always** be visible, leading to the most interesting signatures.

Consider the normal hierarchy. The right handed sneutrino has a specific flavor,

and thus the flavor of the lepton in the decay leads to a muon 50% of the time and a tau 50% of the time (see Appendix A for a discussion). As before, the  $\tilde{\chi}^{+*}$  will decay with the same 50-50 split. Thus, one expects Branch B2 to give  $\mu\tilde{\mu}$ ,  $\mu\tilde{\tau}$ ,  $\tau\tilde{\mu}$  and  $\tau\tilde{\tau}$  each 25% of the time. For the inverted hierarchy, the flavor of the lepton in the decay of the right handed electron sneutrino is always that of an electron, and the decay of the right handed muon or tau sneutrino is into a muon 50% of the time, and tau 50% of the time. The  $\tilde{\chi}^{+*}$  also decays with the 50-25-25 split in flavor so that branch B2 in the inverse hierarchy yields  $e\tilde{e}$ ,  $e\tilde{\mu}$ ,  $e\tilde{\tau}$ ,  $\mu\tilde{e}$ ,  $\mu\tilde{\mu}$ ,  $\mu\tilde{\tau}$ ,  $\tau\tilde{e}$ ,  $\tau\tilde{\mu}$ , and  $\tau\tilde{\tau}$  with respective probabilities of 25%, 12.5%, 12.5%, 12.5%, 6.25%, 6.25%, 12.5%, 6.25%, and 6.25%. Finally, the slepton decays are given in Table 1 of Freitas et al. [31].

Putting all of these together, we find the decays of the  $\tilde{\chi}^0$  given in Table 5 and Table 6. We have only included decays whose branching ratios exceed 0.5%. Of course, each of the  $\tau$  leptons will decay 17% of the time into electrons and 17% of the time into muons.

$\tilde{\chi}^0$		$\tilde{\chi}^\pm$	
Signature	Branching Fraction	Signature	Branching Fraction
Invisible	66%	$(\tau^\pm)$	40%
$\tau^\pm\mu^\mp$	14%	$(\mu^\pm)$	23%
$\tau^\pm\tau^\mp$	12%	$(\mu^\pm)\tau^+\tau^-$	12%
$\mu^\pm\mu^\mp$	3.1%	$(\tau^\pm)\tau^+\tau^-$	8.2%
$\tau^\pm\tau^+\tau^-\mu^\mp$	2.0%	$(\tau^\pm)\mu^+\mu^-$	4.7%
$\tau^+\tau^-\mu^+\mu^-$	1.1%	$(\tau^\mp)(\mu^\pm\mu^\pm)$	2.9%
$\tau^+\tau^-\tau^+\tau^-$	0.94%	$(\mu^\pm)(\tau^\pm\tau^\pm)$	2.9%
		$(\mu^\pm)\mu^+\mu^-$	1.8%
		$(\tau^\pm)\tau^+\tau^-\mu^+\mu^-$	1.0%
		$(\mu^\pm)\tau^+\tau^-\tau^+\tau^-$	1.0%
		$(\mu^\pm)\mu^+\mu^-\tau^+\tau^-$	0.56%

Table 5: Decay branching fractions for the nu-Higgsinos assuming a normal hierarchy. For the charged nu-Higgsino, the lepton in parenthesis has the upper sign for  $\tilde{\chi}^+$  and the lower sign for  $\tilde{\chi}^-$ .

We now turn to the decays of the  $\tilde{\chi}^+$ . Here our work is already done from the discussion of Branch B2 above. The resulting branching ratios are given in Tables 5 and 6. Note that one can have single lepton, tri-lepton or penta-lepton decays.

$\tilde{\chi}^0$		$\tilde{\chi}^\pm$	
Signature	Branching Fraction	Signature	Branching Fraction
Invisible	66%	$(\tau^\pm)$	28%
$\tau^\pm e^\mp$	11%	$(e^\pm)$	23%
$\tau^+ \tau^-$	6.7%	$(\mu^\pm)$	11%
$\tau^\pm \mu^\mp$	5.1%	$(e^\pm) \tau^+ \tau^-$	5.9%
$e^+ e^-$	3.1%	$(\tau^\pm) e^+ e^-$	4.1%
$\mu^\pm e^\mp$	3.0%	$(\mu^\pm) \tau^+ \tau^-$	3.6%
$\tau^+ \tau^- e^+ e^-$	1.1%	$(e^\pm) e^+ e^-$	3.3%
$\tau^+ \tau^- \mu^\pm e^\mp$	1.1%	$(\tau^\mp) (e^\pm e^\pm)$	3.2%
$\tau^+ \tau^- e^\pm \tau^\mp$	1.0%	$(\tau^\pm) \tau^+ \tau^-$	2.9%
$\mu^+ \mu^-$	.91%	$(\mu^\pm) \tau^\pm e^\mp$	2.1%
		$(\mu^\pm) e^+ e^-$	1.7%
		$(e^\mp) (\tau^\pm \tau^\pm)$	1.1%
		$(e^\pm) e^+ e^- \tau^+ \tau^-$	1.1%
		$(\tau^\pm) \mu^+ \mu^-$	0.84%
		$(\mu^\mp) (e^\pm e^\pm)$	0.75%
		$(e^\pm) \mu^+ \mu^-$	0.69%
		$(\mu^\pm) e^+ e^- \tau^+ \tau^-$	0.52%
		$(\tau^\mp) (\mu^\pm \mu^\pm)$	0.51%
		$(\mu^\mp) (\tau^\pm \tau^\pm)$	0.51%
		$(\tau^\pm) e^+ e^- \tau^+ \tau^-$	0.50%

Table 6: Decay branching fractions of nu-Higgsinos assuming an inverted hierarchy. For the charged nu-Higgsino, the lepton in parenthesis has the upper sign for  $\tilde{\chi}^+$  and the lower sign for  $\tilde{\chi}^-$ .

### 2.4.3 Signatures

The high multiplicity of charged leptons in the nu-Higgsino decays gives some remarkable signatures. From pair production of the  $\tilde{\chi}^+ \tilde{\chi}^-$ , one can have very dramatic hexalepton and tetra-lepton events. Associated production of  $\tilde{\chi}^\pm$  with  $\tilde{\chi}^0$  leads to pentalepton events, and pair production of  $\tilde{\chi}^0 \tilde{\chi}^0$  leads to tetra-lepton events. The

production cross sections were given earlier.

$M_{\tilde{\chi}^\pm}$	Normal Hierarchy			Inverted Hierarchy		
	100 GeV	200 GeV	300 GeV	100 GeV	200 GeV	300 GeV
6 Leptons	260	26	5.1	240	24	4.8
0 $\tau$ 6 $\ell$	11	1.1	0.21	15	1.5	0.31
1 $\tau$ 5 $\ell$	17	1.7	0.35	20	2.0	0.39
2 $\tau$ 4 $\ell$	12	1.2	0.25	10	1.0	0.20
3 $\tau$ 3 $\ell$	4.6	0.46	0.092	2.5	0.25	0.050
4 $\tau$ 2 $\ell$	0.98	0.098	0.020	0.35	0.035	0.0070
5 $\tau$ 1 $\ell$	0.11	0.011	0.0020	0.024	0.0020	0.000
6 $\tau$ 0 $\ell$	0.0050	0.0010	0.000	0.0010	0.000	0.000

Table 7: Cross sections, in femtobarns, for hexalepton signatures for various values of the charged nu-Higgsino mass and for the two different neutrino mass hierarchies. The first line gives the total event rate into six leptons. For the other lines, we include the fact that leptonic  $\tau$  decays lead to additional  $\mu$ 's and  $e$ 's and that hadronic  $\tau$  decays are detected with a 40% efficiency. In the table  $\ell$  refers to either muons or electrons, and  $\tau$  refers to an identified hadronically decaying tau. The quoted cross sections are assuming a center of mass energy of 14 TeV at the LHC. A center of mass energy of 7 TeV reduces the cross section roughly by a factor of 3.

### *Hexalepton Events*

Perhaps the most dramatic events are hexalepton events which arise from the decay of a charged nu-Higgsino pair. From Tables 5 and 6, one can see that the  $\tilde{\chi}^\pm$  has three charged leptons in the decay 31 – 32% of the time, for either hierarchy, and thus the pair will yield six leptons roughly 10% of the time. Note that the production rate at the 14 TeV LHC for a light  $\tilde{\chi}^\pm$  pair can be as large as 2600 fb, leading to an enormous hexalepton rate of over 200 fb.

One will get a distribution of lepton flavors depending on the hierarchy. How robust are these results? If the  $\tilde{\chi}^\pm$  is lighter than the slepton or sneutrino, the flavor structure will not change - it simply means that the slepton or sneutrino is virtual,

thus these results won't change. We did choose a specific point in the mSUGRA parameter space, and that will change the flavor distribution, and thus these precise percentages should be taken with a grain of salt. Nonetheless, one does expect a huge production rate for hexalepton events if the  $\tilde{\chi}^\pm$  is not too heavy.

In Table 7, we have summarized the signatures as follows. In the first row, for both hierarchies and  $\tilde{\chi}^\pm$  masses of 100, 200, 300 GeV, we give the total production rate for hexalepton events. The tau's in the decays will either decay leptonically or hadronically. If they decay hadronically, roughly 40% will be identified. If they decay leptonically, they will be indistinguishable from a muon or an electron. In the remaining rows, we have listed the possible signatures, depending on the number of hadronic tau-identifications, weighted by the 40% factor. Since the electrons and muons are detected with virtually 100% efficiency, **all** of the decays listed in Table 7 are detectable.

One sees that each of the various signatures can be well within reach of the LHC, and some can have production cross sections of many tens of femtobarns. We assumed here that  $\sqrt{s} = 14$  TeV. If it is 7 TeV, then the above figures show that the production rates are lower by a factor of roughly 3. At the Tevatron, one can scale the results as shown in the production cross section figures. One might be able to extend the sensitivity by consider the explicit charges. For example, one combination in the normal hierarchy case would be  $\mu^+\mu^+\mu^+\mu^-\tau^-\tau^-$  which might have lower backgrounds compared with three charge pairs. Given the number of combinations, a detailed analysis of these possibilities would be premature. Note that the total rate of identified hexalepton events, for a  $\tilde{\chi}^\pm$  mass of 100 GeV is approximately 50 femtobarns at the LHC for  $\sqrt{s} = 14$  TeV and approximately 16 femtobarns for  $\sqrt{s} = 7$  TeV. At the Tevatron, the rate would be roughly 4 fb, leading to a couple of dozen events for the current integrated luminosity. Note that

the production rate at the Tevatron will drop more quickly with the  $\tilde{\chi}^\pm$  mass than the LHC.

$M_{\tilde{\chi}^\pm}$	Normal Hierarchy			Inverted Hierarchy		
	100 GeV	200 GeV	300 GeV	100 GeV	200 GeV	300 GeV
4 Leptons	580	57	11	570	56	11
0 $\tau$ 4 $\ell$	27	2.6	0.52	120	11	2.3
1 $\tau$ 3 $\ell$	43	4.2	0.83	140	14	2.7
2 $\tau$ 2 $\ell$	24	2.3	0.46	47	4.6	0.92
3 $\tau$ 1 $\ell$	5.5	0.53	0.11	7.2	0.71	0.14
4 $\tau$ 0 $\ell$	0.44	0.043	0.010	0.37	0.037	0.0070

Table 8: Cross sections, in femtobarns, for tetralepton signatures for various values of the charged nu-Higgsino mass and for the two different neutrino mass hierarchies. The first line gives the total event rate into four leptons. For the other lines, we include the fact that leptonic  $\tau$  decays lead to additional  $\mu$ 's and  $e$ 's and that hadronic  $\tau$  decays are detected with a 40% efficiency. In the table  $\ell$  refers to either muons or electrons, and  $\tau$  refers to an identified hadronically decaying tau. The quoted cross sections are assuming a center of mass energy of 14 TeV at the LHC. A center of mass energy of 7 TeV reduces the cross section roughly by a factor of 3.

Suppose hexalepton events are not detected? It could simply be that the charged nu-Higgsinos are too heavy, and thus failure to detect their decays would effectively place a lower limit on their mass. Could a 100 GeV charged nu-Higgsino evade detection? The choice of hierarchy and the choice of the particular mSUGRA point will affect the flavor distribution (which can thus affect the tau content of the events and thus the efficiency of detection), but those will not substantially affect the size of the signal. If the sneutrinos are heavy, this will also not affect the decays, unless they are so heavy that charged nu-Higgsino decays into a nu-Higgs plus the LSP can dominate, leading to only two leptons in the decay. Perhaps the simplest way to reduce the signal is to have the right-handed sneutrino be substantially heavier than the left-handed sneutrino, since the latter decays are much more likely to be invisible. Nonetheless, for most of parameter space, the charged nu-Higgsino mass

is the primary factor in the signal rate. Note also that, independent of any of these factors, failure to detect these events at the Tevatron would imply a lower bound on the necessary luminosity to detect them at the LHC, as one can read off from the production cross sections.

### *Tetralepton and Pentalepton Events*

$\tilde{\chi}^\pm$  pair production can also lead to tetra-lepton events, as well as  $\tilde{\chi}^0$  pair production. In Table 8, we have listed the total production rate, as well as the various signatures, for these events. Finally, associated production from a  $W$  will lead to pentalepton events, and these are also shown in Table 9.

The cross sections are larger than for hexalepton events, however backgrounds will also be larger. For example, a tetralepton signature of  $\mu^+\mu^-e^+e^-$  would have backgrounds from real or virtual  $\gamma$ 's and  $Z$ 's. One would expect the pentalepton signature to have smaller backgrounds, and yet the cross sections are still much larger. They are much more sensitive to the flavor distribution, as one can see in the table. It may very well be that the pentalepton signatures will be the most sensitive. The cross sections are somewhat lower than for tetraleptons, but one would expect the backgrounds to be substantially lower. The hexaleptons are more dramatic, with even smaller backgrounds, but the cross sections are substantially higher for the pentalepton events.

How sensitive is the Tevatron? Consider a nu-Higgsino mass of 200 GeV. The cross section for pentaleptons at the LHC for  $\sqrt{s} = 14$  TeV is approximately 50 fb, as seen in Table 9. Comparing cross sections between Figure 1a and 1c, one sees that the cross section at the Tevatron is roughly a factor of 50 smaller, giving a cross section of only 1 fb. Thus, with  $8 \text{ fb}^{-1}$  integrated luminosity, one would

expect 8 events, **if and only if** all  $\tau$ 's could be identified. Obviously, they can't, and Table 9 shows that events with five non-taus occur at a rate of roughly 20% of the total. Of course, we have not done a detailed analysis. Some hadronic  $\tau$ 's would be identified, and some of the leptons might not be identified (some would not have enough transverse momentum, for example). Although we are not aware of any backgrounds that large, a full simulation should be carried out. It does appear that a lower bound of approximately 200 GeV on the nu-Higgsino masses could be obtained at the Tevatron. Certainly, at a mass of 100 GeV, the event rate is a factor of 10-20 larger and detection should be straightforward.

$M_{\tilde{\chi}^\pm}$	Normal Hierarchy			Inverted Hierarchy		
	100 GeV	200 GeV	300 GeV	100 GeV	200 GeV	300 GeV
5 Leptons	770	64	13	600	50	10
0 $\tau$ 5 $\ell$	29	2.4	0.50	110	9.0	1.8
1 $\tau$ 4 $\ell$	49	4.1	0.84	100	8.3	1.7
2 $\tau$ 3 $\ell$	36	3.0	0.61	41	3.4	0.69
3 $\tau$ 2 $\ell$	12	0.97	0.20	8.9	0.74	0.15
4 $\tau$ 1 $\ell$	1.8	0.15	0.031	0.76	0.063	0.013
5 $\tau$ 0 $\ell$	0.11	0.0090	0.0020	0.015	0.0010	0.000

Table 9: Cross sections, in femtobarns, for pentalepton signatures for various values of the charged nu-Higgsino mass and for the two different neutrino mass hierarchies. The first line gives the total event rate into five leptons. For the other lines, we include the fact that leptonic  $\tau$  decays lead to additional  $\mu$ 's and  $e$ 's and that hadronic  $\tau$  decays are detected with a 40% efficiency. In the table  $\ell$  refers to either muons or electrons, and  $\tau$  refers to an identified hadronically decaying tau. The quoted cross sections are assuming a center of mass energy of 14 TeV at the LHC. A center of mass energy of 7 TeV reduces the cross section roughly by a factor of 3.

## 2.5 Conclusion

The discovery of nonzero neutrino masses has led to a new type of two Higgs doublet model in which a second Higgs doublet couples only to the lepton doublets and

right-handed neutrinos, leading to Dirac neutrino masses. We consider a supersymmetrized version of this model, which thus contains four Higgs doublets. A global symmetry which is only very weakly broken prevents substantial mixing between the additional doublets, called nu-Higgs multiplets, and the MSSM Higgs sector.

We study two aspects of the phenomenology of these new states. For the scalar nu-Higgs fields, a new production mechanism leads to the possibility of a  $5\sigma$  detection with  $100 \text{ fb}^{-1}$  of integrated luminosity. The second aspect contains extremely exciting possibilities. For the nu-Higgsino states, we find remarkable phenomenological signatures. The most dramatic of these signatures are hexalepton events, which contain six charged leptons and missing energy and which are produced with a cross section of up to  $250 \text{ fb}$  for a nu-Higgsino mass of  $100 \text{ GeV}$ . Many of these leptons are tau's, and when we fold in the 40% detection efficiency, we find roughly 50, 5, 1 fb cross sections for events in which all six leptons can be identified for nu-Higgsino masses of 100, 200, 300 GeV respectively. For  $\sqrt{s} = 7 \text{ TeV}$ , these numbers are lower by a factor of three, and for the Tevatron are lower by another factor of four. Thus, this model gives the exciting possibility of substantial multi-lepton events which can be detected at the LHC and may, for lower nu-Higgsino masses, be detectable at the Tevatron.

# CHAPTER 3

## 3 The Supersymmetric Leptophilic Higgs

### Model \*

#### 3.1 Introduction

The main purpose of the Large Hadron Collider (LHC) is the study of the mechanism of electroweak symmetry breaking (EWSB). As discussed previously, the 2HDM is among the simplest and most studied extensions of the Standard Model. It achieves EWSB via two scalar Higgs doublets that receive vevs. In order to avoid unobserved tree-level flavor changing neutral currents (FCNCs), all fermions with the same quantum numbers (and which are thus capable of mixing) must couple to the same Higgs multiplet. The Glashow-Weinberg theorem [14] states that a necessary and sufficient condition for the absence of FCNCs at tree-level is that all fermions of a given charge and helicity transform according to the same irreducible representation of  $SU(2)$ , correspond to the same eigenvalue of  $T_3$ , and that a basis exists in which they receive their contributions in the mass matrix from a single source. In the 2HDM, this is due to the introduction of discrete or continuous symmetries. Generally one may either take both up and down type quarks to couple to the same doublet or have each couple to its own doublet. It is usually assumed

---

\*This chapter was previously published in Reference [32].

that the leptons couple to the same doublet as the down type quarks, in which case the former scenario describes the Type I 2HDM while the latter describes the Type II 2HDM. Such couplings can be enforced by imposing a suitable  $\mathbb{Z}_2$  symmetry, which may simply be imposed *ad hoc* or which may arise as a subgroup of a continuous symmetry (as in Peccei-Quinn or supersymmetric models).

Despite the traditional convention that leptons couple to the same doublet as the down type quarks, there is no a priori reason why this must be the case. An alternative possibility is that both the up and down type quarks couple to one doublet while the leptons couple to the remaining doublet. While the traditional 2HDMs have received a great deal of attention, relatively little work has been done in investigating this alternative possibility. Those who have focused on this model [33, 34, 66, 36, 37] have referred to it by several names, our selection of which is the Leptophilic Two Higgs Doublet Model (L2HDM). As noted by Su and Thomas [33], the consequences of a L2HDM could drastically alter the possible detection channels for a light Higgs at the LHC, so it is important that it be considered as incoming data begins to arrive. Furthermore, the possibility of substantially enhanced leptonic couplings (which can only occur in leptophilic models) may shed some insight into explaining recent experimental results from PAMELA, Fermi LAT, and H.E.S.S. [66].

There also remain alternative possibilities. One can couple the up-type quarks and leptons to one Higgs doublet and the down-type quarks to the other (referred to as the “flipped” model [38]) or one can couple all of the charged fermions to one doublet and the right-handed neutrino to another (referred to as the “neutrino-specific” model) [39]. While interesting in their own right, these models do not offer the possibility of substantially enhanced leptonic couplings, and we will not focus on them.

The most popular extension of the Standard Model is supersymmetry, which can solve the hierarchy problem and which has a very tightly constrained Higgs sector. Thus, one is led to consider the supersymmetric versions of these alternative 2HDM models. Recently, with McCaskey, we considered [20] the supersymmetric version of the “neutrino-specific” model, and found some remarkable signatures, including pentalepton and hexalepton events with very high rates at the Tevatron and the LHC. In this work, we extend the L2HDM to incorporate supersymmetry. The resulting Supersymmetric Leptophilic Higgs Model (SLHM) leads to exciting phenomenological prospects. In the scalar sector, the strong constraints on the Higgs potential will substantially alter the phenomenology of the lightest Higgs boson, since decays to leptons can be substantially enhanced, and the decrease in the coupling to the gauge bosons means that the current LEP bounds will not apply, and much lighter Higgs bosons can be tolerated. In addition, the supersymmetric partners to the leptons and the leptonic Higgs doublet are influenced by the unusual Yukawa structure. In the case of R-parity violation, the lightest supersymmetric particle (LSP) could decay into leptons. Without R-parity violation the LSP might annihilate into leptons [66]. In this thesis, we will focus on the scalar sector, since the results may be testable in the very near future at the Tevatron.

The layout of this chapter is as follows. In Section 3.2 we review the setup of the L2HDM. In Section 3.3 we introduce the SLHM and calculate the scalar mass matrices. In Section 3.4 we consider various constraints on the model’s parameter space by focusing on the neutral scalar sector. By combining results from Yukawa coupling perturbativity considerations, unitarity requirements, and direct searches for Higgs bosons at LEP, we obtain severe restrictions on the model’s parameter space. In Section 3.5 we discuss the phenomenology of the lightest and next-to-lightest Higgs bosons at the Tevatron and the LHC, and then in Section 3.6, we

conclude.

### 3.2 The Leptophilic Two Higgs Doublet Model

The L2HDM contains two scalar  $SU(2)_L$  doubles  $\Phi_q$  and  $\Phi_\ell$ . A discrete  $\mathbb{Z}_2$  symmetry is imposed under which  $\Phi_\ell \rightarrow -\Phi_\ell$  and  $e_{R_i} \rightarrow -e_{R_i}$ , but all other fields are invariant. The resulting Yukawa lagrangian is given by

$$\mathcal{L}_Y = -\left\{ Y_{ij}^{u\bar{u}} \tilde{\Phi}_q^\dagger \cdot Q_{L_j} + Y_{ij}^{d\bar{d}} \tilde{\Phi}_q^\dagger \cdot Q_{L_j} + Y_{ij}^{\ell\bar{e}} \Phi_\ell^\dagger \cdot E_{L_j} + \text{h.c.} \right\}, \quad (27)$$

where

$$Q_{L_i} = \begin{pmatrix} u_{L_i} \\ d_{L_i} \end{pmatrix}, \quad E_{L_i} = \begin{pmatrix} \nu_{L_i} \\ e_{L_i} \end{pmatrix}, \quad \text{and} \quad \Phi_X = \begin{pmatrix} \phi_X^+ \\ \frac{1}{\sqrt{2}}(v_X + \phi_{Xr}^0 + i\phi_{Xi}^0) \end{pmatrix}$$

for  $X = q, \ell$  and  $\tilde{\Phi}_q = i\sigma_2 \Phi_q$ . The Higgs sector potential is given by [33, 40]

$$\begin{aligned} V = & m_q^2 |\Phi_q|^2 + m_\ell^2 |\Phi_\ell|^2 + \left( m_{q\ell}^2 \Phi_q^\dagger \Phi_\ell + \text{h.c.} \right) + \frac{\lambda_1}{2} |\Phi_q|^4 + \frac{\lambda_2}{2} |\Phi_\ell|^4 \\ & + \lambda_3 |\Phi_q|^2 |\Phi_\ell|^2 + \lambda_4 |\Phi_q^\dagger \Phi_\ell|^2 + \frac{\lambda_5}{2} \left[ (\Phi_q^\dagger \Phi_\ell)^2 + \text{h.c.} \right]. \end{aligned} \quad (28)$$

The physical scalars consist of two neutral scalars  $h$  and  $H$ , a pseudoscalar  $\chi^0$ , and a charged pair  $H^\pm$ . The other three degrees of freedom are the Goldstone bosons  $G^\pm$  and  $G^0$ , which are eaten by the  $W^\pm$  and  $Z^0$  respectively. If one defines the mixing angle  $\tan \beta = v_q/v_\ell$ , the physical charged scalars can be expressed as

$$\begin{pmatrix} G^+ \\ H^+ \end{pmatrix} = \begin{pmatrix} \cos \beta & \sin \beta \\ -\sin \beta & \cos \beta \end{pmatrix} \begin{pmatrix} \Phi_\ell^+ \\ \Phi_q^+ \end{pmatrix}. \quad (29)$$

The physical neutral scalar states are expressed in terms of the mixing angle  $\tan \alpha$ ,

which can be solved for in terms of the entries of the neutral scalar mass-squared matrix  $\tan 2\alpha = 2M_{12}^2/(M_{11}^2 - M_{22}^2)$ . One then finds the following relation

$$\begin{pmatrix} H \\ h \end{pmatrix} = \sqrt{2} \begin{pmatrix} \cos \alpha & \sin \alpha \\ -\sin \alpha & \cos \alpha \end{pmatrix} \begin{pmatrix} \phi_{\ell r}^0 - v_\ell \\ \phi_{qr}^0 - v_q \end{pmatrix}. \quad (30)$$

The vertex factors for the couplings between the charged scalar and fermions are given by [34]

$$\begin{aligned} H^+ u_i d_j &\rightarrow \left( \frac{ig \cot \beta}{2\sqrt{2}M_W} \right) V_{ij} [(m_{u_i} - m_{d_j}) - (m_{u_i} + m_{d_j})\gamma_5], \\ H^+ \nu_i e_i &\rightarrow \left( \frac{ig \tan \beta}{2\sqrt{2}M_W} \right) m_{e_i} (1 - \gamma_5). \end{aligned} \quad (31)$$

For large  $\tan \beta$  the neutrino-lepton coupling to  $H^+$  is magnified while the quarks' coupling to  $H^+$  is diminished. The neutral scalar couplings to the charged leptons will similarly be magnified. An interesting feature of the model is that  $\tan \beta$  can be much larger than in the conventional 2HDMs without causing problems with perturbativity and unitarity, since the Standard Model leptonic couplings are smaller than the quark couplings.

### 3.3 The Supersymmetric Leptophilic Higgs Model

In this section we introduce the minimal leptophilic model required to incorporate supersymmetry. A SLHM will require a minimum of four Higgs doublets in order to achieve anomaly cancelation. Therefore, we add to the MSSM two Higgs doublets  $H_0$  and  $H_\ell$  with weak hypercharge assignments  $+1/2$  and  $-1/2$  respectively. The four Higgs doublets along with their weak hypercharges are listed in the table.

$\Phi$	$H_u$	$H_d$	$H_0$	$H_\ell$
$U_Y(1)$	$+1/2$	$-1/2$	$+1/2$	$-1/2$

The scalar doublets  $H_u$  and  $H_d$  are responsible for giving mass to the up and down quarks respectively. We refer to these doublets as the quark friendly doublets. Of the new doublets, the lepton friendly doublet  $H_\ell$  gives mass to the leptons, while the remaining inert doublet  $H_0$  does not couple to quarks or leptons. This Yukawa structure is enforced by a discrete  $\mathbb{Z}_2$  symmetry, under which the superfields  $E$ ,  $H_0$ , and  $H_\ell$  transform as  $X \rightarrow -X$  while all other fields remain unchanged. The most general superpotential respecting R-parity, gauge symmetry, and the  $\mathbb{Z}_2$  symmetry is

$$W = y_u U Q H_u - y_d D Q H_d - y_\ell E L H_\ell + \tilde{\mu}_1 H_u H_d + \tilde{\mu}_2 H_0 H_\ell. \quad (32)$$

The  $\mathbb{Z}_2$  symmetry is softly broken by the terms  $(\mu_3^2 H_u H_\ell + \mu_4^2 H_0 H_d + \text{h.c.})$  contained in the Higgs sector soft SUSY breaking potential  $V_{\text{Soft}}$  given by

$$V_{\text{Soft}} = \mu_u^2 |H_u|^2 + \mu_d^2 |H_d|^2 + \mu_0^2 |H_0|^2 + \mu_\ell^2 |H_\ell|^2 \\ + \left( \mu_1^2 H_u H_d + \mu_2^2 H_0 H_\ell + \mu_3^2 H_u H_\ell + \mu_4^2 H_0 H_d + \text{h.c.} \right).$$

The Higgs sector potential is given by the sum of the F-terms, D-terms, and  $V_{\text{Soft}}$  respectively

$$V = \sum_{i=1}^k \left| \frac{\partial W}{\partial H_i} \right|^2 + \frac{1}{2} \sum_a \left| \sum_{i=1}^k g^a H_i^\dagger T^a H_i \right|^2 + V_{\text{Soft}}.$$

Expanding the above expression results in

$$V = m_u^2 |H_u|^2 + m_d^2 |H_d|^2 + m_0^2 |H_0|^2 + m_\ell^2 |H_\ell|^2 \\ + (\mu_1^2 H_u H_d + \mu_2^2 H_0 H_\ell + \mu_3^2 H_u H_\ell + \mu_4^2 H_0 H_d + \text{h.c.}) \\ + \frac{g_1^2}{8} \sum_a \left| H_u^\dagger \sigma^a H_u + H_d^\dagger \sigma^a H_d + H_0^\dagger \sigma^a H_0 + H_\ell^\dagger \sigma^a H_\ell \right|^2 \\ + \frac{g_2^2}{8} \left| |H_u|^2 - |H_d|^2 + |H_0|^2 - |H_\ell|^2 \right|^2,$$

where  $m_u^2 = (|\tilde{\mu}_1|^2 + \mu_u^2)$ ,  $m_d^2 = (|\tilde{\mu}_1|^2 + \mu_d^2)$ ,  $m_0^2 = (|\tilde{\mu}_2|^2 + \mu_0^2)$ ,  $m_\ell^2 = (|\tilde{\mu}_2|^2 + \mu_\ell^2)$ , and  $\sigma^a$  ( $a = 1, 2, 3$ ) are the Pauli matrices. To achieve spontaneous symmetry breaking, the Higgs doublets acquire the following vevs:

$$\begin{aligned} \langle H_u \rangle &= \frac{1}{\sqrt{2}} \begin{pmatrix} 0 \\ v_u \end{pmatrix}, & \langle H_d \rangle &= \frac{1}{\sqrt{2}} \begin{pmatrix} v_d \\ 0 \end{pmatrix}, \\ \langle H_0 \rangle &= \frac{1}{\sqrt{2}} \begin{pmatrix} 0 \\ v_0 \end{pmatrix}, & \langle H_\ell \rangle &= \frac{1}{\sqrt{2}} \begin{pmatrix} v_\ell \\ 0 \end{pmatrix}. \end{aligned} \tag{33}$$

We define  $v^2 = v_u^2 + v_d^2 + v_0^2 + v_\ell^2$  so that we have  $v^2 = 4M_Z^2/(g_1^2 + g_2^2) \approx (246 \text{ GeV})^2$ . Between the quark friendly doublets we define the mixing angle  $\tan \beta = v_u/v_d$  while between the lepton friendly and inert doublets we define the mixing angle  $\tan \beta_\ell = v_0/v_\ell$ . We also define  $\tan \alpha = v_q/v_L$ , where  $v_q^2 = v_u^2 + v_d^2$  and  $v_L^2 = v_0^2 + v_\ell^2$ . These definitions allow us to express the individual vevs in terms of the Standard Model vev and the three mixing angles  $\alpha$ ,  $\beta$ , and  $\beta_\ell$

$$v_u = v \sin \alpha \sin \beta, \quad v_d = v \sin \alpha \cos \beta, \quad v_0 = v \cos \alpha \sin \beta_\ell, \quad v_\ell = v \cos \alpha \cos \beta_\ell. \tag{34}$$

Each of the four complex Higgs doublets contains four real degrees of freedom, so there are a total of sixteen degrees of freedom. Three of these are eaten to give mass to the  $W^\pm$  and  $Z^0$ , while those remaining result in a scalar mass spectrum that includes four neutral scalars, three pseudoscalars, and three charged pairs. From the scalar potential above, the mass matrices can be calculated. We parameterize them in terms of the gauge boson masses and the three mixing angles appearing in equation 34.

The neutral scalar mass matrix is  $M_N^2 =$

$$\begin{pmatrix} M_1^2 & -\frac{1}{2}M_Z^2 s_\alpha^2 s_{2\beta} - \mu_1^2 & \frac{1}{2}M_Z^2 s_{2\alpha} s_\beta s_{\beta_\ell} & -\frac{1}{2}M_Z^2 s_{2\alpha} s_\beta c_{\beta_\ell} - \mu_3^2 \\ -\frac{1}{2}M_Z^2 s_\alpha^2 s_{2\beta} - \mu_1^2 & M_2^2 & -\frac{1}{2}M_Z^2 s_{2\alpha} c_\beta s_{\beta_\ell} - \mu_4^2 & \frac{1}{2}M_Z^2 s_{2\alpha} c_\beta c_{\beta_\ell} \\ \frac{1}{2}M_Z^2 s_{2\alpha} s_\beta s_{\beta_\ell} & -\frac{1}{2}M_Z^2 s_{2\alpha} c_\beta s_{\beta_\ell} - \mu_4^2 & M_3^2 & -\frac{1}{2}M_Z^2 c_\alpha^2 s_{2\beta_\ell} - \mu_2^2 \\ -\frac{1}{2}M_Z^2 s_{2\alpha} s_\beta c_{\beta_\ell} - \mu_3^2 & \frac{1}{2}M_Z^2 s_{2\alpha} c_\beta c_{\beta_\ell} & -\frac{1}{2}M_Z^2 c_\alpha^2 s_{2\beta_\ell} - \mu_2^2 & M_4^2 \end{pmatrix}$$

where  $s_x$  and  $c_x$  are shorthand for  $\sin x$  and  $\cos x$  respectively, and the diagonal terms are given by

$$\begin{aligned} M_1^2 &= M_Z^2 \sin^2 \alpha \sin^2 \beta + \lambda_1, & \lambda_1 &= \mu_1^2 \cot \beta + \mu_3^2 \cot \alpha \left( \frac{\cos \beta_\ell}{\sin \beta} \right), \\ M_2^2 &= M_Z^2 \sin^2 \alpha \cos^2 \beta + \lambda_2, & \lambda_2 &= \mu_1^2 \tan \beta + \mu_4^2 \cot \alpha \left( \frac{\sin \beta_\ell}{\cos \beta} \right), \\ M_3^2 &= M_Z^2 \cos^2 \alpha \sin^2 \beta_\ell + \lambda_3, & \lambda_3 &= \mu_2^2 \cot \beta_\ell + \mu_4^2 \tan \alpha \left( \frac{\cos \beta}{\sin \beta_\ell} \right), \\ M_4^2 &= M_Z^2 \cos^2 \alpha \cos^2 \beta_\ell + \lambda_4, & \lambda_4 &= \mu_2^2 \tan \beta_\ell + \mu_3^2 \tan \alpha \left( \frac{\sin \beta}{\cos \beta_\ell} \right). \end{aligned}$$

The pseudoscalar mass matrix is

$$M_A^2 = \begin{pmatrix} \lambda_1 & \mu_1^2 & 0 & \mu_3^2 \\ \mu_1^2 & \lambda_2 & \mu_4^2 & 0 \\ 0 & \mu_4^2 & \lambda_3 & \mu_2^2 \\ \mu_3^2 & 0 & \mu_2^2 & \lambda_4 \end{pmatrix}. \quad (35)$$

The charged scalar mass matrix is

$$M_{H^\pm}^2 = M_A^2 + \Delta M^2, \quad (36)$$

where

$$\Delta M^2 = M_W^2 \begin{pmatrix} s_\alpha^2 c_\beta^2 + c_\alpha^2 c_{2\beta_\ell} & \frac{1}{2} s_\alpha^2 s_{2\beta} & \frac{1}{2} s_{2\alpha} s_\beta s_{\beta_\ell} & \frac{1}{2} s_{2\alpha} s_\beta c_{\beta_\ell} \\ \frac{1}{2} s_\alpha^2 s_{2\beta} & s_\alpha^2 s_\beta^2 - c_\alpha^2 c_{2\beta_\ell} & \frac{1}{2} s_{2\alpha} c_\beta s_{\beta_\ell} & \frac{1}{2} s_{2\alpha} c_\beta c_{\beta_\ell} \\ \frac{1}{2} s_{2\alpha} s_\beta s_{\beta_\ell} & \frac{1}{2} s_{2\alpha} c_\beta s_{\beta_\ell} & c_\alpha^2 c_{\beta_\ell}^2 + s_\alpha^2 c_{2\beta} & \frac{1}{2} c_\alpha^2 s_{2\beta_\ell} \\ \frac{1}{2} s_{2\alpha} s_\beta c_{\beta_\ell} & \frac{1}{2} s_{2\alpha} c_\beta c_{\beta_\ell} & \frac{1}{2} c_\alpha^2 s_{2\beta_\ell} & c_\alpha^2 s_{\beta_\ell}^2 - s_\alpha^2 c_{2\beta} \end{pmatrix}.$$

In Section 3.3 of [41] Gupta and Wells outline a procedure for obtaining an upper bound on the tree-level mass of the lightest neutral scalar,  $h$ , in the limit of large SUSY breaking masses (as compared to the  $Z$ -mass). The procedure consists of transforming the mass matrices into the so called ‘‘Runge basis,’’ in which one doublet obtains all of the vev while the others are orthogonal to one another. Details on the Runge basis can be found in [42]. In this basis all but one diagonal entry of the neutral scalar mass matrix grow large in the limit of large SUSY breaking masses. This entry acts as an upper bound on  $M_h^2$  since, for a positive definite matrix, the smallest eigenvalue is bounded above by the smallest diagonal entry. Their result holds in our case as well and results in the inequality

$$M_h \leq M_Z |\sin^2 \alpha \cos 2\beta + \cos^2 \alpha \cos 2\beta_\ell|. \quad (37)$$

Leading order radiative corrections to the Higgs masses will be important in constraining parameter space. As usual, the dominant contributions come from top quark loops, governed by the top quark Yukawa coupling. In this section we have written the neutral scalar mass matrix,  $M_N^2$ , in the  $\{u, d, 0, \ell\}$  basis. Hence the 1-1 entry receives a correction from top quark loop diagrams given by

$$\Delta M_{11}^2 = \frac{3\alpha}{\pi} \left( \frac{m_t^4}{M_Z^2} \right) \frac{\ln(m_t^2/m_t^2)}{\sin^2 2\theta_W \sin^2 \alpha \sin^2 \beta}, \quad (38)$$

where  $m_{\tilde{t}}$  is the stop squark mass, which we take to be  $\sim 1$  TeV. In addition to top quark loop corrections, other corrections are potentially significant because of the possibility of very large values for  $\tan\beta$  and  $\tan\beta_\ell$ . We therefore also consider the leading correction to the 2-2 and 4-4 entries of  $M_N^2$ , which come from bottom quark loop diagrams and a tau loop diagram respectively. The 3-3 entry receives no correction since the inert doublet,  $H_0$ , does not couple to quarks or leptons. There are other sub-leading-log corrections to the masses, and these can contribute 5 – 10 GeV to the masses (see Ref. [43] for a detailed discussion).

### 3.4 Constraints on The Supersymmetric Leptophilic Higgs Model

In this section we outline the main constraints that limit the viable parameter space of the SLHM. The free parameters arising from the scalar sector consist of the four couplings  $\mu_1^2$ ,  $\mu_2^2$ ,  $\mu_3^2$ , and  $\mu_4^2$ , which mix pairs of Higgs doublets in the scalar potential, as well as the three mixing angles  $\tan\alpha$ ,  $\tan\beta$ , and  $\tan\beta_\ell$ , which appear in equation 34. The constraints arising from the charged scalar sector are similar to those of the L2HDM, which is studied in [34]. Our interest therefore lies in the neutral sector. We find that LEP data and other constraints severely restrict the size of the allowable parameter space, but leave enough room to comfortably fit the model a lightest neutral scalar mass substantially less than 110 GeV.

#### 3.4.1 Yukawa Coupling Perturbativity

The first constraints come from requiring that the Yukawa couplings remain perturbative. By demanding that each Yukawa coupling remains smaller than  $4\pi$  we

obtain the following three inequalities

$$\begin{aligned}
\left(1 + \frac{1}{\tan^2 \alpha}\right) \left(1 + \frac{1}{\tan^2 \beta}\right) &< \frac{8\pi^2 v^2}{m_t^2} \approx 13^2, \\
\left(1 + \frac{1}{\tan^2 \alpha}\right) \left(1 + \tan^2 \beta\right) &< \frac{8\pi^2 v^2}{m_b^2} \approx 520^2, \\
\left(1 + \tan^2 \alpha\right) \left(1 + \tan^2 \beta_\ell\right) &< \frac{8\pi^2 v^2}{m_\tau^2} \approx 1235^2.
\end{aligned} \tag{39}$$

One can see that the top quark Yukawa coupling becomes non-perturbative for small values of  $\tan \alpha$  or  $\tan \beta$  while the bottom quark Yukawa coupling does so for small values of  $\tan \alpha$  or large values of  $\tan \beta$ . In addition, the tau Yukawa coupling becomes non-perturbative for large values of  $\tan \alpha$  or  $\tan \beta_\ell$ .

### 3.4.2 Tree Level Unitarity

Requiring perturbative unitarity of fermion anti-fermion scattering places upper bounds on the fermion masses. The unitarity condition that must be satisfied is  $|\Re(a_J)| \leq 1/2$ , where  $a_J$  is the  $J$ th partial wave amplitude in the partial wave expansion of the fermion anti-fermion scattering amplitude. The scattering we consider occurs by the exchange of a Higgs boson. We obtain bounds from imposing the unitarity condition on the  $J = 0$  partial wave amplitude, which is calculated from a sum over s- and t-channel helicity amplitudes in the high energy limit. The procedure is described in detail in [44], where contributions to the partial wave amplitudes are provided for a general model. These contributions depend on combinations of the vector and axial vector Yukawa couplings. For the SLHM the resultant bounds

are found to be (see [44] for a clear discussion)

$$\begin{aligned}
\frac{G_F m_t^2}{4\pi\sqrt{2}} &< \sin^2 \alpha \sin^2 \beta, \\
\frac{G_F m_b^2}{4\pi\sqrt{2}} &< \sin^2 \alpha \cos^2 \beta, \\
\frac{G_F m_\tau^2}{4\pi\sqrt{2}} &< \cos^2 \alpha \cos^2 \beta_\ell.
\end{aligned}
\tag{40}$$

Here we have used the bounds obtained for third generation fermions as their larger masses yield the most stringent results. The unitarity constraint prevents very large values for  $\tan \beta$ , capping it at around 300. Several combinations of  $\tan \alpha$  and  $\tan \beta$  values on the order of several tenths are also eliminated.

### 3.4.3 The Anomalous Muon Magnetic Moment

As in the Standard Model, the magnetic moment of the muon receives a contribution from the one-loop diagram formed by connecting the muon lines on a muon-muon-photon vertex with a neutral Higgs boson. Only the lightest neutral Higgs is relevant since the contribution goes as the square of the ratio between the muon and Higgs masses. For the SLHM the contribution is

$$\Delta a_\mu = K^2 \frac{m_\mu^2}{8\pi^2 v^2} \int_0^1 \frac{z^2(2-z)}{z^2 + x^2(1-z)} dz,
\tag{41}$$

where  $x = M_h/m_\mu$  and

$$K^2 = \frac{|U_{41}|^2}{\cos^2 \alpha \cos^2 \beta_\ell}.$$

If the Higgs mass,  $M_h$ , is assumed to be the same in the SLHM and the Standard Model then the contribution to the muon's magnetic moment from a light scalar in the SLHM is simply its Standard Model value multiplied by  $K^2$ . The value of  $K^2$  however, remains  $\lesssim 1$  across the entire spectrum of parameter space, even for very

large values of  $\tan \alpha$  and  $\tan \beta_\ell$ . A review on the anomalous muon magnetic moment is given by [45] while current results and uncertainties can be found in [46, 47]. In our case the contribution is much too small to produce any bounds.

In addition however, there is a two-loop Barr-Zee effect [48], which is generally more significant than the one-loop contribution discussed above. The Barr-Zee effect occurs by connecting an internal Higgs to an internal photon through a massive fermion loop and is given by [49, 50]. We consider such effects with third generation fermions in the SLHM and find that the contribution to the muon magnetic moment is

$$\Delta a_\mu = -\frac{\alpha m_\mu^2 U_{41}}{4\pi^3 v^2 \cos \beta_\ell} \left\{ \frac{8U_{11}f(x_t)}{3 \sin 2\alpha \sin \beta} + \frac{2U_{21}f(x_b)}{3 \sin 2\alpha \cos \beta} + \frac{U_{41}f(x_\tau)}{\cos^2 \alpha \cos \beta_\ell} \right\}, \quad (42)$$

where  $x_f = m_f^2/M_h^2$  and the function  $f(x)$  is given by

$$f(x) = \frac{x}{2} \int_0^1 \frac{1 - 2z(1-z)}{z(1-z) - x} \ln \left[ \frac{z(1-z)}{x} \right] dz.$$

Though the contribution from the tau loop diagram is suppressed by  $m_\tau^2/M_h^2$ , it is enhanced for very large  $\tan \beta_\ell$ . In following [51] we measure how well these contributions compare to experiment with the quantity

$$\chi_{a_\mu}^2 = \left( \frac{\Delta a_\mu^{\text{SLHM}}}{6.8 \times 10^{-10}} \right)^2,$$

where  $6.8 \times 10^{-10}$  is the theoretical uncertainty for  $a_\mu$  in the Standard Model (used because it is larger than the experimental uncertainty). The result is that, though larger than the one-loop contributions, the two-loop Barr-Zee effect contributions are still too small to provide significant constraints on the parameter space.

### 3.4.4 LEP Higgs Search Data

The largest source of constraints for the neutral sector of the SLHM consists of LEP's failure to discover a neutral Higgs boson. If the lightest neutral scalar's mass is too small, one would expect LEP to have seen it, whereas for a mass  $M_h > 114.4$  GeV, LEP data becomes irrelevant and no bounds can be obtained [52]. The production mechanism at LEP is the Higgs-strahlung process  $e^+e^- \rightarrow hZ$ , and thus if the coupling,  $g_{ZZh}$ , between the lightest neutral scalar and  $Z$ -pairs is sufficiently small, the scalar's non-discovery at LEP can be explained [53, 54, 82, 56].

In addition, there is an effect which suppresses the sensitivity with which the experimental results may be applied to constrain models beyond the Standard Model [57, 51]. Bounds from LEP were produced under the assumption that the Higgs boson decays exclusively into  $b\bar{b}$  pairs or exclusively into  $\tau^+\tau^-$  pairs. LEP has provided a bound on the quantity  $\text{BR}(h \rightarrow X\bar{X})\xi^2$  for  $X = b$  and  $X = \tau$ , where  $\xi$  is the ratio of the  $ZZh$  coupling in a model to that of the Standard model i.e.  $\xi = g_{ZZh}/g_{ZZh}^{SM}$ . In Appendix C we derive the expression for  $\xi^2$  in the SLHM and find that it is given by

$$\xi^2 = \left| U_{11} \sin \alpha \sin \beta + U_{21} \sin \alpha \cos \beta + U_{31} \cos \alpha \sin \beta_\ell + U_{41} \cos \alpha \cos \beta_\ell \right|^2. \quad (43)$$

We will employ both of these bounds to exclude regions of parameter space in the SLHM. Naively, one expects  $\text{BR}(h \rightarrow b\bar{b})$  to approach unity when  $\tan \beta$  is large and  $\tan \alpha$ ,  $\tan \beta_\ell$  are small since in that case the down-type quark Yukawa couplings are doubly enhanced while the lepton Yukawa couplings remains small. On the other hand, when  $\tan \alpha$  and  $\tan \beta_\ell$  are large while  $\tan \beta$  is small, the lepton Yukawa couplings are enhanced and the down-type quark Yukawa couplings remain small, resulting in an increase in the branching ratio  $\text{BR}(h \rightarrow \tau^+\tau^-)$ .

Since in the interesting region of parameter space, the  $ZZh$  and  $WWh$  couplings are small, we can approximate the total decay width as simply  $\Gamma(h \rightarrow b\bar{b}) + \Gamma(h \rightarrow \tau^+\tau^-)$ . The two branching ratios for the SLHM can therefore be conveniently expressed as  $\text{BR}(h \rightarrow b\bar{b}) = 1/(1 + \kappa)$  and  $\text{BR}(h \rightarrow \tau^+\tau^-) = \kappa/(1 + \kappa)$ , where  $\kappa = \Gamma(h \rightarrow \tau^+\tau^-)/\Gamma(h \rightarrow b\bar{b})$ . The variable  $\kappa$  is straightforward to calculate and is given by

$$\kappa = \left( \frac{m_\tau^2}{3m_b^2} \right) \tan^2 \alpha \frac{\cos^2 \beta}{\cos^2 \beta_\ell} \left| \frac{U_{41}}{U_{21}} \right|^2 \left( \frac{M_h^2 - 4m_\tau^2}{M_h^2 - 4m_b^2} \right)^{3/2}, \quad (44)$$

where the  $U_{ij}$  are entries of the  $4 \times 4$  diagonalizing matrix defined by  $U^\dagger M_N^2 U = M_{\text{diag}}^2$ .

We have numerically scanned through parameter space, calculating the values of  $\text{BR}(h \rightarrow b\bar{b})\xi^2$ ,  $\text{BR}(h \rightarrow \tau^+\tau^-)\xi^2$ , and  $M_h$  in the SLHM. Those points in parameter space for which either  $\text{BR}(h \rightarrow b\bar{b})\xi^2$  or  $\text{BR}(h \rightarrow \tau^+\tau^-)\xi^2$  is greater than its LEP bound at the corresponding value of  $M_h$  are excluded. By imposing these two LEP bounds as well as the perturbativity requirements of Section 3.4.1 and the unitarity requirements of Section 3.4.2, we are able to exclude substantial regions of the model's parameter space. In Figures 2 and 3 the allowed region of the three-dimensional parameter space for the variables  $\tan \alpha$ ,  $\tan \beta$ , and  $\tan \beta_\ell$  is shown. For these plots the values of  $\mu_1$ ,  $\mu_2$ ,  $\mu_3$ , and  $\mu_4$  have been fixed at 200, 250, 300, and 100 GeV respectively. The plots depict several sections of viable parameter space in the  $\tan \alpha \times \tan \beta$  plane, each being a slice of constant  $\tan \beta_\ell$ . As  $\tan \beta_\ell$  varies over its allowed range, one can see how the sections grow in area, change shape, and eventually shrink back away.

Though the values of  $\mu_1$ ,  $\mu_2$ ,  $\mu_3$ , and  $\mu_4$  are fixed, the size and shape of the allowed parameter space remains largely unchanged when  $\mu_1$  and  $\mu_3$  are allowed to vary between 50 and 1000 GeV. Their values are consequentially relatively unconstrained. Increasing the value of  $\mu_4$  however, has the effect of sharply cutting down on the

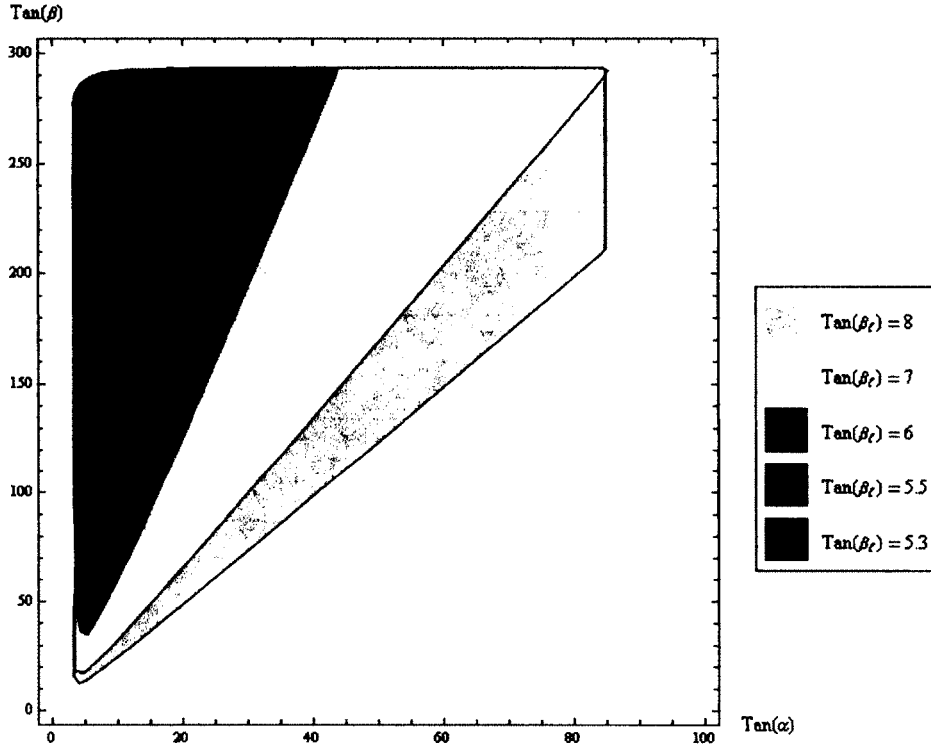


Figure 2: The colored regions illustrate the allowed points in the  $\tan \alpha$ ,  $\tan \beta$ ,  $\tan \beta_\ell$  parameter space. Each region is a slice of constant  $\tan \beta_\ell$  in the  $\tan \alpha \times \tan \beta$  plane. The values of  $\mu_1$ ,  $\mu_2$ ,  $\mu_3$ , and  $\mu_4$  are fixed at 200, 250, 300, and 100 GeV respectively, but changing  $\mu_1$  and/or  $\mu_3$  has relatively little effect. Increasing  $\mu_2$  and/or  $\mu_4$  shrinks the above space. Increasing  $\tan \beta_\ell$  enlarges the size of the allowed space quite rapidly until around  $\tan \beta_\ell \approx 8$ , when the space stops enlarging and begins to slowly shrink - this can be seen in Figure 3.

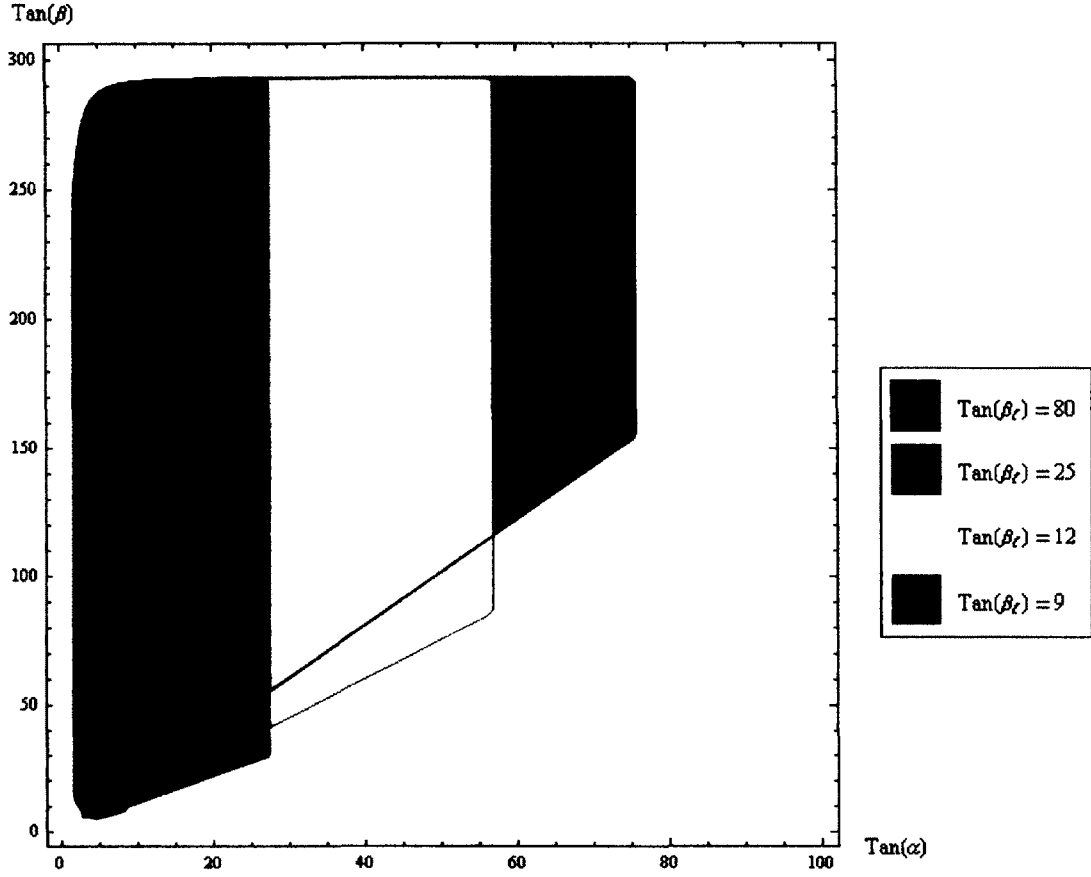


Figure 3: A continuation of figure 2 for larger values of  $\tan \beta_\ell$ . As  $\tan \beta_\ell$  increases beyond 80, the space very slowly shrinks into an extremely thin sliver of possible  $\tan \alpha$  values centered near 2; it finally disappears completely at  $\tan \beta_\ell \approx 350$ .

size of the allowed region of parameter space. So too does increasing  $\mu_2$ , though to a slightly lesser degree. Merely increasing  $\mu_4$  to 200 GeV results in a drastically smaller allowed region than that shown in Figure 2 and completely eliminates the regions corresponding to  $\tan \beta_\ell$  values of 5.3 and 5.5. The other regions are compressed so that  $3 \lesssim \tan \alpha \lesssim 20$  and  $50 \lesssim \tan \beta \lesssim 290$ , while their overall shape remains the same. Enlarging either  $\mu_2$  or  $\mu_4$  further rapidly shrinks the allowed space away until it vanishes completely.

Figure 4 plots an assortment of possible  $\text{BR}(h \rightarrow b\bar{b})\xi^2$  values as a function of the lightest neutral scalar mass  $M_h$ . Each value plotted corresponds to some point in the

allowed region of parameter space. The LEP curve is shown in blue. For very large values of  $\tan \beta_\ell$ , the curves continue down to approximately 25 GeV, with the value of  $\text{BR}(h \rightarrow b\bar{b})\xi^2$  becoming extremely small. We see that Higgs bosons below 114.4 GeV are certainly allowed, but below approximately 90 GeV their couplings to vector bosons become negligible, making detection through vector boson fusion or Higgsstrahlung off a vector boson impossible. The analogous result for  $\text{BR}(h \rightarrow \tau^+\tau^-)$  is plotted in Figure 5, with similar conclusions.

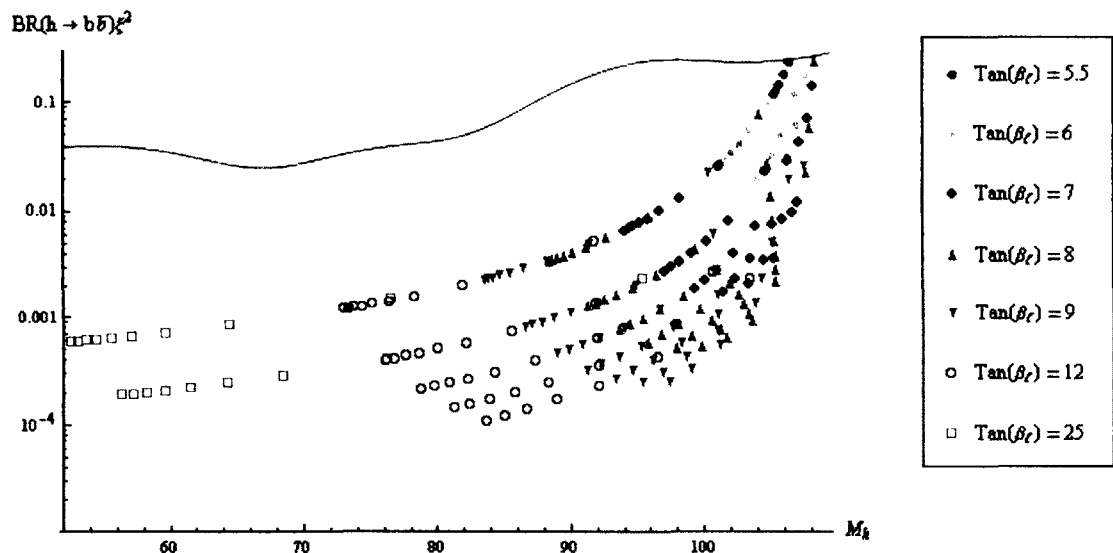


Figure 4: Various values of the quantity  $\text{BR}(h \rightarrow b\bar{b})\xi^2$  plotted as a function of the lightest neutral scalar mass  $M_h$ . The plotted values correspond to a uniform sampling of points within the allowed regions of the  $\tan \alpha \times \tan \beta$  plane for the different values of  $\tan \beta_{\ell i}$  that are plotted in figures 2 and 3. The LEP bound of reference [54] is shown in blue.

### 3.5 Phenomenology

In this section we discuss the possibility of detecting a supersymmetric leptophilic Higgs. We have focused on the neutral sector, as the charged sector strongly resembles the non-SUSY leptophilic scenario covered in [34]. The quantity of importance

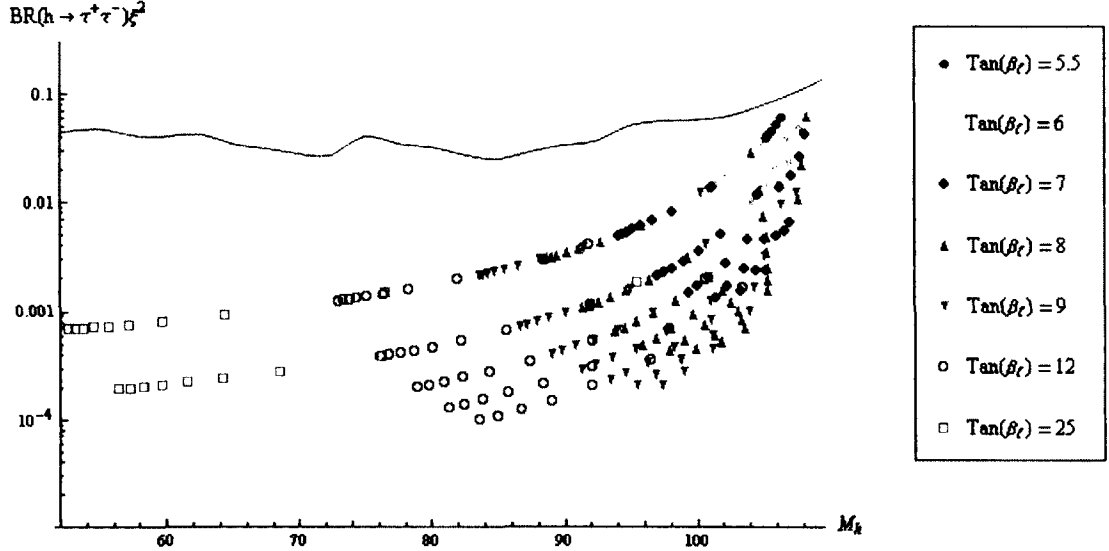


Figure 5: Various values of the quantity  $\text{BR}(h \rightarrow \tau^+\tau^-)\xi^2$  plotted as a function of the lightest neutral scalar mass  $M_h$ .

to the decay of the lightest neutral scalar is the ratio  $\kappa = \text{BR}(h \rightarrow \tau^+\tau^-)/\text{BR}(h \rightarrow b\bar{b})$ , which is given by equation 44 in Section 3.4.4.

For the region of parameter space discussed in the previous section, we have shown various values of  $\kappa$  in Figure 6. For Higgs bosons near 114.4 GeV, the allowed value of  $\kappa$  approaches its Standard Model value of approximately 0.1. However, for lighter Higgs bosons,  $\kappa$  is much bigger, approaching unity for Higgs masses below 100 GeV.

We see that in this model, the Higgs can be relatively light, and will have a much larger branching ratio to  $\tau^+\tau^-$  than in the Standard Model. In order to detect the Higgs at the Tevatron or the LHC, however, one also must consider the production rate. As we have seen, for Higgs bosons below 90 GeV, the  $ZZh$  and  $WW_h$  couplings are quite small, and thus Higgs-strahlung is negligible. What about gluon fusion, which is the primary production mechanism for a light Higgs? Here, one must include both top and bottom loops, and the coupling to the Higgs will

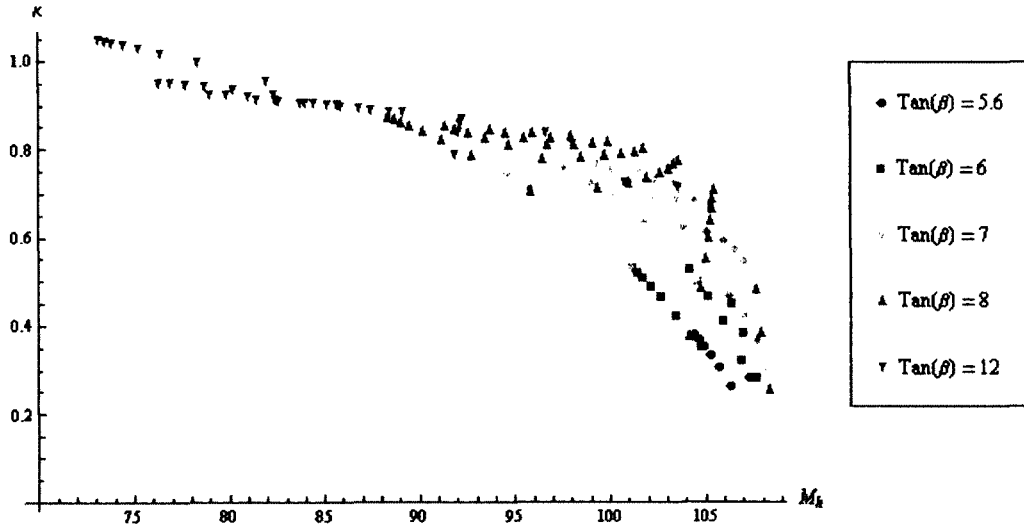


Figure 6: Various values of  $\kappa$  plotted as a function of the lightest neutral scalar mass  $M_h$ .

be different. We find that the ratio of the gluon fusion cross section to that of the Standard Model is

$$\frac{\sigma_{SLHM}}{\sigma_{SM}} = \left| \frac{U_{11}}{\sin \alpha \sin \beta} + \frac{A(m_b)}{A(m_t)} \frac{U_{21}}{\sin \alpha \cos \beta} \right|^2, \quad (45)$$

and this is plotted in Figure 7 for various parameters. The function  $A(m_f)$  is given by  $A(m_f) = 2[x_f + (x_f - 1)f(x_f)]x_f^{-2}$ , where  $x_f = M_h^2/4m_f^2$  and  $f(x_f)$  is given by equation 2.47 in [58]. For much of parameter space, the gluon fusion rate is also very small, making Higgs detection extremely difficult. In the Standard Model, the only other production mechanism that doesn't involve gluon fusion or the  $WW_h$  or  $ZZh$  vertex is Higgs-strahlung off a top quark. That is difficult in the Standard Model, and in this model is even weaker since the top quark Yukawa coupling is smaller. One can think about Higgs-strahlung off a tau, but this is likely to be swamped by backgrounds.

In any event, this is just a specific model. One might have other possibilities

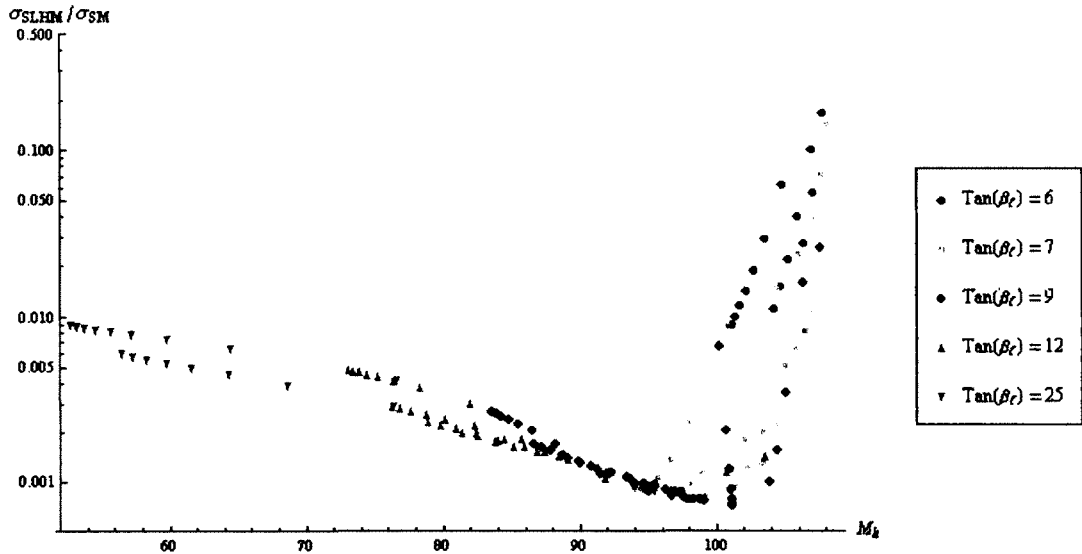


Figure 7: Logplot of the ratio of the production cross section of the lightest neutral scalar by gluon fusion in the SLHM to the Standard Model.

for Higgs production, such as production in the decay of one of the charged Higgs bosons in the model, or production through supersymmetric particles. In both of these scenarios, the production rate would depend on many additional parameters. Thus, experimenters should look for Higgs bosons in the 75 – 110 GeV range with a substantially enhanced coupling to  $\tau$  pairs (below 75 GeV, a very small sliver of parameter space does remain). A study of  $\tau$  pair detection in leptophilic Higgs decays at the LHC was carried out in Ref. [59]. Since they did not consider the supersymmetric version, they concentrated on Higgs in the 100 – 160 GeV mass range, and gluon fusion production was not particularly suppressed, as it is here. They also focussed on models with dark matter candidates (usually involving an additional singlet or an additional inert doublet). Nonetheless, their techniques show that detection of a Higgs decay into  $\tau$  pairs is feasible in the early stages at the LHC. At the Tevatron, CDF and D0 did explicitly search for Higgs decays to  $\tau$  pairs [60], but did not consider Higgs masses below 90 GeV.

Throughout this analysis, we have ignored the effects of the heavier neutral Higgs scalars. Consider the second lightest neutral scalar,  $\eta$ . As we scan the entire allowed parameter space, we find that the  $\eta$  always appears to be very close to 110 GeV. This may not be too surprising. Imagine that there was no mixing at all between the quarkophilic and leptophilic Higgs sectors. Then each sector would have a similar mass matrix to that of the MSSM (although with smaller overall vevs), and thus one would find two relatively light Higgs. Mixing can't be eliminated, of course, due to D-terms, but it is not surprising that there are two relatively light scalars in the model. In the region of parameter space in which the couplings of the  $h$  to the gauge bosons is severely suppressed, however, the couplings of the  $\eta$  will not be, and thus the  $\eta$  will be similar to the Standard Model Higgs. Given the uncertainty in our calculations, including the effects of non-leading-log and higher order corrections to the masses, it is premature to conclude that the current LEP bounds would rule out this 110 GeV Higgs, but an increase of just a few GeV in the current lower bound on the Standard Model Higgs would rule out this model.

In the region of parameter space of interest, the  $h$  and  $\eta$  are primarily linear combinations of  $H_0$  and  $H_u$ , with small admixtures of  $H_d$  and  $H_\ell$ . Nonetheless, the ratios of vacuum expectation values are large enough that the dominant decay of the  $h$ , for example, is primarily into  $\tau$ 's and  $b$ 's through these small admixtures. The two heaviest Higgs bosons are each almost entirely  $H_d$  and  $H_\ell$ , respectively, with little mixing.

Consider these two heavier Higgs bosons,  $H_1$  and  $H_2$ . Since the coupling of the  $\eta$ , in the region of interest, to  $Z$ -pairs is very close to that of the Standard Model, then the fact that the sum of the squares of the Higgs couplings to  $Z$ -pairs must equal the square of the Standard Model coupling implies that the coupling of  $H_1$  and  $H_2$  with  $W, Z$ -pairs is negligible. We have confirmed this numerically. Another

way to say this is that the narrow window of parameter space forces the direction of the vacuum expectation value to be almost entirely in the  $\eta$  direction, leaving little room for vev-dependent couplings of the other neutral Higgs. This will also cause a suppression in the  $H_1 hh$  and  $H_2 hh$  couplings. The  $H_1$  and  $H_2$  will thus be both Higgs-phobic and gauge-phobic and will only decay into fermion pairs. One of the two,  $H_1$ , will decay almost entirely into  $b\bar{b}$ , and the other,  $H_2$ , will decay almost entirely into  $\tau^+\tau^-$ . This leads to interesting phenomenological consequences. The  $H_1$  can be copiously produced through gluon fusion (through its coupling to the  $b$ -quark), and its dominant decay into  $b\bar{b}$  will be quite dramatic. The  $H_2$  would be a heavy Higgs boson that decays entirely into  $\tau$  pairs. However, gluon fusion occurs at a small rate, and thus production through heavier particles or supersymmetric partners would be necessary. This possibility is currently under investigation.

### 3.6 Conclusion

In this work, we have studied the Higgs sector of the supersymmetric version of leptophilic models. The model contains four Higgs doublets, which couple to the up quarks, down quarks, charged leptons and no fermions, respectively. The Higgs sector, as in all supersymmetric models, is tightly constrained. We consider constraints from perturbativity, unitarity, the muon anomalous magnetic moment and we also impose constraints from experimental searches at LEP.

We find that in most of parameter space, the lightest Higgs,  $h$ , has a mass between 75 and 110 GeV (with a very small sliver of parameter space giving smaller masses). For lighter values of the mass, the decay branching ratio into  $\tau$  pairs is substantial, and can even be the dominant decay mode. This would lead to some spectacular signatures at the Tevatron and the LHC. However, the conventional production mechanisms, such as W-fusion, Higgs-strahlung and gluon fusion are

suppressed in this region of parameter space.

The second lightest Higgs,  $\eta$ , has a mass throughout the allowed parameter space of approximately 110 GeV. Its production cross section is not as strongly suppressed, and would appear similar to a Standard Model Higgs. The remaining two neutral scalars are typically heavier, are gauge-phobic and Higgs-phobic, and would decay into fermions. One decays almost entirely into  $b\bar{b}$  and would be copiously produced through gluon fusion. The other decays almost entirely into  $\tau^+\tau^-$ , but conventional production mechanisms are suppressed.

There are also three charged scalars and three pseudoscalars in the model. We do not expect the phenomenology to differ substantially from the detailed analysis of Logan and MacLennan [34], who used MSSM parameters to constrain their parameter space (even though the model was not supersymmetric), and thus there would only be  $\mathcal{O}(1)$  changes in their results due to mixing angles. Exploration of the supersymmetric particles in the model are currently under investigation.

# CHAPTER 4

## 4 A Supersymmetric Leptophilic Higgs to Explain an Observed Gamma Ray Excess from The Galactic Center \*

### 4.1 Introduction

Recently, Hooper and Goodenough examined the first two years of Fermi Gamma Ray Space Telescope (FGST) data from the inner  $10^\circ$  around the Galactic Center [21]. They found that the gamma ray emissions coming from between  $1.25^\circ$  and  $10^\circ$  of the Galactic Center is consistent with what is expected from known emission mechanisms such as cosmic rays colliding with gas to produce subsequently decaying pions, inverse Compton scattering of cosmic ray electrons, and known gamma ray point sources. In order to model the gamma ray background within  $2^\circ$  of the Galactic Center, Hooper and Goodenough model the emission of the Galactic black hole Sgr A\* as a power-law extrapolated from higher energy HESS observations. Comparing the FGST measurements to this background, Hooper and Goodenough found that it agrees very well with FGST data between  $1.25^\circ - 2^\circ$  but found an excess in the observed gamma ray intensity within  $1.25^\circ$ . It has been pointed out by Ref. [62]

---

\*This chapter was previously published in Reference [61].

however, that a simple power-law extrapolation of HESS data may understate the flux of the central point source Sgr A\* as the slope of its spectrum may deviate from the constant HESS results below an energy of 100 GeV.

The authors of Ref. [21] showed that the increased gamma ray emissions are well described by annihilating dark matter that has a cusped halo profile ( $\rho \propto r^{-\gamma}$ , with  $\gamma = 1.18$  to  $1.33$ ) provided that the dark matter satisfies three basic conditions. The conditions required of the dark matter are 1) that it have a mass between 7 – 10 GeV, 2) that it annihilate into  $\tau$ -pairs most of the time, but into hadronic channels 15 – 40% of the time, and 3) that its total annihilation cross section yield a thermal average within the range  $\langle\sigma v\rangle = 4.6 \times 10^{-27} - 5.3 \times 10^{-26} \text{ cm}^3/\text{s}$ . It should be noted that the results of Hooper and Goodenough are controversial, and the Fermi-LAT collaboration itself has not yet published official results. In addition, other background related explanations for the gamma ray excess have been proposed such as the existence of a pulsar near the Galactic Center [63]. In this thesis we proceed with the assumption that the analysis of Hooper and Goodenough is correct. The astrophysical and particle physics implications of this finding are discussed in Refs. [64, 65].

In this chapter we construct a dark matter model satisfying the above conditions by adding a singlet to the supersymmetric leptophilic Higgs model (SLHM) [32]. In the SLHM the up quarks, down quarks, and leptons, each receive mass from a separate Higgs doublet. For our purposes, the salient characteristic of the SLHM is that it endows the leptons with an enhanced coupling to one of the scalars. This provides a natural mechanism for dark matter particles to annihilate predominantly into  $\tau$ -pairs. This model of dark matter is able to successfully account for the FGST observations, yields the correct relic density, and evades relevant collider bounds such as measurements of the  $Z$  width and direct production at LEP. The idea of

a leptophilic Higgs has been studied as a possible explanation for the  $e^\pm$  excess observed by PAMELA and ATIC in Ref. [66]. However, this entails a 100 GeV - 1 TeV dark matter particle, while our model requires a light,  $\mathcal{O}(10)$  GeV dark matter particle. There also exist some other models that can explain the Galactic Center gamma ray excess [67].

In addition to explaining the FGST observations, such a model of light dark matter is also capable of describing observations by the CoGeNT [68] and DAMA collaborations [69]. CoGeNT has recently reported direct detection signals that hint at the presence of  $\mathcal{O}(10)$  GeV dark matter compatible with the light dark matter interpretation of DAMA's annual event rate modulation. Ref. [70] showed that dark matter with a mass between 7 – 8 GeV that has a spin independent cross section approximately between  $\sigma_{SI} = 1 \times 10^{-40} - 3 \times 10^{-40} \text{ cm}^2$  is consistent with both CoGeNT and DAMA signals. Although the XENON [71] and CDMS [72] collaborations challenge this report, Ref. [65] has pointed out that “zero-charge” background events lie in the signal region. The authors suggest that the bound could possibly be loosened if a modest uncertainty or systematic error is introduced in the energy scale calibration near the energy threshold. Although our model is able to explain the reported observations of the CoGeNT and DAMA collaborations, it is not dependent upon their validity. By simply moving to another region of parameter space our model can coexist with the absolute refutation of CoGeNT and DAMA while continuing to explain the FGST results and avoiding collider bounds.

This chapter is organized as follows. In Section 4.2 we introduce the setup of the model and calculate the mass matrices for the scalars and the neutralinos. In Section 4.3 we describe the process by which the dark matter annihilates into Standard model particles and calculate the relevant cross sections for a benchmark point in parameter space. We also show that the resultant relic density is consistent

with current cosmological measurements. In Section 4.4 we discuss possible direct detection and in Section 4.5 we discuss relevant bounds for this model and show that it is currently viable. Lastly, we conclude with Section 4.6 and summarize the results of this chapter.

## 4.2 The Model

In this model the quark and lepton content is that of the MSSM. To this we add four Higgs doublets,  $\widehat{H}_u$ ,  $\widehat{H}_d$ ,  $\widehat{H}_0$ , and  $\widehat{H}_\ell$ , with weak hypercharge assignment  $+1/2$ ,  $-1/2$ ,  $+1/2$ , and  $-1/2$  respectively. The third Higgs doublet is necessary to achieve a leptonic structure, while the fourth doublet is required for anomaly cancellation. In order to avoid problems with the  $Z$  decay width, we introduce a singlet  $\widehat{S}$  that acts as  $\mathcal{O}(10)$  GeV dark matter. The idea of adding a light singlet to the MSSM to act as dark matter was also considered in [73], while the use of a singlet for other purposes such as solving the  $\mu$  problem was first developed in [74]. The superpotential is given by

$$\begin{aligned}
W = & y_u \widehat{U} \widehat{Q} \widehat{H}_u - y_d \widehat{D} \widehat{Q} \widehat{H}_d - y_\ell \widehat{E} \widehat{L} \widehat{H}_\ell + \mu_q \widehat{H}_u \widehat{H}_d + \mu_\ell \widehat{H}_0 \widehat{H}_\ell \\
& + \kappa_q \widehat{S} \widehat{H}_u \widehat{H}_d + \kappa_\ell \widehat{S} \widehat{H}_0 \widehat{H}_\ell + \lambda_1^2 \widehat{S} + \frac{1}{2} \lambda_2 \widehat{S}^2 + \frac{1}{3} \kappa_s \widehat{S}^3,
\end{aligned} \tag{46}$$

where the hats denote superfields. In the superpotential we introduced a  $\mathbb{Z}_2$  symmetry under which  $\widehat{H}_0$ ,  $\widehat{H}_\ell$  and  $\widehat{E}$  are odd while all other fields are even. The symmetry enforces a Yukawa structure in which  $\widehat{H}_u$  gives mass to up-type quarks,  $\widehat{H}_d$  to down-type quarks, and  $\widehat{H}_\ell$  to leptons, while  $\widehat{H}_0$  does not couple to the quarks or leptons and is called the inert doublet. It is introduced to ensure anomaly cancellation. The

$\mathbb{Z}_2$  symmetry is broken in  $V_{\text{soft}}$  so that we have: \*

$$\begin{aligned}
V_{\text{soft}} = & m_u^2 |H_u|^2 + m_d^2 |H_d|^2 + m_0^2 |H_0|^2 + m_\ell^2 |H_\ell|^2 + m_s^2 |S|^2 \\
& + \left( \mu_1^2 H_u H_d + \mu_2^2 H_0 H_\ell + \mu_3^2 H_u H_\ell + \mu_4^2 H_0 H_d \right. \\
& + \mu_a S H_u H_d + \mu_b S H_0 H_\ell + \mu_c S H_u H_\ell + \mu_d S H_0 H_d \\
& \left. + m_{u0}^2 H_u^\dagger H_0 + m_{d\ell}^2 H_d^\dagger H_\ell + t^3 S + b_s^2 S^2 + a_s S^3 + \text{h.c.} \right).
\end{aligned} \tag{47}$$

The breaking of the  $\mathbb{Z}_2$  symmetry is discussed in greater detail in Appendix D. The Higgs sector potential is given by  $V = V_D + V_F + V_{\text{soft}}$ . Letting  $\sigma^a$  denote the Pauli matrices for  $a = 1, 2, 3$ , the D-term is simply

$$\begin{aligned}
V_D = & \frac{g^2}{8} \sum_a \left| H_u^\dagger \sigma^a H_u + H_d^\dagger \sigma^a H_d + H_0^\dagger \sigma^a H_0 + H_\ell^\dagger \sigma^a H_\ell \right|^2 \\
& + \frac{g'^2}{8} \left| |H_u|^2 - |H_d|^2 + |H_0|^2 - |H_\ell|^2 \right|^2,
\end{aligned} \tag{48}$$

where  $g$  and  $g'$  are the  $SU(2)$  and  $U(1)$  gauge couplings respectively. The F-term

---

\*In Ref. [32] the soft breaking terms  $m_{u0}^2 H_u^\dagger H_0 + m_{d\ell}^2 H_d^\dagger H_\ell + \text{h.c.}$  were omitted.

and  $V_{\text{soft}}$  combine with the D-term to yield the following potential

$$\begin{aligned}
V = & (\mu_q^2 + m_u^2)|H_u|^2 + (\mu_q^2 + m_d^2)|H_d|^2 + (\mu_\ell^2 + m_0^2)|H_0|^2 + (\mu_\ell^2 + m_\ell^2)|H_\ell|^2 \\
& + \left[ (\mu_1^2 + \kappa_q \lambda_1^2)H_u H_d + (\mu_2^2 + \kappa_\ell \lambda_1^2)H_0 H_\ell + \mu_3^2 H_u H_\ell + \mu_4^2 H_0 H_d + \text{h.c.} \right] \\
& + \left| \kappa_q H_u H_d + \kappa_\ell H_0 H_\ell \right|^2 + \left( m_{u0}^2 H_u^\dagger H_0 + m_{d\ell}^2 H_d^\dagger H_\ell + \text{h.c.} \right) + (m_s^2 + \lambda_2^2)|S|^2 \\
& + \left[ (t^3 + \lambda_1^2 \lambda_2)S + (b_s^2 + \kappa_s \lambda_2^2)S^2 + a_s S^3 + \text{h.c.} \right] + \kappa_s \lambda_2 |S|^2 (S + S^*) + \kappa_s^2 |S|^4 \\
& + \left[ \mu_a (H_u H_d)S + \mu_b (H_0 H_\ell)S + \mu_c (H_u H_\ell)S + \mu_d (H_0 H_d)S + \text{h.c.} \right] \\
& + \left\{ \lambda_2 \left[ \kappa_q (H_u H_d) + \kappa_\ell (H_0 H_\ell) \right] S^* + \kappa_s \left[ \kappa_q (H_u H_d) + \kappa_\ell (H_0 H_\ell) \right] (S^2)^* + \text{h.c.} \right\} \\
& + \left\{ \kappa_q \mu_q \left( |H_u|^2 + |H_d|^2 \right) + \kappa_\ell \mu_\ell \left( |H_0|^2 + |H_\ell|^2 \right) \right\} (S + S^*) \\
& + \kappa_q^2 \left( |H_u|^2 + |H_d|^2 \right) |S|^2 + \kappa_\ell^2 \left( |H_0|^2 + |H_\ell|^2 \right) |S|^2 + V_D.
\end{aligned} \tag{49}$$

The singlet  $S$  acquires the vev  $\langle S \rangle = v_s/\sqrt{2}$  while the Higgs doublets acquire the vevs:

$$\begin{aligned}
\langle H_u \rangle &= \frac{1}{\sqrt{2}} \begin{pmatrix} 0 \\ v_u \end{pmatrix}, & \langle H_d \rangle &= \frac{1}{\sqrt{2}} \begin{pmatrix} v_d \\ 0 \end{pmatrix}, \\
\langle H_0 \rangle &= \frac{1}{\sqrt{2}} \begin{pmatrix} 0 \\ v_0 \end{pmatrix}, & \langle H_\ell \rangle &= \frac{1}{\sqrt{2}} \begin{pmatrix} v_\ell \\ 0 \end{pmatrix}.
\end{aligned} \tag{50}$$

Letting  $v_{\text{cw}}^2 = v_u^2 + v_d^2 + v_0^2 + v_\ell^2$  so that  $v_{\text{cw}}^2 = 4M_Z^2/(g^2 + g'^2) \approx (246 \text{ GeV})^2$ , we define the mixing angles  $\alpha$ ,  $\beta$ , and  $\beta_\ell$  by the relations  $\tan \beta = v_u/v_d$ ,  $\tan \beta_\ell = v_0/v_\ell$ , and  $\tan^2 \alpha = (v_u^2 + v_d^2)/(v_0^2 + v_\ell^2)$ . These definitions lead to the following parameterization

of the Higgs vevs:

$$\begin{aligned} v_u &= v_{\text{cw}} \sin \alpha \sin \beta, & v_d &= v_{\text{cw}} \sin \alpha \cos \beta, \\ v_0 &= v_{\text{cw}} \cos \alpha \sin \beta_\ell, & v_\ell &= v_{\text{cw}} \cos \alpha \cos \beta_\ell. \end{aligned} \tag{51}$$

In order to avoid increasing the  $Z$  width or violating other known bounds, we want the light dark matter to separate from the other neutralinos and be mostly singlino  $\tilde{s}$ , the fermionic component of the singlet  $\widehat{S}$ . This is accomplished by taking the parameters  $\kappa_q$  and  $\kappa_\ell$  to be small, which eliminates most of the mixing between the singlino and the Higgsinos [see Eq. (55)]. It can then be easily arranged to have the singlino be the lightest of the neutralinos. A possible mechanism for explaining the small size of  $\kappa_q$  and  $\kappa_\ell$  is discussed in Appendix D. Small values of  $\kappa_q$  and  $\kappa_\ell$  also leads to reduced mixing between the scalar singlet and the Higgs doublets as can be seen from Eq. (49). A small amount of mixing is of course required since we desire the lightest scalar, which is mostly singlet, to couple to  $\tau$ -pairs in order for the dark matter to annihilate to  $\tau^+\tau^-$  and other Standard Model particles. This mixing is generated by the soft supersymmetry-breaking parameters  $\mu_a$ ,  $\mu_b$ ,  $\mu_c$ , and  $\mu_d$ .

It is sufficient for  $\kappa_q$  and  $\kappa_\ell$  to be  $\mathcal{O}(10^{-2})$ , which is what we use in our numerical calculations (see Table 10 and 11). Though the scalar mass matrices are quite complicated in general, they simplify considerably in the limit of vanishing  $\kappa_q$  and  $\kappa_\ell$ . The numerical calculations in the sections that follow have been determined using the general matrices, but for compactness we present only the simplified matrices here. In the  $\{h_u, h_d, h_0, h_\ell, h_s\}$  basis, the neutral scalar mass matrix is given by

$$M_N^2 = \begin{pmatrix} M^2 & \vec{m}^2 \\ \vec{m}^{2T} & M_{SS}^2 \end{pmatrix}, \tag{52}$$

where the matrix  $M^2$  is given by  $M^2 = M_{\text{SLHM}}^2 + \Delta M_1^2 + \Delta M_2^2$  and the terms  $\vec{m}^2$  and  $M_{SS}$  are given by

$$\vec{m}^2{}^T = -\frac{1}{\sqrt{2}} (\mu_a v_d + \mu_c v_\ell, \mu_a v_u + \mu_d v_0, \mu_b v_\ell + \mu_d v_d, \mu_b v_0 + \mu_c v_u)$$

and

$$M_{SS}^2 = \frac{3(a_s + \kappa_s \lambda_2) v_s^2 + 2(\sqrt{2} \kappa_s^2 v_s^3 - t^3 - \lambda_1^2 \lambda_2) + \hat{m}_\circ}{\sqrt{2} v_s},$$

where  $\hat{m}_\circ = \mu_a v_u v_d + \mu_b v_0 v_\ell + \mu_c v_u v_\ell + \mu_d v_0 v_d$ . The matrix  $M_{\text{SLHM}}^2$  is the neutral scalar mass matrix from the ordinary SLHM, which can be found in [32], while the matrices  $\Delta M_1^2$  and  $\Delta M_2^2$  are given by

$$\Delta M_1^2 = \begin{pmatrix} -m_{u0}^2 \frac{v_0}{v_u} & 0 & m_{u0}^2 & 0 \\ 0 & -m_{d\ell}^2 \frac{v_\ell}{v_d} & 0 & m_{d\ell}^2 \\ m_{u0}^2 & 0 & -m_{u0}^2 \frac{v_u}{v_0} & 0 \\ 0 & m_{d\ell}^2 & 0 & -m_{d\ell}^2 \frac{v_d}{v_\ell} \end{pmatrix},$$

and

$$\Delta M_2^2 = \frac{1}{\sqrt{2}} \begin{pmatrix} \frac{v_s}{v_u} (\mu_a v_d + \mu_c v_\ell) & -v_s \mu_a & 0 & -v_s \mu_c \\ -v_s \mu_a & \frac{v_s}{v_d} (\mu_a v_u + \mu_d v_0) & -v_s \mu_d & 0 \\ 0 & -v_s \mu_d & \frac{v_s}{v_0} (\mu_b v_\ell + \mu_d v_d) & -v_s \mu_b \\ -v_s \mu_c & 0 & -v_s \mu_b & \frac{v_s}{v_\ell} (\mu_b v_0 + \mu_c v_u) \end{pmatrix}.$$

The pseudoscalar mass matrix, in the  $\{a_u, a_d, a_0, a_\ell, a_s\}$  basis, is similarly given by

$$M_A^2 = \begin{pmatrix} \widetilde{M}^2 & -\vec{m}^2 \\ -\vec{m}^2{}^T & \widetilde{M}_{SS}^2 \end{pmatrix}, \quad (53)$$

where  $\widetilde{M}^2 = \widetilde{M}_{\text{SLHM}}^2 + \Delta M_1^2 + \Delta \widetilde{M}_2^2$ . The matrix  $\widetilde{M}_{\text{SLHM}}^2$  is the pseudoscalar mass

matrix from the ordinary SLHM while  $\Delta\widetilde{M}_2^2$  is the matrix obtained from  $\Delta M_2^2$  by changing the sign of every off-diagonal entry. Lastly,  $\widetilde{M}_{SS}^2$  is given by

$$\widetilde{M}_{SS}^2 = \frac{1}{\sqrt{2}v_s} \left[ \widehat{m}_\phi - 2\lambda_1^2\lambda_2 - 2t^3 - (9a_s + \kappa_s\lambda_2)v_s^2 - 4\sqrt{2}(b_s^2 + \kappa_s\lambda_2^2)v_s \right].$$

The chargino mass matrix, on the other hand, is rather simple even with nonvanishing  $\kappa_q$  and  $\kappa_\ell$ . Letting  $\tilde{h}_u, \tilde{h}_d, \tilde{h}_0$ , and  $\tilde{h}_\ell$  denote the Higgsino gauge eigenstates, the chargino mass matrix, in the  $\{\widetilde{W}^+, \tilde{h}_u^+, \tilde{h}_0^+, \widetilde{W}^-, \tilde{h}_d^-, \tilde{h}_\ell^-\}$  basis, is given by

$$M_{\chi^\pm} = \begin{pmatrix} 0 & 0 & 0 & M_2 & gv_d & gv_\ell \\ 0 & 0 & 0 & gv_u & \mu_q + \frac{\kappa_q}{\sqrt{2}}v_s & 0 \\ 0 & 0 & 0 & gv_0 & 0 & \mu_\ell + \frac{\kappa_\ell}{\sqrt{2}}v_s \\ M_2 & gv_u & gv_0 & 0 & 0 & 0 \\ gv_d & \mu_q + \frac{\kappa_q}{\sqrt{2}}v_s & 0 & 0 & 0 & 0 \\ gv_\ell & 0 & \mu_\ell + \frac{\kappa_\ell}{\sqrt{2}}v_s & 0 & 0 & 0 \end{pmatrix}. \quad (54)$$

Like the chargino mass matrix, the neutralino mass matrix is simple. The neutralino mass matrix, in the  $\{\widetilde{B}^0, \widetilde{W}^0, \tilde{h}_u, \tilde{h}_d, \tilde{h}_0, \tilde{h}_\ell, \bar{s}\}$  basis, is given by

$$M_\chi = \begin{pmatrix} M_1 & 0 & \frac{1}{2}g'v_u & -\frac{1}{2}g'v_d & \frac{1}{2}g'v_0 & -\frac{1}{2}g'v_\ell & 0 \\ 0 & M_2 & -\frac{1}{2}gv_u & \frac{1}{2}gv_d & -\frac{1}{2}gv_0 & \frac{1}{2}gv_\ell & 0 \\ \frac{1}{2}g'v_u & -\frac{1}{2}gv_u & 0 & \mu_q + \frac{\kappa_q}{\sqrt{2}}v_s & 0 & 0 & \frac{\kappa_q}{\sqrt{2}}v_d \\ -\frac{1}{2}g'v_d & \frac{1}{2}gv_d & \mu_q + \frac{\kappa_q}{\sqrt{2}}v_s & 0 & 0 & 0 & \frac{\kappa_q}{\sqrt{2}}v_u \\ \frac{1}{2}g'v_0 & -\frac{1}{2}gv_0 & 0 & 0 & 0 & \mu_\ell + \frac{\kappa_\ell}{\sqrt{2}}v_s & \frac{\kappa_\ell}{\sqrt{2}}v_\ell \\ -\frac{1}{2}g'v_\ell & \frac{1}{2}gv_\ell & 0 & 0 & \mu_\ell + \frac{\kappa_\ell}{\sqrt{2}}v_s & 0 & \frac{\kappa_\ell}{\sqrt{2}}v_0 \\ 0 & 0 & \frac{\kappa_q}{\sqrt{2}}v_d & \frac{\kappa_q}{\sqrt{2}}v_u & \frac{\kappa_\ell}{\sqrt{2}}v_\ell & \frac{\kappa_\ell}{\sqrt{2}}v_0 & \lambda_2 + \sqrt{2}\kappa_s v_s \end{pmatrix}. \quad (55)$$

When  $\kappa_q$  and  $\kappa_\ell$  are small, the singlino part of the above matrix separates from the

$\kappa_q$	=	0.01	$v_s$	=	50 GeV	$\mu_\ell$	=	125 GeV
$\kappa_\ell$	=	0.01	$v_u$	=	245.6 GeV	$\lambda_1^2$	=	$(100 \text{ GeV})^2$
$\kappa_s$	=	0.6	$v_d$	=	4.9 GeV	$\lambda_2$	=	-35 GeV
$\tan \alpha$	=	20	$v_0$	=	12.2 GeV	$M_1$	=	500 GeV
$\tan \beta$	=	50	$v_\ell$	=	1.2 GeV	$M_2$	=	500 GeV
$\tan \beta_t$	=	10	$\mu_q$	=	125 GeV	$m_{u0}^2$	=	$-(100 \text{ GeV})^2$
$\mu_1^2$	=	$(400 \text{ GeV})^2$	$\mu_a$	=	100 GeV	$m_{dt}^2$	=	$(100 \text{ GeV})^2$
$\mu_2^2$	=	$(200 \text{ GeV})^2$	$\mu_b$	=	200 GeV	$t^3$	=	$(60.6 \text{ GeV})^3$
$\mu_3^2$	=	$(200 \text{ GeV})^2$	$\mu_c$	=	200 GeV	$b_s^2$	=	$(63.4 \text{ GeV})^2$
$\mu_4^2$	=	$(400 \text{ GeV})^2$	$\mu_d$	=	200 GeV	$a_s$	=	-42.4 GeV

Table 10: Benchmark Point A

wino, bino, and higgsinos, and the singlino mass can be well approximated by

$$m_{\chi_1} \approx \lambda_2 + \sqrt{2} \kappa_s v_s. \quad (56)$$

The  $\mathcal{O}(10)$  GeV LSP can be arranged with some tuning of the parameters in order to achieve a cancelation between  $\lambda_2$  and the product  $\kappa_s v_s$  in Eq. (56). Though the smallness of  $\kappa_q$  and  $\kappa_\ell$  is technically unnatural, we remind the reader that a possible mechanism to make them small is discussed in Appendix D.

In the following sections, we calculate the relevant cross sections and quantities of interest using benchmark points A and B, found in Tables 10 and 11 respectively. While both of these benchmark points can explain the Galactic Central region gamma ray excess, the spin independent direct detection cross section corresponding to benchmark point A lies within the region favored by CoGeNT and DAMA. In contrast, we will show that benchmark point B satisfies CDMS bounds that exclude CoGeNT and DAMA. Relevant quantities have been calculated for several additional benchmark points as well, and their values are summarized in Table 15 of Appendix E.

$\kappa_q$	=	0.01	$v_s$	=	50 GeV	$\mu_\ell$	=	125 GeV
$\kappa_\ell$	=	0.01	$v_u$	=	245.6 GeV	$\lambda_1^2$	=	(100 GeV) <sup>2</sup>
$\kappa_s$	=	0.6	$v_d$	=	4.9 GeV	$\lambda_2$	=	-35 GeV
$\tan \alpha$	=	20	$v_0$	=	12.2 GeV	$M_1$	=	500 GeV
$\tan \beta$	=	50	$v_\ell$	=	1.2 GeV	$M_2$	=	500 GeV
$\tan \beta_l$	=	10	$\mu_q$	=	125 GeV	$m_{u0}^2$	=	-(100 GeV) <sup>2</sup>
$\mu_1^2$	=	(400 GeV) <sup>2</sup>	$\mu_a$	=	100 GeV	$m_{d\ell}^2$	=	(100 GeV) <sup>2</sup>
$\mu_2^2$	=	(200 GeV) <sup>2</sup>	$\mu_b$	=	200 GeV	$t^3$	=	(55.0 GeV) <sup>3</sup>
$\mu_3^2$	=	(200 GeV) <sup>2</sup>	$\mu_c$	=	200 GeV	$b_s^2$	=	(66.3 GeV) <sup>2</sup>
$\mu_4^2$	=	(400 GeV) <sup>2</sup>	$\mu_d$	=	200 GeV	$a_s$	=	-42.2 GeV

Table 11: Benchmark Point B

### 4.3 Annihilation to Fermions

In this section, we will show that this model can achieve the conditions needed to explain the gamma ray excess in the Galactic Center region. In order to calculate the dark matter cross section, we need the interactions between Higgs and fermions:

$$\begin{aligned}
\mathcal{L} \supset & -\frac{\kappa_s}{\sqrt{2}} [h_s \bar{s} \tilde{s} - i a_s \bar{s} \gamma^5 \tilde{s}] \\
& -\frac{\kappa_q}{2\sqrt{2}} [h_u \bar{s} \tilde{h}_d - i a_u \bar{s} \gamma^5 \tilde{h}_d + h_d \bar{s} \tilde{h}_u - i a_d \bar{s} \gamma^5 \tilde{h}_u + h.c.] \\
& -\frac{\kappa_\ell}{2\sqrt{2}} [h_0 \bar{s} \tilde{h}_\ell - i a_0 \bar{s} \gamma^5 \tilde{h}_\ell + h_\ell \bar{s} \tilde{h}_0 - i a_\ell \bar{s} \gamma^5 \tilde{h}_0 + h.c.] \\
& - \sum_{f=\{u,d,\ell\}} \sum_j \frac{m_{f_j}}{v_f} (h_f \bar{f}_j f_j - i a_f \bar{f}_j \gamma^5 f_j),
\end{aligned} \tag{57}$$

where  $m_{f_j}$  is the mass of the fermion  $f_j$ ,  $v_f$  is the vev of  $f$ -type scalars, and  $j$  runs over the fermion generations. In the limit  $\kappa_q, \kappa_\ell \rightarrow 0$ , the higgs-higgsino-singlino interactions vanish.

We can expand  $\langle \sigma v \rangle$  in powers of the dark matter velocity squared  $v^2$ :

$$\langle \sigma v \rangle = a + b v^2 + \dots \tag{58}$$

Only the  $s$ -wave contribution to  $a$  is relevant in discussing the gamma ray excess

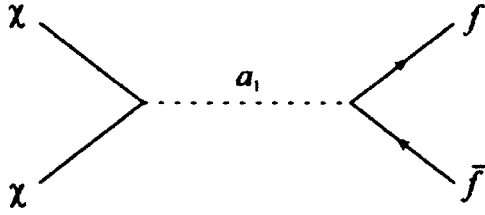


Figure 8: The dominant diagram of dark matter annihilation into fermions. Here  $a_1$  is the lightest pseudoscalar.

coming from dark matter annihilation since the velocity of the dark matter in the Galactic Center region is relatively low. An exception to this is within the sphere of influence of the Milky Way supermassive black hole, but this region corresponds to only a fraction of an arc second and is below FGST accuracy. As we see later,  $a_1$  is mostly singlet for benchmark points A and B. Therefore the  $s$ -wave contribution to dark matter annihilation to fermions comes mostly from the  $s$ -channel diagram involving an exchange of the lightest pseudoscalar  $a_1$  given in Fig. 8. It is approximately given by

$$a \approx \frac{N_c \kappa_s^2 U_{1f}^2 m_f^2}{4\pi v_f^2} \frac{m_{\chi_1}^2}{(4m_{\chi_1}^2 - m_{a_1}^2)^2} \sqrt{1 - \frac{m_f^2}{m_{\chi_1}^2}}, \quad (59)$$

where  $N_c$  is the number of fermion colors,  $U_{1f}$  is the  $(1, f)$  element of the pseudoscalar diagonalizing matrix and  $m_{a_1}$  is the mass of the lightest pseudoscalar. The  $s$ -wave contributions from heavier pseudoscalars are suppressed by larger masses as well as smaller mixings with the singlet. Moreover,  $s$ -channel scalar exchange diagrams are  $s$ -wave suppressed, i.e.  $a(\chi_1 \chi_1 \rightarrow h_i \rightarrow \bar{f} f) = 0$ .

For benchmark point A, the dark matter mass is  $m_{\chi_1} = 7.4$  GeV. The physical dark matter can be expressed in terms of gauge eigenstates as:

$$\chi_1 = 0.0017 \tilde{B}^0 - 0.0031 \tilde{W}^0 - 0.0141 \tilde{h}_u - 0.0046 \tilde{h}_d - 0.0001 \tilde{h}_0 - 0.0008 \tilde{h}_\ell + 0.9999 \tilde{s}.$$

We need a light pseudoscalar,  $\mathcal{O}(10)$  GeV, to get a sizeable annihilation cross section. This requires 1% tuning in the parameter space in addition to the tuning needed to make the singlino the LSP. The lightest pseudoscalar in the benchmark point is mostly singlet with a mixing with other types of pseudoscalar given by

$$a_1 = -0.000002 a_u - 0.002193 a_d - 0.001203 a_0 - 0.003679 a_\ell + 0.999990 a_s,$$

with its mass is  $m_{a_1} = 18.7$  GeV.

Having the masses and mixing, we can calculate the total annihilation cross section into fermion pairs which gives

$$\langle\sigma v\rangle = 4.0 \times 10^{-26} \text{ cm}^3/\text{s} \quad (60)$$

where the hadronic final states cross section is 23% of the total cross section and  $\tau$  pairs final state makes up the rest. For benchmark point B given in Table 11, the mass of dark matter is  $m_{\chi_1} = 7.4$  GeV and  $\langle\sigma v\rangle = 3.0 \times 10^{-26} \text{ cm}^3/\text{s}$ , with the hadronic final states make up 23% of it. The annihilation cross sections given above are within the range of suggested cross section for explaining the gamma ray excess in the Galactic Center region given in Ref. [21].

In this model, dark matter annihilation into SM fermions given in Fig. 8 is also responsible for giving the dark matter the correct thermal relic abundance. To show this, we calculate the relic abundance which is given by [75]

$$\Omega_{\chi_1} h^2 \approx 2.82 \times 10^8 Y_\infty(m_{\chi_1}/\text{GeV}), \quad (61)$$

where

$$Y_\infty^{-1} = 0.264 \sqrt{g_*} m_P m_{\chi_1} \left\{ a/x_f + 3(b - \frac{1}{4}a)/x_f^2 \right\}. \quad (62)$$

In the equation above,  $m_P$  is the Planck mass and  $g_*$  is the number of relativistic degrees of freedom at freeze-out. The freeze-out epoch  $x_f$  is related to the freeze-out temperature  $T_f$  by  $x_f = m_{\chi_1}/T_f$ , and  $x_f$  is determined by [75]

$$x_f = \ln \left[ 0.0764 m_P (a + 6b/x_f) c(2 + c) m_{\chi_1} / \sqrt{g_* x_f} \right]. \quad (63)$$

The value of  $c$  is usually taken as  $c = 1/2$ . Approximating  $g_*$  to be a ladder function, we get that, for both of our benchmark points, the freeze-out epoch is  $x_f = 21$  and the relic abundance is

$$\Omega_{\chi_1} h^2 \approx 0.1, \quad (64)$$

which agrees with the cosmologically measured abundance [76]. Since the freeze-out temperature happens to be around the QCD phase transition temperature,  $g_*$  varies significantly over the change of temperature [77] and the result (64) can change up to  $\mathcal{O}(1)$ . However the relic density is in the correct ballpark, therefore we do not expect that the correction will invalidate our result. An adjustment of parameters can be done when taking into account of the variation of  $g_*$  to get the correct density and annihilation cross section.

The benchmark points A and B serve as examples to show that in principle this model can explain the gamma ray excess in the Galactic Center region. However, the excess could also be obtained by some other regions in the parameter space as shown in the Appendix E. One could do a scan on the parameter space to find the favored region of the model.

Note that in our relic density calculation, we have neglected possible chargino and sfermion contributions coming from resonance and coannihilation effects. This is because the charginos have masses  $\mathcal{O}(100)$  GeV for all of our benchmark points, and we assume that the sfermion masses are at least  $\mathcal{O}(100)$  GeV, which is consistent

with current LEP bounds.

## 4.4 Direct Detection

Having shown that this model can account for the gamma ray excess in the Galactic Center region, we now discuss direct detection of dark matter of this model. In this section, we will consider constraints from the search for spin independent, elastic scattering of dark matter off target nuclei. The most relevant contribution for the cross section is given by the  $t$ -channel scalar exchange diagram with the effective Lagrangian:

$$\mathcal{L}_{int} = \sum_q \alpha_q \bar{\chi}_1 \chi_1 \bar{q} q. \quad (65)$$

In our benchmark points, the only relevant contribution to dark matter detection comes from the lightest scalar and  $\alpha_q$  can be approximated by

$$\alpha_q \approx \frac{\kappa_s m_q V_{1q}}{\sqrt{2} v_q m_{h_1}^2}, \quad (66)$$

where  $m_q$  is the mass of quark  $q$ ,  $v_q$  is the scalar vev associated with quark flavor  $q$ ,  $V_{1q}$  is the  $(1, q)$  element of the scalar diagonalizing matrix, and  $m_{h_1}$  is the mass of the lightest scalar. Given the partonic interaction between dark matter and quarks, we can follow Ref. [78] to get the effective interaction with nucleons:

$$\mathcal{L}_{eff} = f_p \bar{\chi}_1 \chi_1 \bar{p} p + f_n \bar{\chi}_1 \chi_1 \bar{n} n, \quad (67)$$

where  $f_p$  and  $f_n$  are related to  $\alpha_q$  through the relation [78]

$$\frac{f_{p,n}}{m_{p,n}} = \sum_{q=u,d,s} \frac{f_{Tq}^{(p,n)} \alpha_q}{m_q} + \frac{2}{27} f_{Tg}^{(p,n)} \sum_{q=c,b,t} \frac{\alpha_q}{m_q}, \quad (68)$$

and  $\langle n|m_q\bar{q}q|n\rangle = m_n f_{Tq}^n$ . Numerically, the  $f_{Tq}^{(p,n)}$  are given by [79]

$$\begin{aligned} f_{Tu}^p &= 0.020 \pm 0.004, f_{Td}^p = 0.026 \pm 0.005, f_{Ts}^p = 0.118 \pm 0.062 \\ f_{Tu}^n &= 0.014 \pm 0.0043, f_{Td}^n = 0.036 \pm 0.008, f_{Ts}^n = 0.118 \pm 0.062, \end{aligned} \quad (69)$$

while  $f_{Tg}^{(p,n)}$  is defined by

$$f_{Tg}^{(p,n)} = 1 - \sum_{q=u,d,s} f_{Tq}^{(p,n)}. \quad (70)$$

We can approximate  $f_p \approx f_n$  since  $f_{Ts}$  is larger than other  $f_{Tq}$ 's and  $f_{Tg}$ . For the purpose of comparing the predicted cross section with existing bounds, we evaluate the cross section for scattering off a single nucleon. The result can be approximated as

$$\sigma_{SI} \approx \frac{4m_r^2 f_p^2}{\pi} \quad (71)$$

where  $m_r$  is nucleon-dark matter reduced mass  $1/m_r = 1/m_n + 1/m_{\chi_1}$ .

We are now ready to show that benchmark point A can explain signals reported by CoGeNT [68] and DAMA [69]. For this benchmark point, the lightest scalar mass is  $m_{h_1} = 11.3$  GeV. This lightest scalar is mostly singlet and its mixing with other scalars is given by

$$h_1 = 0.089 h_u + 0.004 h_d + 0.010 h_0 + 0.004 h_\ell + 0.996 h_s.$$

As in the case of pseudoscalar, contributions from higher mass scalars are suppressed by their masses and their mixings with the singlet. The spin independent cross section for the benchmark point now can be calculated and is given by

$$\sigma_{SI} = 1.7 \times 10^{-40} \text{ cm}^2, \quad (72)$$

which is inside the CoGeNT and DAMA favored region [70].

Similarly, we can show that benchmark point B given in Table 11 has the lightest scalar mass  $m_{h_1} = 41.5$  GeV and spin independent cross section  $\sigma_{SI} = 1.2 \times 10^{-42}$  cm<sup>2</sup>. This cross section is two orders of magnitude lower than the present CDMS and XENON bound [71, 72].

## 4.5 Bounds on The Model

In this section we discuss various collider bounds that apply to the model. We will spend most of the discussions in this section for the benchmark point A given in Table 10. The bounds for benchmark point B as well as the summary of the bounds for benchmark point A are given in Table 12.

In this model, the decays  $Z \rightarrow \chi_1 \chi_1$  and  $Z \rightarrow h_1 a_1$  are allowed kinematically. The  $Z$  decay width has been measured precisely and is given by  $\Gamma = 2.4952 \pm 0.0023$  GeV [80]. Corrections to the decay width can be used as a bound on the mixing between the singlet and the Higgs sector. The partial decay width of  $Z \rightarrow \chi_1 \chi_1$  is given by

$$\Gamma_{Z \rightarrow \chi_1 \chi_1} = \frac{G_F \theta_\chi^2}{48\sqrt{2}\pi} m_Z^3 \left(1 - \frac{4m_{\chi_1}^2}{m_Z^2}\right)^{\frac{3}{2}}, \quad (73)$$

where  $G_F$  is the Fermi constant,  $m_Z$  is  $Z$  mass, and  $\theta_\chi$  is given by

$$\theta_\chi = |W_{u1}|^2 - |W_{d1}|^2 + |W_{01}|^2 - |W_{e1}|^2. \quad (74)$$

In the equation above,  $W_{f1}$  is the  $(f, 1)$  element of the neutralino diagonalizing matrix. The decay width of  $Z \rightarrow h_1 a_1$  is given by

$$\Gamma_{Z \rightarrow h_1 a_1} = \frac{G_F |\theta_{ha}|^2}{3\sqrt{2}\pi} p^3, \quad (75)$$

Benchmark point	A	B
$m_{\chi_1}$ (GeV)	7.4	7.4
$m_{\chi_1^\pm}$ (GeV)	118	118
$m_{h_1}$ (GeV)	11.3	41.5
$m_{a_1}$ (GeV)	18.7	19.3
$\Gamma_{Z \rightarrow \chi_1 \chi_1}$ (GeV)	$1.4 \times 10^{-9}$	$1.4 \times 10^{-9}$
$\Gamma_{Z \rightarrow h_1 a_1}$ (GeV)	$1.1 \times 10^{-11}$	$4.9 \times 10^{-12}$
$k$	$8.0 \times 10^{-3}$	$1.3 \times 10^{-2}$
$S_{model}(e^+e^- \rightarrow h_1 a_1)$	$1 \times 10^{-10}$	$1 \times 10^{-10}$
$S_{model}(e^+e^- \rightarrow h_2 a_1)$	$1 \times 10^{-12}$	$2 \times 10^{-12}$
$\sigma_{e^+e^- \rightarrow \chi_1 \chi_2}$ (pb)	$1 \times 10^{-5}$	$1 \times 10^{-5}$

Table 12: Mass spectrum and bounds for benchmark points A and B. The variable  $k$  is given by  $k = \sigma_{hZ}/\sigma_{hZ}^{SM}$  and  $S_{model} = \sigma_{h_i a_j}/\sigma_{ref}$ , where  $\sigma_{h_i a_j}$  is the  $h_i a_j$  production cross section and  $\sigma_{ref}$  is the reference cross section defined in Ref. [82].

where

$$\theta_{ha} = U_{u1}V_{u1} - U_{d1}V_{d1} + U_{01}V_{01} - U_{\ell 1}V_{\ell 1}, \quad (76)$$

and

$$p^2 = \frac{1}{4m_Z^2} [(m_Z^2 - (m_{h_1} + m_{a_1})^2)(m_Z^2 - (m_{h_1} - m_{a_1})^2)]. \quad (77)$$

For the benchmark point, the partial decay widths in both cases are given by

$$\begin{aligned} \Gamma_{Z \rightarrow \chi_1 \chi_1} &= 1.4 \times 10^{-9} \text{ GeV}, \\ \Gamma_{Z \rightarrow h_1 a_1} &= 1.1 \times 10^{-11} \text{ GeV}, \end{aligned} \quad (78)$$

which is well within the measurement error.

Another bound on the model comes from scalar and pseudoscalar direct production at LEP. At LEP a light scalar can be produced by Higgsstrahlung process  $e^+e^- \rightarrow Z \rightarrow Zh_1$ . Ref. [81] gives a bound on the coupling strength of  $Z$  pairs to scalars regardless of the scalar's decay mode. The bound is given in terms of the quantity

$$k(m_h) = \frac{\sigma_{hZ}}{\sigma_{hZ}^{SM}}. \quad (79)$$

In our model,  $k(m_h)$  is given by

$$k(m_{h_i}) = \frac{1}{v_{ew}^2} |v_u V_{ui} + v_d V_{di} + v_0 V_{0i} + v_\ell V_{\ell i}|^2, \quad (80)$$

and its value for the lightest scalar at our benchmark point is

$$k(m_{h_1}) = 8.0 \times 10^{-3}. \quad (81)$$

The bound on  $k(m_h)$  for the benchmark point  $h_1$  mass is given by

$$k(11.3 \text{ GeV}) \leq 0.09. \quad (82)$$

Therefore  $k(m_{h_1})$  does not exceed the bound from Higgsstrahlung process in our benchmark point. The pseudoscalar can also be produced at LEP by the process  $e^+e^- \rightarrow Z \rightarrow ha$ . In the benchmark point, both  $h_1 a_1$  and  $h_2 a_1$  production are kinematically allowed. LEP bounds on scalar and pseudoscalar production for various final states are given in Ref. [82]. The bound is given in term of  $S_{95} = \sigma_{max}/\sigma_{ref}$  where  $\sigma_{max}$  is the largest cross section compatible with data and  $\sigma_{ref}$  is the standard model  $hZ$  production cross section multiplied by a kinematic scaling factor. Defining  $S_{model} = \sigma_{h_i a_j}/\sigma_{ref}$ , where  $\sigma_{h_i a_j}$  is the model's  $h_i a_j$  production cross section, the bound on the model is given by  $S_{model} < S_{95}$ . For our benchmark point,  $S_{model}$  is given by

$$\begin{aligned} S_{model}(e^+e^- \rightarrow h_1 a_1) &= 1 \times 10^{-10}, \\ S_{model}(e^+e^- \rightarrow h_2 a_1) &= 1 \times 10^{-12}, \end{aligned} \quad (83)$$

which is lower than the bound,  $S_{95} \sim \mathcal{O}(10^{-2})$ , in both cases.

We note that the lightest chargino mass is 118 GeV for the benchmark point,

which exceeds the PDG bound of 94 GeV [80]. In the case of a long lived chargino however, the bound can be made much stronger and is currently at 171 GeV. We have calculated the lifetime of the chargino in our model assuming a stau mass of 110 GeV and have found that it is short lived, thus this latter bound is not of concern. We should point out however, that our analysis has been done at tree level. Loop corrections could change these results but are beyond the scope of this thesis.

Finally, we need to calculate the bound on neutralino productions. Ref. [83] discusses the bound on production of the lightest and second to lightest neutralinos at LEP,  $e^+e^- \rightarrow \chi_1\chi_2$ , where  $\chi_2$  decays into  $\chi_1 f \bar{f}$ . Assuming that the selectron is much heavier than the  $Z$ , the main contribution comes from s-channel  $Z$  exchange. For our benchmark point, we calculate the cross section to be

$$\sigma_{e^+e^- \rightarrow \chi_1\chi_2} = 1 \times 10^{-5} \text{ pb}, \quad (84)$$

while the bound is  $\mathcal{O}(0.1)$  pb. A summary of all these bounds is given in Table 12.

The light particles are mostly singlet and have very little mixing with the Higgs sector. This make the particles unlikely to be produced at near future experiments. However the heavier sector has a richer phenomenology. For example, heavier scalars are mostly  $h_u$ ,  $h_d$ ,  $h_0$ , and  $h_\ell$  therefore they have a better chance of being detected in future colliders [32].

## 4.6 Conclusion

In this chapter, we have presented a supersymmetric model of 7 – 10 GeV dark matter, which is capable of describing the FGST observations. In a recent analysis of FGST data, Hooper and Goodenough found an excess in gamma ray emission from within  $1.25^\circ$  of the Galactic Center. They showed that this can be explained

by annihilating dark matter if the dark matter has a mass between  $7 - 10$  GeV, annihilates into  $\tau$ -pairs most of the time, but into hadronic channels the other  $15 - 40\%$  of the time, and  $\langle\sigma v\rangle$  falls within the range  $4.6 \times 10^{-27} - 5.3 \times 10^{-26}$  cm<sup>3</sup>/s [21]. Our model achieves these requirements by minimally extending the SLHM to include a scalar singlet whose superpartner is the dark matter particle. Due to the Yukawa structure of the SLHM the scalar particles mediating the dark matter annihilation have an enhanced coupling to leptons. This provides a natural means for satisfying the second requirement put forward by Hooper and Goodenough.

We have shown that this model produces the correct dark matter thermal relic density and is consistent with current collider bounds. In addition, we have shown that this model is consistent with the direct detection signals reported by both CoGeNT and DAMA for certain regions of parameter space, while for other regions of parameter space, the model yields a spin independent cross section far below the present CDMS bound, but maintains the right relic density and continues to explain the FGST observations. Thus our model is fully able to accommodate the results reported by CoGeNT and DAMA in the case of their vindication, but it is in no way contingent upon their validity.

# APPENDICES

## A The PMNS Mixing Matrix Parameters

The decay rate of  $\chi^+ \rightarrow \ell_i^+ \nu_j$  (as well as the rate for supersymmetric versions) is proportional to the square of the  $ij$ -element of the neutrino mass matrix in the flavor eigenstate basis. It, in turn, is related to the physical neutrino masses through the PMNS matrix  $U_{ij}$  by  $m_{\nu_{ij}}^D = U_{ik}^\dagger m_{\nu_{kl}} U_{lj}$ , where  $m_{\nu_{ij}}^D$  is the diagonalized neutrino mass matrix. This gives

$$\Gamma(\chi^+ \rightarrow \ell_i^+ \nu_j) \propto m_{\nu_{ij}}^2 = \left( U_{ik} m_{\nu_{kl}}^D U_{lj}^\dagger \right)^2. \quad (\text{A.1})$$

The diagonalizing matrix and diagonalized mass matrix are given by (in the limit where  $\theta_{13} = 0$ )

$$U_{ij} = \begin{pmatrix} \cos(\theta_{12}) & \sin(\theta_{12}) & 0 \\ -\sin(\theta_{12}) \cos(\theta_{23}) & \cos(\theta_{12}) \cos(\theta_{23}) & \sin(\theta_{23}) \\ \sin(\theta_{12}) \sin(\theta_{23}) & -\cos(\theta_{12}) \sin(\theta_{23}) & \cos(\theta_{23}) \end{pmatrix} \quad (\text{A.2})$$

and

$$m_{\nu_{ij}}^D = \begin{pmatrix} m_{\nu_1} & 0 & 0 \\ 0 & m_{\nu_2} & 0 \\ 0 & 0 & m_{\nu_3} \end{pmatrix}. \quad (\text{A.3})$$

Although there is a range of allowed values for  $\theta_{12}$ ,  $\theta_{13}$ , and  $\theta_{23}$ , we will choose them to be given by  $34^\circ$ ,  $0^\circ$ , and  $45^\circ$ , respectively. We will also assume that the lightest neutrino has negligible mass (thus not considering the fully degenerate case). The reason for these assumption is that, in determining branching ratios, we are already choosing a specific point in mSUGRA parameter space, and thus our quantitative results should not be taken too precisely. Choosing the central values of the neutrino parameters keeps the presentation simple. With these assumptions,

the diagonalizing matrix becomes

$$U_{ij} \approx \begin{pmatrix} .83 & .56 & 0 \\ -.4 & .59 & .71 \\ .4 & -.59 & .71 \end{pmatrix}. \quad (\text{A.4})$$

For the normal hierarchy we have  $m_{\nu_1} \approx m_{\nu_2} \ll m_{\nu_3} \equiv M$ , while for the inverted hierarchy we have  $m_{\nu_3} \ll m_{\nu_1} \approx m_{\nu_2} \equiv M$ .

We therefore find

$$\Gamma(\chi^+ \rightarrow \ell_i^+ \nu_j) \propto m_{ij}^2 = \begin{cases} M^2 |U_{i3} U_{j3}^*|^2 & \text{Normal Hierarchy} \\ M^2 |U_{i1} U_{j1}^* + U_{i2} U_{j2}^*|^2 & \text{Inverted Hierarchy} \end{cases} \quad (\text{A.5})$$

The branching ratio  $\text{BR}(\chi^+ \rightarrow \ell_i^+ \nu_j) = \Gamma(\chi^+ \rightarrow \ell_i^+ \nu_j) / \Gamma(\chi^+ \rightarrow \text{any } \ell^+ \nu)$  is given by  $m_{ij}^2 / \sum_{kl} m_{kl}^2$ , which is easily evaluated as

$$\text{BR}(\chi^+ \rightarrow \ell_i^+ \nu_j) = \begin{pmatrix} 0 & 0 & 0 \\ 0 & 25\% & 25\% \\ 0 & 25\% & 25\% \end{pmatrix} \quad \text{for the normal hierarchy,} \quad (\text{A.6})$$

$$\text{BR}(\chi^+ \rightarrow \ell_i^+ \nu_j) = \begin{pmatrix} 50\% & 0 & 0 \\ 0 & 12.5\% & 12.5\% \\ 0 & 12.5\% & 12.5\% \end{pmatrix} \quad \text{for the inverted hierarchy.} \quad (\text{A.7})$$

In the case of final state neutrinos, one sums over all flavors since they are not detected. All of the above holds for the analogous decays involving SUSY partners:  $\tilde{\chi}^+ \rightarrow \tilde{\ell}_i^+ \nu_j$  and also will give us the flavor structure when, for example, a  $\tilde{\nu}_R$  of flavor  $j$  decays into a  $\tilde{\chi}^{+*}$  and a lepton  $\ell_i^-$

## B Gauge Boson Masses in The SLHM

To calculate gauge boson masses we look at the kinetic terms of the Higgs doublets. The process is exactly as in Standard Model; the only difference is that there are four kinetic terms instead of only one. We follow the procedure of Reference [84] The kinetic term for each doublet  $H_i$  is given by

$$\begin{aligned}
(\mathcal{D}_\mu H_i)^\dagger \mathcal{D}^\mu H_i &= \left( \partial_\mu H_i - i\frac{g_1}{2} A_\mu^\alpha \sigma^a H_i - ig_2 Y_i B_\mu H_i \right)^\dagger \left( \partial^\mu H_i - i\frac{g_1}{2} A^{b\mu} \sigma^b H_i - ig_2 Y_i B^\mu H_i \right) \\
&= \left( \partial_\mu H_i^\dagger + i\frac{g_1}{2} A_\mu^\alpha H_i^\dagger \sigma^a + ig_2 Y_i B_\mu H_i^\dagger \right) \left( \partial^\mu H_i - i\frac{g_1}{2} A^{b\mu} \sigma^b H_i - ig_2 Y_i B^\mu H_i \right) \\
&= \partial_\mu H_i^\dagger \partial^\mu H_i + \left\{ i\frac{g_1}{2} A_\mu^\alpha H_i^\dagger \sigma^a \partial^\mu H_i + ig_2 Y_i B_\mu H_i^\dagger \partial^\mu H_i + \text{h.c.} \right\} \\
&\quad + H_i^\dagger \left( \frac{g_1}{2} A_\mu^\alpha \sigma^a + g_2 Y_i B_\mu \right) \left( \frac{g_1}{2} A^{b\mu} \sigma^b + g_2 Y_i B^\mu \right) H_i.
\end{aligned}$$

Mass terms are quadratic in both the gauge boson fields and the Higgs vev. Consequently, mass terms can only come from the last line above. We will denote that portion of the lagrangian by  $\Delta\mathcal{L}$ . Using the identity  $\{\sigma^a, \sigma^b\} = 2\delta_{ab}$  we have  $A_\mu^\alpha A^{b\mu} \sigma^a \sigma^b = A_\mu^\alpha A^{b\mu}$ , which allows us to simplify this portion

$$\begin{aligned}
\Delta\mathcal{L} &= H_i^\dagger \left( \frac{g_1^2}{4} A_\mu^\alpha A^{a\mu} + g_1 g_2 Y_i A_\mu^\alpha B^\mu \sigma^a + g_2^2 Y_i^2 B_\mu B^\mu \right) H_i \\
&= H_i^\dagger \left( \frac{g_1^2}{4} A_\mu^1 A^{1\mu} + \frac{g_1^2}{4} A_\mu^2 A^{2\mu} + \frac{g_1^2}{4} A_\mu^3 A^{3\mu} + g_1 g_2 Y_i A_\mu^\alpha B^\mu \sigma^a + g_2^2 Y_i^2 B_\mu B^\mu \right) H_i.
\end{aligned} \tag{B.1}$$

To find the masses we set the Higgs doublets equal to their vacuum expectation values, which are as follows

$$\begin{aligned}
\langle H_u \rangle &= \frac{1}{\sqrt{2}} \begin{pmatrix} 0 \\ v_u \end{pmatrix}, & \langle H_d \rangle &= \frac{1}{\sqrt{2}} \begin{pmatrix} v_d \\ 0 \end{pmatrix}, \\
\langle H_0 \rangle &= \frac{1}{\sqrt{2}} \begin{pmatrix} 0 \\ v_0 \end{pmatrix}, & \langle H_\ell \rangle &= \frac{1}{\sqrt{2}} \begin{pmatrix} v_\ell \\ 0 \end{pmatrix}.
\end{aligned}$$

Using the fact that  $\langle H_i \rangle^\dagger Y_i A_\mu^a \sigma^a \langle H_i \rangle = -\langle H_i \rangle^\dagger A_\mu^3 |Y_i| \langle H_i \rangle$ , which can be easily seen by a direct calculation, we may rewrite the last three terms in the parenthesis as a square. The result is

$$\begin{aligned}
\Delta\mathcal{L} &= \langle H_i \rangle^\dagger \left( \frac{g_1^2}{4} (A_\mu^1 A^{1\mu} + A_\mu^2 A^{2\mu}) + \left( \frac{g_1}{2} A_\mu^3 - g_2 |Y_i| B_\mu \right)^2 \right) \langle H_i \rangle \\
&= \langle H_i \rangle^\dagger \left( \frac{g_1^2}{2} W_\mu^+ W^{-\mu} + \frac{1}{4} (g_1^2 + g_2^2) Z_\mu^0 Z^{0\mu} \right) \langle H_i \rangle \\
&= \left( \frac{g_1 v_i}{2} \right)^2 W_\mu^+ W^{-\mu} + \frac{v_i^2}{8} (g_1^2 + g_2^2) Z_\mu^0 Z^{0\mu}.
\end{aligned} \tag{B.2}$$

Here we have used the fact that  $|Y_i| = 1/2$  for all four Higgs doublets. The expressions for  $W^\pm$ ,  $Z^0$ , and  $A_\mu$  (the photon) are consequently given by

$$W_\mu^\pm = \frac{1}{\sqrt{2}} (A_\mu^1 \mp i A_\mu^2), \tag{B.3}$$

and

$$\begin{pmatrix} Z_\mu^0 \\ A_\mu \end{pmatrix} = \begin{pmatrix} \cos \theta_W & -\sin \theta_W \\ \sin \theta_W & \cos \theta_W \end{pmatrix} \begin{pmatrix} A_\mu^3 \\ B_\mu \end{pmatrix}, \tag{B.4}$$

where

$$\cos \theta_W = \frac{g_1}{\sqrt{g_1^2 + g_2^2}} \quad \text{and} \quad \sin \theta_W = \frac{g_2}{\sqrt{g_1^2 + g_2^2}}.$$

The two terms in the last line of Equation B.2 are mass terms for the  $W^\pm$  and  $Z^0$  contributed by the Higgs doublet  $H_i$ . Each of the four Higgs doublets contributes a pair of terms in this way. The  $W^\pm$  and  $Z^0$  masses are simple the sum of these terms.

Hence we have

$$M_W^2 = \frac{g_1^2}{4} (v_u^2 + v_d^2 + v_0^2 + v_\ell^2) \quad \text{and} \quad M_Z^2 = \frac{1}{4} (g_1^2 + g_2^2) (v_u^2 + v_d^2 + v_0^2 + v_\ell^2). \tag{B.5}$$

Additionally, we may use Equations B.3 and B.4 to write the covariant derivative in terms of the physical gauge bosons. For notational convenience we first define  $T^\pm = (T^1 \pm iT^2)$  and  $Q = T^3 + Y$ , where the  $T^a$  are the generators of  $SU(2)$  for an arbitrary representation. Up until now, when we were working specifically with a complex 2-dimensional representation of  $SU(2)$ , the Higgs doublets, we had  $T^a = \sigma^a/2$ . Now however, we leave the generators to be for a general representation

$$\begin{aligned}\mathcal{D}_\mu &= \partial_\mu - ig_1 A_\mu^a T^a - ig_2 Y B_\mu \\ &= \partial_\mu - ig_1 \left( A_\mu^1 T^1 + A_\mu^2 T^2 \right) - ig_1 A_\mu^3 T^3 - ig_2 Y B_\mu\end{aligned}\tag{B.6}$$

We may use equation B.4 to substitute  $A_\mu^3 = \cos\theta_W Z_\mu + \sin\theta_W A_\mu$  and  $B_\mu = -\sin\theta_W Z_\mu + \cos\theta_W A_\mu$  into equation B.6. Doing this and noting that

$$\begin{aligned}\left( A_\mu^1 T^1 + A_\mu^2 T^2 \right) &= \frac{1}{2} \left( A_\mu^1 - iA_\mu^2 \right) \left( T^1 + iT^2 \right) + \frac{1}{2} \left( A_\mu^1 + iA_\mu^2 \right) \left( T^1 - iT^2 \right) \\ &= \frac{1}{\sqrt{2}} \left( W_\mu^+ T^+ + W_\mu^- T^- \right),\end{aligned}$$

Equation B.6 becomes

$$\mathcal{D}_\mu = \partial_\mu - \frac{g_1}{\sqrt{2}} \left( W_\mu^+ T^+ + W_\mu^- T^- \right) - \frac{ig_1}{\cos\theta_W} Z_\mu^0 \left( T^3 - \sin^2\theta_W Q \right) - ieQ A_\mu.\tag{B.7}$$

## C Derivation of $\xi^2$ in The SLHM

In order to calculate the  $g_{zzh}$  coupling we look at the kinetic terms for the Higgs doublets. The kinetic term for the doublet  $H_i$  takes the form

$$\begin{aligned} (\mathcal{D}_\mu H_i)^\dagger \mathcal{D}^\mu H_i &= \left( \langle \text{Stuff} \rangle_\mu H_i + B Z_\mu^0 H_i \right)^\dagger \left( \langle \text{Stuff} \rangle^\mu H_i + B Z^{0\mu} H_i \right) \\ &= \langle \text{Other Stuff} \rangle + H_i^\dagger |B|^2 Z_\mu^0 Z^{0\mu} H_i. \end{aligned} \quad (\text{C.1})$$

Since we are only interested in terms quadratic in  $Z^0$ , we need only look at the last term above. We may write the four Higgs doublets in terms of their real degrees of freedom as

$$\begin{aligned} H_u &= \langle H_u \rangle + \frac{1}{\sqrt{2}} \begin{pmatrix} \phi_1 + i\phi_2 \\ \phi_3 + i\phi_4 \end{pmatrix}, & H_d &= \langle H_d \rangle + \frac{1}{\sqrt{2}} \begin{pmatrix} \phi_5 + i\phi_6 \\ \phi_7 + i\phi_8 \end{pmatrix}, \\ H_0 &= \langle H_0 \rangle + \frac{1}{\sqrt{2}} \begin{pmatrix} \phi_9 + i\phi_{10} \\ \phi_{11} + i\phi_{12} \end{pmatrix}, & H_\ell &= \langle H_\ell \rangle + \frac{1}{\sqrt{2}} \begin{pmatrix} \phi_{13} + i\phi_{14} \\ \phi_{15} + i\phi_{16} \end{pmatrix}. \end{aligned} \quad (\text{C.2})$$

Each of the four neutral scalars can be written as a linear combination of the four fields  $\phi_3, \phi_5, \phi_{11}$ , and  $\phi_{13}$ . For each Higgs doublet, we are only interested in its real degree of freedom that is a part of the lightest neutral scalar  $h^0$ . For each of these fields  $Q = 0$  since the field will reside in the component of the Higgs doublet for which  $T^3 = -Y$ . Since  $|T^3|^2 = 1/4$  for all four doublets, Equation B.7 tells us that  $|B|^2 = g_1^2/4 \cos^2 \theta_W$ . Setting  $\phi_i = 0$  for all  $i$  except  $i = 3, 5, 11, 13$  the last term in Equation C.1 becomes

$$\begin{aligned} H_i^\dagger |B|^2 Z_\mu^0 Z^{0\mu} H_i &= \left( \frac{g_1^2}{4 \cos^2 \theta_W} \right) Z_\mu^0 Z^{0\mu} \frac{1}{2} (v_i + \phi_{h(i)})^2 \\ &= \langle \text{Stuff} \rangle + \left( \frac{g_1^2 v_i}{4 \cos^2 \theta_W} \right) Z_\mu^0 Z^{0\mu} \phi_{h(i)}. \end{aligned}$$

We do not care about the “stuff” since we only need the coupling between two  $Z^0$ -bosons and one scalar Higgs. The notation  $\phi_{h(i)}$  is intended to mean the nonzero field inside the Higgs doublet  $H_i$ , e.g. for  $H_d$  we would have  $\phi_{h(d)} = \phi_5$ . Each of the four Higgs doublets contributes a relevant term so that we obtain

$$\sum_{i=1}^4 H_i^\dagger |B|^2 Z_\mu^0 Z^{0\mu} H_i = \left( \frac{g_1}{2 \cos \theta_W} \right)^2 Z_\mu^0 Z^{0\mu} (v_u \phi_3 + v_d \phi_5 + v_0 \phi_{11} + v_\ell \phi_{13}) + \langle \text{Irrelevant Stuff} \rangle.$$

The above term, which we will denote by  $\Delta\mathcal{L}$ , contains the couplings between  $Z^0 Z^0$  pairs and each of the four neutral scalars, but it is currently expressed in terms of the gauge eigenstate components  $\phi_i$ . We need to reexpress it in terms of the physical mass eigenstates (of which  $h^0$  is one) in order to extract any coupling constants. Let us arrange the four neutral scalar gauge eigenstate components into the vector  $\Phi = (\phi_3, \phi_5, \phi_{11}, \phi_{13})^T$  and let  $M$  be the neutral scalar mass matrix with  $U$  its unitary diagonalizing matrix, i.e.

$$U^\dagger M U = M_{\text{diag}}.$$

If we let  $\Phi' = U^\dagger \Phi$  then we have

$$\begin{aligned} \Phi^\dagger M \Phi &= \Phi^\dagger U U^\dagger M U U^\dagger \Phi \\ &= (U^\dagger \Phi)^\dagger (U^\dagger M U) (U^\dagger \Phi) \\ &= \Phi'^\dagger M_{\text{diag}} \Phi'. \end{aligned}$$

In other words,  $\Phi^\dagger M \Phi = \sum_{i=1}^4 m_i^2 |\Phi'_i|^2$ , which indicates that  $\Phi'$  is the vector of neutral scalar mass eigenstates  $\Phi' = (h^0, \eta^0, H_1^0, H_2^0)^T$ . These are the physical states in terms of which we wish to express  $\Delta\mathcal{L}$ . Using  $\Phi_i = U_{ij} \Phi'_j$ , this can now be easily

accomplished

$$\begin{aligned}\Delta\mathcal{L} &= \left(\frac{g_1}{2\cos\theta_W}\right)^2 Z_\mu^0 Z^{0\mu} (v_u\phi_3 + v_d\phi_5 + v_0\phi_{11} + v_\ell\phi_{13}) \\ &= \left(\frac{g_1}{2\cos\theta_W}\right)^2 Z_\mu^0 Z^{0\mu} (v_u U_{1j}\Phi'_j + v_d U_{2j}\Phi'_j + v_0 U_{3j}\Phi'_j + v_\ell U_{4j}\Phi'_j)\end{aligned}\tag{C.3}$$

This gives the coupling of each of the four physical neutral scalars  $h^0, \eta^0, H_1^0, H_2^0$  to  $Z^0$ -pairs. If we now define  $v^2 = v_u^2 + v_d^2 + v_0^2 + v_\ell^2$ ,  $\tan\beta = v_u/v_d$ ,  $\tan\beta_\ell = v_0/v_\ell$ , and  $\tan^2\alpha = (v_u^2 + v_d^2)/(v_0^2 + v_\ell^2)$  then we have

$$v_u = v \sin\alpha \sin\beta, \quad v_d = v \sin\alpha \cos\beta, \quad v_0 = v \cos\alpha \sin\beta_\ell, \quad v_\ell = v \cos\alpha \cos\beta_\ell.\tag{C.4}$$

We are only interested in extracting the  $Z^0 Z^0 h^0$  coupling from equation C.3. Using the above relations we find

$$\begin{aligned}g_{zzh} &= \left(\frac{g_1}{2\cos\theta_W}\right)^2 (v_u U_{11} + v_d U_{21} + v_0 U_{31} + v_\ell U_{41}) \\ &= \left(\frac{g_1 M_Z}{2\cos\theta_W}\right) (U_{11} \sin\alpha \sin\beta + U_{21} \sin\alpha \cos\beta + U_{31} \cos\alpha \sin\beta_\ell + U_{41} \cos\alpha \cos\beta_\ell),\end{aligned}$$

The factor out front is simply the Standard Model value for the  $g_{zzh}$  coupling, thus we find that the ratio  $\xi^2 = (g_{zzh}/g_{zzh}^{SM})^2$  is given by

$$\xi^2 = \left| U_{11} \sin\alpha \sin\beta + U_{21} \sin\alpha \cos\beta + U_{31} \cos\alpha \sin\beta_\ell + U_{41} \cos\alpha \cos\beta_\ell \right|^2.\tag{C.5}$$

Note that the second subscript for each  $U_{ij}$  is always 1 because  $h^0$  is the first component of  $\Phi'$ . This follows from the way we have implicitly defined  $U$ . It is the diagonalizing matrix of  $M$ , and so its columns are the orthonormalized eigenvectors of  $M$ . We have specifically chosen to order the eigenvectors of  $M$  as columns in  $U$  so that  $U^\dagger \Phi = \Phi' = (h^0, \eta^0, H_1^0, H_2^0)^T$ . If we had chosen some other order, it

would corresponding to a permutation of the columns of  $U$  and the second subscript on each  $U_{ij}$  in Equation C.3 would change accordingly. What is important however, is to remember that it is the subscript that corresponds to the component  $h^0$ , which is defined as the lightest neutral scalar (i.e. the eigenstate with the smallest eigenvalue).

## D Breaking Terms

Field	$\mathbb{Z}_{3q}$	$\mathbb{Z}_{3\ell}$	Field	$\mathbb{Z}_{3q}$	$\mathbb{Z}_{3\ell}$
$\widehat{H}_u$	$\omega$	1	$\widehat{X}_{01}$	1	1
$\widehat{H}_d$	$\omega$	1	$\widehat{X}_{02}$	$\omega^2$	$\omega^2$
$\widehat{H}_0$	1	$\omega$	$\widehat{X}_{q1}$	$\omega$	1
$\widehat{H}_\ell$	1	$\omega$	$\widehat{X}_{q2}$	$\omega^2$	1
$\widehat{E}$	1	$\omega^2$	$\widehat{X}_{\ell1}$	1	$\omega$
$\widehat{Q}$	$\omega^2$	1	$\widehat{X}_{\ell2}$	1	$\omega^2$

Table 13: Transformation rule for the  $\mathbb{Z}_{3q} \times \mathbb{Z}_{3\ell}$  symmetry. Each field transforms as  $\phi \rightarrow X\phi$ , where  $X$  is the corresponding factor shown in the table. For each case,  $\omega^3 = 1$ . Other fields not shown in the table are neutral under  $\mathbb{Z}_{3q} \times \mathbb{Z}_{3\ell}$

In this appendix, we discuss a possible source of the terms in  $V_{\text{soft}}$  that break the  $\mathbb{Z}_2$  symmetry of the superpotential. Generally, one can imagine such breaking terms arising from the  $F$ -term of some hidden sector superfield receiving a vacuum expectation value. To be more specific, we consider a possible scenario that results in such breaking terms and also explains the smallness of  $\kappa_q$  and  $\kappa_\ell$ . In this scenario there is a hidden sector, which contains the six fields  $\widehat{X}_{01}$ ,  $\widehat{X}_{02}$ ,  $\widehat{X}_{q1}$ ,  $\widehat{X}_{q2}$ ,  $\widehat{X}_{\ell1}$  and  $\widehat{X}_{\ell2}$ . The  $F$ -terms of the fields receive vevs

$$\langle F_{X_i} \rangle \sim \mathcal{O}(10^{11} \text{GeV})^2, \quad (\text{D.1})$$

so that

$$M_{\text{SUSY}} \sim \frac{\langle F_{X_i} \rangle}{M_P} \quad (\text{D.2})$$

is at the TeV scale. The index  $i$  denotes 01, 02,  $q1$ ,  $q2$ ,  $\ell1$ , and  $\ell2$ . A  $\mathbb{Z}_{3q} \times \mathbb{Z}_{3\ell}$  symmetry is imposed, under which the fields transform according to Table 13. The hidden sector fields  $\widehat{X}_i$  couple to visible sector fields in a high energy, fundamental theory, and are Planck suppressed in the low energy effective theory. Consequen-

tially, the lagrangian contains terms such as

$$\Delta\mathcal{L} = \frac{f'}{M_P^2} \int d^4\theta \widehat{X}_{01}^\dagger \widehat{X}_{02} \widehat{H}_u \widehat{H}_\ell + \frac{m'}{M_P} \int d^2\theta \widehat{X}_{02} \widehat{S} \widehat{H}_u \widehat{H}_\ell + \text{h.c.}, \quad (\text{D.3})$$

where  $d^2\theta = d(\theta\theta)$  and  $d^4\theta = d(\theta\theta)d(\bar{\theta}\bar{\theta})$  represent integration over Grassmann variables and  $f'$  and  $m'$  are coupling constants. When the  $F$ -terms of  $\widehat{X}_{01}$  and  $\widehat{X}_{02}$  receive vevs, the terms in Eq. (D.3) give rise to

$$\begin{aligned} \Delta\mathcal{L} &= \frac{f'\langle F_{01}\rangle\langle F_{02}\rangle}{M_P^2} \int d^4\theta(\bar{\theta}\bar{\theta})(\theta\theta)\widehat{H}_u\widehat{H}_\ell + \frac{m'\langle F_{02}\rangle}{M_P} \int d^2\theta(\theta\theta)\widehat{S}\widehat{H}_u\widehat{H}_\ell + \text{h.c.} \\ &= \frac{f'\langle F_{01}\rangle\langle F_{02}\rangle}{M_P^2} H_u H_\ell + \frac{m'\langle F_{02}\rangle}{M_P} S H_u H_\ell + \text{h.c.} \\ &\rightarrow \mu_3^2 H_u H_\ell + \mu_c S H_u H_\ell + \text{h.c.} \end{aligned} \quad (\text{D.4})$$

Similarly, the breaking parameters  $\mu_4^2$  and  $\mu_d$  arise from the Planck suppressed terms

$$\begin{aligned} \Delta\mathcal{L} &= \frac{g'}{M_P^2} \int d^4\theta \widehat{X}_{01}^\dagger \widehat{X}_{02} \widehat{H}_0 \widehat{H}_d + \frac{n'}{M_P} \int d^2\theta \widehat{X}_{02} \widehat{S} \widehat{H}_0 \widehat{H}_d + \text{h.c.} \\ &\rightarrow \frac{g'\langle F_{01}\rangle\langle F_{02}\rangle}{M_P^2} H_0 H_d + \frac{n'\langle F_{02}\rangle}{M_P} S H_0 H_d + \text{h.c.} \\ &\rightarrow \mu_4^2 H_0 H_d + \mu_d S H_0 H_d + \text{h.c.}, \end{aligned} \quad (\text{D.5})$$

while the parameters  $m_{u0}^2$  and  $m_{d\ell}^2$  arise from

$$\begin{aligned} \Delta\mathcal{L} &= \frac{h'}{M_P^2} \int d^4\theta \widehat{X}_{02}^\dagger \widehat{X}_{\ell 1} \widehat{H}_u^\dagger \widehat{H}_0 + \frac{i'}{M_P^2} \int d^4\theta \widehat{X}_{02}^\dagger \widehat{X}_{\ell 1} \widehat{H}_d^\dagger \widehat{H}_\ell + \text{h.c.} \\ &\rightarrow \frac{h'\langle F_{02}\rangle\langle F_{\ell 1}\rangle}{M_P^2} H_u^\dagger H_0 + \frac{i'\langle F_{02}\rangle\langle F_{\ell 1}\rangle}{M_P^2} H_d^\dagger H_\ell + \text{h.c.} \\ &\rightarrow m_{u0}^2 H_u^\dagger H_0 + m_{d\ell}^2 H_d^\dagger H_\ell + \text{h.c.} \end{aligned} \quad (\text{D.6})$$

In this way, all of the  $\mathbb{Z}_2$  breaking terms are generated. At this point it should be noted that the  $\mathbb{Z}_{3q} \times \mathbb{Z}_{3\ell}$  symmetry actually prohibits the terms  $\mu_q \widehat{H}_u \widehat{H}_d$ ,  $\mu_\ell \widehat{H}_0 \widehat{H}_\ell$ ,

$\frac{1}{M_P} \int d^4\theta \hat{X}_{q2}^\dagger \hat{H}_u \hat{H}_d$	$\int d^2\theta \mu_q \hat{H}_u \hat{H}_d$
$\frac{1}{M_P} \int d^4\theta \hat{X}_{\ell2}^\dagger \hat{H}_0 \hat{H}_\ell$	$\int d^2\theta \mu_\ell \hat{H}_0 \hat{H}_\ell$
$\frac{1}{M_P} \int d^4\theta \hat{X}_{01}^\dagger \hat{S}^2$	$\int d^2\theta \lambda_2 \hat{S}^2$
$\frac{1}{M_P^2} \int d^4\theta \left( \hat{X}_{01}^\dagger \hat{X}_{q1} + \hat{X}_{q2}^\dagger \hat{X}_{01} + \hat{X}_{02}^\dagger \hat{X}_{\ell2} + \hat{X}_{q1}^\dagger \hat{X}_{q2} \right) \hat{H}_u \hat{H}_d$	$\mu_1^2 H_u H_d$
$\frac{1}{M_P^2} \int d^4\theta \left( \hat{X}_{01}^\dagger \hat{X}_{\ell1} + \hat{X}_{\ell2}^\dagger \hat{X}_{01} + \hat{X}_{02}^\dagger \hat{X}_{q2} + \hat{X}_{\ell1}^\dagger \hat{X}_{\ell2} \right) \hat{H}_0 \hat{H}_\ell$	$\mu_2^2 H_0 H_\ell$
$\frac{1}{M_P^2} \int d^4\theta \left( \hat{X}_{01}^\dagger \hat{X}_{02} + \hat{X}_{q1}^\dagger \hat{X}_{\ell2} + \hat{X}_{\ell1}^\dagger \hat{X}_{q2} \right) \hat{H}_u \hat{H}_\ell$	$\mu_3^2 H_u H_\ell$
$\frac{1}{M_P^2} \int d^4\theta \left( \hat{X}_{01}^\dagger \hat{X}_{02} + \hat{X}_{q1}^\dagger \hat{X}_{\ell2} + \hat{X}_{\ell1}^\dagger \hat{X}_{q2} \right) \hat{H}_0 \hat{H}_d$	$\mu_4^2 H_0 H_d$
$\frac{1}{M_P^2} \int d^4\theta \left( \hat{X}_{02}^\dagger \hat{X}_{\ell1} + \hat{X}_{q1}^\dagger \hat{X}_{02} + \hat{X}_{q2}^\dagger \hat{X}_{\ell2} + \hat{X}_{\ell1}^\dagger \hat{X}_{q1} \right) \hat{H}_u^\dagger \hat{H}_0$	$m_{u0}^2 H_u^\dagger H_0$
$\frac{1}{M_P^2} \int d^4\theta \left( \hat{X}_{02}^\dagger \hat{X}_{\ell1} + \hat{X}_{q1}^\dagger \hat{X}_{02} + \hat{X}_{q2}^\dagger \hat{X}_{\ell2} + \hat{X}_{\ell1}^\dagger \hat{X}_{q1} \right) \hat{H}_d^\dagger \hat{H}_\ell$	$m_{d\ell}^2 H_d^\dagger H_\ell$
$\frac{1}{M_P^2} \int d^4\theta \sum_i \hat{X}_i^\dagger \hat{X}_i \hat{H}_f^\dagger \hat{H}_f$	$m_f^2  H_f ^2$
$\frac{1}{M_P} \int d^2\theta \hat{X}_{q1} \hat{S} \hat{H}_u \hat{H}_d$	$\mu_a S H_u H_d$
$\frac{1}{M_P} \int d^2\theta \hat{X}_{\ell1} \hat{S} \hat{H}_0 \hat{H}_\ell$	$\mu_b S H_0 H_\ell$
$\frac{1}{M_P} \int d^2\theta \hat{X}_{02} \hat{S} \hat{H}_u \hat{H}_\ell$	$\mu_c S H_u H_\ell$
$\frac{1}{M_P} \int d^2\theta \hat{X}_{02} \hat{S} \hat{H}_0 \hat{H}_d$	$\mu_d S H_0 H_d$
$\frac{1}{M_P^2} \int d^4\theta \sum_i \hat{X}_i^\dagger \hat{X}_i \hat{S}^2$	$b_s^2 S^2$
$\frac{1}{M_P} \int d^2\theta \hat{X}_0 \hat{S}^3$	$a_s S^3$

Table 14: Half of the complete list of superpotential and  $V_{\text{soft}}$  terms generated by the  $X_i$  in this example. The other half simply consists of the hermitian conjugates of the terms shown in this table. Please note that we have suppressed the constant coefficient in front of each of the couplings listed on the left side of the table. They provide no meaningful information for our purposes and severely clutter the table.

$\kappa_q \hat{S} \hat{H}_u \hat{H}_d$ , and  $\kappa_\ell \hat{S} \hat{H}_0 \hat{H}_\ell$  from appearing in the superpotential [see Eq. (46)]. As far as the  $\mu_q$  and  $\mu_\ell$  terms are concerned, this is not a problem since they are generated by the vevs of the  $\hat{X}_{q2}$  and  $\hat{X}_{\ell 2}$  fields in the same manner:

$$\begin{aligned}
\Delta\mathcal{L} &= \frac{a'}{M_P} \int d^4\theta \hat{X}_{q2}^\dagger \hat{H}_u \hat{H}_d + \frac{b'}{M_P} \int d^4\theta \hat{X}_{\ell 2}^\dagger \hat{H}_0 \hat{H}_\ell \\
&\rightarrow \frac{a' \langle F_{q2} \rangle}{M_P} \int d^2\theta d^2\bar{\theta} (\bar{\theta}\theta) \hat{H}_u \hat{H}_d + \frac{b' \langle F_{\ell 2} \rangle}{M_P} \int d^2\theta d^2\bar{\theta} (\bar{\theta}\theta) \hat{H}_0 \hat{H}_\ell \\
&= \frac{a' \langle F_{q2} \rangle}{M_P} \int d^2\theta \hat{H}_u \hat{H}_d + \frac{b' \langle F_{\ell 2} \rangle}{M_P} \int d^2\theta \hat{H}_0 \hat{H}_\ell \\
&\rightarrow \mu_q \int d^2\theta \hat{H}_u \hat{H}_d + \mu_\ell \int d^2\theta \hat{H}_0 \hat{H}_\ell.
\end{aligned} \tag{D.7}$$

In this UV completion scenario, the terms corresponding to  $\kappa_q$ ,  $\kappa_\ell$ ,  $\lambda_1$  and  $t$  are not generated in this way. Because of the  $\mathbb{Z}_{3q} \times \mathbb{Z}_{3\ell}$  symmetry, they are entirely absent at tree level. Benchmark points II and V in Table 15 satisfy  $\kappa_q = \kappa_\ell = \lambda_1 = t = 0$  and yield results consistent with our goals. Since we are not committing to this particular UV completion scheme, we consider several other benchmark points that include nonzero values for these parameters. A list of the soft breaking terms relevant to this thesis, which are generated by the fields  $X_i$ , is given in Table 14.

## E List of Benchmark Points

In this appendix, we show several benchmark points given in Table 15. Benchmarks point I-III lie in the suggested CoGeNT and DAMA range, while benchmarks point IV-VI satisfy CDMS bound. Benchmark point I is identical with benchmark point A discussed in the text. Benchmark point IV is identical with benchmark point B. Benchmark points II and V are motivated by mechanism described in Appendix D.

Table 15: Additional benchmark points

Benchmark point	I	II	III	IV	V	VI
$\kappa_q$	0.01	0	0.01	0.01	0	0.01
$\kappa_l$	0.01	0	0.01	0.01	0	0.01
$\kappa_s$	0.6	0.6	0.5	0.6	0.6	0.5
$\tan \alpha$	20	15	30	20	30	25
$\tan \beta$	50	30	30	50	25	25
$\tan \beta_\ell$	10	10	5	10	5	5
$v_s$ (GeV)	50	50	100	50	50	100
$v_u$ (GeV)	245.6	245.3	245.7	245.6	245.7	245.6
$v_d$ (GeV)	4.9	8.2	8.2	4.9	9.8	9.8
$v_0$ (GeV)	12.2	16.2	8.0	12.2	8.0	9.6
$v_\ell$ (GeV)	1.2	1.6	1.6	1.2	1.6	1.9
$\mu_q$ (GeV)	125	125	200	125	125	150
$\mu_\ell$ (GeV)	125	125	150	125	150	150
$\lambda_1^2$ (GeV <sup>2</sup> )	100 <sup>2</sup>	0	150 <sup>2</sup>	100 <sup>2</sup>	0	50 <sup>2</sup>
$\lambda_2$ (GeV)	-35	-35	-63	-35	-35	-63
$M_1$ (GeV)	500	500	250	500	250	200
$M_2$ (GeV)	500	500	500	500	500	400
$m_{u0}^2$ (GeV <sup>2</sup> )	-100 <sup>2</sup>	-150 <sup>2</sup>	-150 <sup>2</sup>	-100 <sup>2</sup>	-150 <sup>2</sup>	-150 <sup>2</sup>
$m_{dt}^2$ (GeV <sup>2</sup> )	100 <sup>2</sup>	200 <sup>2</sup>	100 <sup>2</sup>	100 <sup>2</sup>	200 <sup>2</sup>	100 <sup>2</sup>
$\mu_1^2$ (GeV <sup>2</sup> )	400 <sup>2</sup>	300 <sup>2</sup>	300 <sup>2</sup>	400 <sup>2</sup>	400 <sup>2</sup>	350 <sup>2</sup>
$\mu_2^2$ (GeV <sup>2</sup> )	200 <sup>2</sup>	300 <sup>2</sup>	250 <sup>2</sup>	200 <sup>2</sup>	200 <sup>2</sup>	300 <sup>2</sup>
$\mu_3^2$ (GeV <sup>2</sup> )	200 <sup>2</sup>	200 <sup>2</sup>	250 <sup>2</sup>	200 <sup>2</sup>	250 <sup>2</sup>	200 <sup>2</sup>
$\mu_4^2$ (GeV <sup>2</sup> )	400 <sup>2</sup>	200 <sup>2</sup>	200 <sup>2</sup>	400 <sup>2</sup>	400 <sup>2</sup>	100 <sup>2</sup>
$\mu_a$ (GeV)	100	75	75	100	100	80
$\mu_b$ (GeV)	200	150	300	200	250	400
$\mu_c$ (GeV)	200	200	400	200	300	200
$\mu_d$ (GeV)	200	100	100	200	250	100

Continued on the next page

Table 15: continued

Benchmark point	I	II	III
$t^3$ (GeV <sup>3</sup> )	60.6 <sup>3</sup>	0	83.9 <sup>3</sup>
$b_s^2$ (GeV <sup>2</sup> )	63.4 <sup>2</sup>	43.6 <sup>2</sup>	98.2 <sup>2</sup>
$a_s$ (GeV)	-42.4	-21.7	-50.2
$m_{\chi_1}$ (GeV)	7.4	7.4	7.7
$m_{\chi_1^\pm}$ (GeV)	118	117	151
$m_{h_1}$ (GeV)	11.3	19.2	12.8
$m_{a_1}$ (GeV)	18.7	16.1	18.8
$\langle\sigma v\rangle$ ( $\frac{\text{cm}^3}{\text{s}}$ )	$4.0 \times 10^{-26}$	$3.4 \times 10^{-26}$	$4.6 \times 10^{-26}$
$\frac{\langle\sigma v(\chi_1\chi_1 \rightarrow \text{hadrons})\rangle}{\langle\sigma v\rangle}$	23%	38%	32%
$\sigma_{SI}$ (cm <sup>2</sup> )	$1.7 \times 10^{-40}$	$1.2 \times 10^{-40}$	$1.5 \times 10^{-40}$
$\Gamma_{Z \rightarrow \chi_1\chi_1}$ (GeV)	$1.4 \times 10^{-9}$	0	$2.1 \times 10^{-10}$
$\Gamma_{Z \rightarrow h_1 a_1}$ (GeV)	$1.1 \times 10^{-11}$	$1.2 \times 10^{-10}$	$1.4 \times 10^{-10}$
$k$	$8.0 \times 10^{-3}$	$3.5 \times 10^{-2}$	$2.2 \times 10^{-2}$
$S_{\text{model}}(e^+e^- \rightarrow h_1 a_1)$	$1 \times 10^{-10}$	$2 \times 10^{-9}$	$2 \times 10^{-9}$
$S_{\text{model}}(e^+e^- \rightarrow h_2 a_1)$	$1 \times 10^{-12}$	$5 \times 10^{-11}$	$3 \times 10^{-11}$
$\sigma_{e^+e^- \rightarrow \chi_1\chi_2}$ (pb)	$1 \times 10^{-5}$	0	$5 \times 10^{-9}$
Benchmark point	IV	V	VI
$t^3$ (GeV <sup>3</sup> )	55.0 <sup>3</sup>	0	-87.9 <sup>3</sup>
$b_s^2$ (GeV <sup>2</sup> )	66.3 <sup>2</sup>	47.1 <sup>2</sup>	99.0 <sup>2</sup>
$a_s$ (GeV)	-42.2	-20.0	-50.2
$m_{\chi_1}$ (GeV)	7.4	7.4	7.7
$m_{\chi_1^\pm}$ (GeV)	118	117	137
$m_{h_1}$ (GeV)	41.5	41.4	23.1
$m_{a_1}$ (GeV)	19.3	19.2	11.7
$\langle\sigma v\rangle$ ( $\frac{\text{cm}^3}{\text{s}}$ )	$3.0 \times 10^{-26}$	$3.1 \times 10^{-26}$	$4.1 \times 10^{-26}$
$\frac{\langle\sigma v(\chi_1\chi_1 \rightarrow \text{hadrons})\rangle}{\langle\sigma v\rangle}$	23%	24%	30%
$\sigma_{SI}$ (cm <sup>2</sup> )	$1.2 \times 10^{-42}$	$6.1 \times 10^{-42}$	$1.5 \times 10^{-41}$
$\Gamma_{Z \rightarrow \chi_1\chi_1}$ (GeV)	$1.4 \times 10^{-9}$	0	$6.3 \times 10^{-10}$
$\Gamma_{Z \rightarrow h_1 a_1}$ (GeV)	$4.9 \times 10^{-12}$	$4.2 \times 10^{-11}$	$1.2 \times 10^{-10}$
$k$	$1.3 \times 10^{-2}$	0.12	$2.8 \times 10^{-2}$
$S_{\text{model}}(e^+e^- \rightarrow h_1 a_1)$	$1 \times 10^{-10}$	$1 \times 10^{-9}$	$2 \times 10^{-9}$
$S_{\text{model}}(e^+e^- \rightarrow h_2 a_1)$	$2 \times 10^{-12}$	$1 \times 10^{-10}$	$4 \times 10^{-11}$
$\sigma_{e^+e^- \rightarrow \chi_1\chi_2}$ (pb)	$1 \times 10^{-5}$	0	$4 \times 10^{-6}$

## References

- [1] J. F. Gunion, H. E. Haber, G. L. Kane and S. Dawson, “THE Higgs Hunter’s Guide,” Addison-Wesley, Reading, USA, 1995.
- [2] M. Sher, Phys. Rept. **179**, 273 (1989).
- [3] G. C. Branco, P. M. Ferreira, L. Lavoura, M. N. Rebelo, M. Sher and J. P. Silva, arXiv:1106.0034 [hep-ph].
- [4] T. D. Lee, Phys. Rev. D **8**, 1226 (1973).
- [5] S. Weinberg, Phys. Rev. Lett. **37**, 657 (1976).
- [6] G. C. Branco and M. N. Rebelo, Phys. Lett. B **160**, 117 (1985).
- [7] J. Liu and L. Wolfenstein, Nucl. Phys. B **289**, 1 (1987).
- [8] S. Weinberg, Phys. Rev. D **42**, 860 (1990).
- [9] Y. L. Wu and L. Wolfenstein, Phys. Rev. Lett. **73**, 1762 (1994) [arXiv:hep-ph/9409421],
- [10] E. Accomando *et al.*, arXiv:hep-ph/0608079.
- [11] A. Riotto and M. Trodden, Ann. Rev. Nucl. Part. Sci. **49**, 35 (1999) [arXiv:hep-ph/9901362].
- [12] M. Dine and A. Kusenko, Rev. Mod. Phys. **76**, 1 (2004) [arXiv:hep-ph/0303065].
- [13] R. D. Peccei and H. R. Quinn, Phys. Rev. Lett. **38**, 1440 (1977).
- [14] S. L. Glashow and S. Weinberg, Phys. Rev. D **15** (1977) 1958; E. A. Paschos, Phys. Rev. D **15** (1977) 1966.

- [15] H. E. Haber and G. L. Kane, *Phys. Rept.* **117**, 75 (1985).
- [16] T. P. Cheng and M. Sher, *Phys. Rev. D* **35**, 3484 (1987).
- [17] A. Antaramian, L. J. Hall and A. Rasin, *Phys. Rev. Lett.* **69**, 1871 (1992) [hep-ph/9206205].
- [18] S. R. Coleman, J. Mandula, *Phys. Rev.* **159**, (1967) 1251.
- [19] A. Signer, *J. Phys. G* **36**, 073002 (2009) [arXiv:0905.4630 [hep-ph]].
- [20] G. Marshall, M. McCaskey and M. Sher, *Phys. Rev. D* **81**, 053006 (2010) [arXiv:0912.1599 [hep-ph]].
- [21] D. Hooper and L. Goodenough, *Phys. Lett. B* **697**, 412 (2011) [arXiv:1010.2752 [hep-ph]].
- [22] R. M. Barnett, G. Senjanovic, L. Wolfenstein and D. Wyler, *Phys. Lett. B* **136**, 191 (1984); R. M. Barnett, G. Senjanovic and D. Wyler, *Phys. Rev. D* **30**, 1529 (1984); Y. Grossman, *Nucl. Phys. B* **426**, 355 (1994) [arXiv:hep-ph/9401311]; V. Barger, H. E. Logan and G. Shaughnessy, *Phys. Rev. D* **79**, 115018 (2009) [arXiv:0902.0170 [hep-ph]].
- [23] H. S. Goh, L. J. Hall and P. Kumar, *JHEP* **0905**, 097 (2009) [arXiv:0902.0814 [hep-ph]]; M. Aoki, S. Kanemura, K. Tsumura and K. Yagyu, *Phys. Rev. D* **80**, 015017 (2009) [arXiv:0902.4665 [hep-ph]]; S. Su and B. Thomas, *Phys. Rev. D* **79**, 095014 (2009) [arXiv:0903.0667 [hep-ph]].
- [24] S. Gabriel and S. Nandi, *Phys. Lett. B* **655**, 141 (2007).
- [25] S. M. Davidson and H. E. Logan, *Phys. Rev. D* **80**, 095008 (2009) [arXiv:0906.3335 [hep-ph]].

- [26] A. Aranda and M. Sher, Phys. Rev. D **62**, 092002 (2000) [arXiv:hep-ph/0005113].
- [27] M. Spira, A. Djouadi, D. Graudenz and P. M. Zerwas, Nucl. Phys. B **453**, 17 (1995) [arXiv:hep-ph/9504378].
- [28] J. Alwall *et al.*, JHEP **0709**, 028 (2007) [arXiv:0706.2334 [hep-ph]].
- [29] J. Pumplin, A. Belyaev, J. Huston, D. Stump and W. K. Tung, JHEP **0602**, 032 (2006) [arXiv:hep-ph/0512167].
- [30] G. Aad *et al.* [The ATLAS Collaboration], arXiv:0901.0512 [hep-ex].
- [31] A. Freitas, A. von Manteuffel and P. M. Zerwas, Eur. Phys. J. C **34**, 487 (2004) [arXiv:hep-ph/0310182].
- [32] G. Marshall and M. Sher, Phys. Rev. D **83**, 015005 (2011) [arXiv:1011.3016 [hep-ph]].
- [33] S. Su and B. Thomas, Phys. Rev. D **79** (2009) 095014 [arXiv:0903.0667 [hep-ph]].
- [34] H. E. Logan and D. MacLennan, Phys. Rev. D **79** (2009) 115022 [arXiv:0903.2246 [hep-ph]].
- [35] H. S. Goh, L. J. Hall and P. Kumar, JHEP **0905** (2009) 097 [arXiv:0902.0814 [hep-ph]].
- [36] J. Cao, P. Wan, L. Wu and J. M. Yang, Phys. Rev. D **80** (2009) 071701 [arXiv:0909.5148 [hep-ph]].
- [37] M. Aoki, S. Kanemura, K. Tsumura and K. Yagyu, Phys. Rev. D **80**, 015017 (2009) [arXiv:0902.4665 [hep-ph]].

- [38] H. E. Logan and D. MacLennan, Phys. Rev. D **81**, 075016 (2010) [arXiv:1002.4916 [hep-ph]].
- [39] S. M. Davidson and H. E. Logan, Phys. Rev. D **80** (2009) 095008 [arXiv:0906.3335 [hep-ph]].
- [40] J. F. Gunion and H. E. Haber, Phys. Rev. D **67**, 075019 (2003) [arXiv:hep-ph/0207010].
- [41] R. S. Gupta and J. D. Wells, Phys. Rev. D **81**, 055012 (2010) [arXiv:0912.0267 [hep-ph]].
- [42] J. D. Wells, arXiv:0909.4541 [hep-ph].
- [43] A. Djouadi, Phys. Rept. **459**, 1 (2008) [arXiv:hep-ph/0503173].
- [44] S. Dawson and P. Jaiswal, Phys. Rev. D **82**, 073017 (2010) [arXiv:1009.1099 [hep-ph]].
- [45] F. Jegerlehner, Acta Phys. Polon. B **38**, 3021 (2007) [arXiv:hep-ph/0703125].
- [46] G. W. Bennett *et al.* [Muon g-2 Collaboration], Phys. Rev. Lett. **92**, 161802 (2004) [arXiv:hep-ex/0401008].
- [47] G. W. Bennett *et al.* [Muon G-2 Collaboration], Phys. Rev. D **73**, 072003 (2006) [arXiv:hep-ex/0602035].
- [48] S. M. Barr and A. Zee, Phys. Rev. Lett. **65**, 21 (1990) [Erratum-ibid. **65**, 2920 (1990)].
- [49] K. Cheung and O. C. W. Kong, Phys. Rev. D **68**, 053003 (2003) [arXiv:hep-ph/0302111].

- [50] A. W. El Kaffas, W. Khater, O. M. Ogreid and P. Osland, Nucl. Phys. B **775**, 45 (2007) [arXiv:hep-ph/0605142].
- [51] A. Wahab El Kaffas, P. Osland and O. M. Ogreid, Phys. Rev. D **76**, 095001 (2007) [arXiv:0706.2997 [hep-ph]].
- [52] C. Amsler *et al.* [Particle Data Group], Phys. Lett. B **667**, 1 (2008).
- [53] P. Teixeira-Dias, J. Phys. Conf. Ser. **110**, 042030 (2008) [arXiv:0804.4146 [hep-ex]].
- [54] R. Barate *et al.* [LEP Working Group for Higgs boson searches and ALEPH Collaboration and and], Phys. Lett. B **565**, 61 (2003) [arXiv:hep-ex/0306033].
- [55] S. Schael *et al.* [ALEPH Collaboration and DELPHI Collaboration and L3 Collaboration and ], Eur. Phys. J. C **47**, 547 (2006) [arXiv:hep-ex/0602042].
- [56] P. Achard *et al.* [L3 Collaboration], Phys. Lett. B **583**, 14 (2004) [arXiv:hep-ex/0402003].
- [57] J. Abdallah *et al.* [DELPHI Collaboration], Eur. Phys. J. C **38**, 1 (2004) [arXiv:hep-ex/0410017].
- [58] A. Djouadi, Phys. Rept. **457**, 1 (2008) [arXiv:hep-ph/0503172].
- [59] A. Belyaev, R. Guedes, S. Moretti and R. Santos, JHEP **1007**, 051 (2010) [arXiv:0912.2620 [hep-ph]].
- [60] I. Kravchenko [CDF and D0 Collaboration], in *In the Proceedings of the 15th International Conference on Supersymmetry and the Unification of Fundamental Interactions (SUSY07), Karlsruhe, Germany, 26 Jul - 1 Aug 2007* arXiv:0710.5141 [hep-ex].

- [61] G. Marshall and R. Primulando, *JHEP* **1105**, 026 (2011) [arXiv:1102.0492 [hep-ph]].
- [62] A. Boyarsky, D. Malyshev and O. Ruchayskiy, *Phys. Lett. B* **705**, 165 (2011) [arXiv:1012.5839 [hep-ph]].
- [63] K. N. Abazajian, *JCAP* **1103**, 010 (2011) [arXiv:1011.4275 [astro-ph.HE]].
- [64] J. Kopp, V. Niro, T. Schwetz and J. Zupan, *PoS IDM 2010*, 118 (2011) [arXiv:1011.1398 [hep-ph]]. M. R. Buckley, D. Hooper and T. M. P. Tait, *Phys. Lett. B* **702**, 216 (2011) [arXiv:1011.1499 [hep-ph]]. D. Hooper and T. Linden, *Phys. Rev. D* **83**, 083517 (2011) [arXiv:1011.4520 [astro-ph.HE]]. K. N. Abazajian, S. Blanchet and J. P. Harding, *Phys. Rev. D* **85**, 043509 (2012) [arXiv:1011.5090 [hep-ph]]. J. M. Siegal-Gaskins, R. Reesman, V. Pavlidou, S. Profumo and T. P. Walker, *Mon. Not. Roy. Astron. Soc.* **415**, 1074S (2011) [arXiv:1011.5501 [astro-ph.HE]]. M. H. G. Tytgat, *PoS IDM 2010*, 126 (2011) [arXiv:1012.0576 [hep-ph]]. K. N. Abazajian, S. Blanchet and J. P. Harding, *Phys. Rev. D* **84**, 103007 (2011) [arXiv:1012.1247 [astro-ph.CO]]. A. Abada, D. Ghaffor and S. Nasri, *Phys. Rev. D* **83**, 095021 (2011) [arXiv:1101.0365 [hep-ph]]. G. Zhu, *Phys. Rev. D* **83**, 076011 (2011) [arXiv:1101.4387 [hep-ph]].
- [65] C. Kelso and D. Hooper, *JCAP* **1102**, 002 (2011) [arXiv:1011.3076 [hep-ph]].
- [66] H. S. Goh, L. J. Hall and P. Kumar, *JHEP* **0905**, 097 (2009) [arXiv:0902.0814 [hep-ph]].
- [67] H. E. Logan, *Phys. Rev. D* **83**, 035022 (2011) [arXiv:1010.4214 [hep-ph]]. V. Barger, Y. Gao, M. McCaskey and G. Shaughnessy, *Phys. Rev. D* **82**, 095011 (2010) [arXiv:1008.1796 [hep-ph]]. A. L. Fitzpatrick, D. Hooper and

- K. M. Zurek, Phys. Rev. D **81**, 115005 (2010) [arXiv:1003.0014 [hep-ph]].  
A. R. Raklev and M. J. White, arXiv:0911.1986 [hep-ph].
- [68] C. E. Aalseth *et al.* [CoGeNT Collaboration], Phys. Rev. Lett. **106**, 131301 (2011) [arXiv:1002.4703 [astro-ph.CO]].
- [69] R. Bernabei *et al.* [ DAMA Collaboration ], Eur. Phys. J. **C56**, 333-355 (2008). [arXiv:0804.2741 [astro-ph]]; R. Bernabei *et al.*, Eur. Phys. J. C **67**, 39 (2010) [arXiv:1002.1028 [astro-ph.GA]].
- [70] D. Hooper, J. I. Collar, J. Hall *et al.*, Phys. Rev. **D82**, 123509 (2010). [arXiv:1007.1005 [hep-ph]].
- [71] E. Aprile *et al.* [XENON100 Collaboration], Phys. Rev. Lett. **105**, 131302 (2010) [arXiv:1005.0380 [astro-ph.CO]].
- [72] Z. Ahmed *et al.* [CDMS-II Collaboration], Phys. Rev. Lett. **106**, 131302 (2011) [arXiv:1011.2482 [astro-ph.CO]].
- [73] R. Kappl, M. Ratz and M. W. Winkler, Phys. Lett. B **695**, 169 (2011) [arXiv:1010.0553 [hep-ph]].
- [74] J. Espinosa and M. Quirós, Phys. Lett. B **279**, 92 (1992); Phys. Lett. B **302**, 51 (1993).  
G. Kane, C. Kolda and J. Wells, Phys. Rev. Lett. **70**, 2686 (1993).
- [75] G. Jungman, M. Kamionkowski and K. Griest, Phys. Rept. **267**, 195 (1996) [arXiv:hep-ph/9506380].
- [76] E. Komatsu *et al.* [WMAP Collaboration], Astrophys. J. Suppl. **180**, 330 (2009) [arXiv:0803.0547 [astro-ph]].

- [77] P. Gondolo and G. Gelmini, Nucl. Phys. B **360**, 145 (1991).
- [78] C. Munoz, Int. J. Mod. Phys. A **19**, 3093 (2004) [arXiv:hep-ph/0309346].
- [79] J. R. Ellis, A. Ferstl and K. A. Olive, Phys. Lett. B **481**, 304 (2000) [arXiv:hep-ph/0001005].
- [80] K. Nakamura *et al.* [Particle Data Group], J. Phys. G **37**, 075021 (2010).
- [81] G. Abbiendi *et al.* [ OPAL Collaboration ], Eur. Phys. J. **C27**, 311-329 (2003). [hep-ex/0206022].
- [82] S. Schael *et al.* [ ALEPH and DELPHI and L3 and OPAL and LEP Working Group for Higgs Boson Searches Collaborations ], Eur. Phys. J. **C47**, 547-587 (2006). [hep-ex/0602042].
- [83] J. Abdallah *et al.* [DELPHI Collaboration], Eur. Phys. J. C **31**, 421 (2003) [arXiv:hep-ex/0311019].
- [84] M. E. Peskin, D. V. Schroeder, *An Introduction to Quantum Field Theory* (Westview Press, Boulder, Colorado, 1995).

## VITA

### Gardner Rush Marshall

Gardner Marshall was born on February 28, 1985. He grew up in Charlottesville, Virginia. As a preschooler, he enjoyed exploring a small bamboo thicket behind his backyard and wanted to find a ladder long enough to climb up to the moon. Sadly, the ladder idea didn't pan out (for a number of reasons). He attended STAB high school, graduated in 2003, and subsequently studied physics and mathematics at the University of Mary Washington. There he met his wife, whom he stopped on the side of the street to ask for a date as a complete stranger. It apparently creeped her out a little bit - but not enough to turn down the offer! He was inducted into Phi Beta Kappa during his junior year and graduated summa cum laude in 2007 with departmental honors in physics and also mathematics. The following fall he entered the graduate program in physics at William & Mary.